Ph.D. Dissertation of Agriculture

Bioreducible Polymers with Crosslinked Structure and Fluorinated Arginine-functionalization for Gene Delivery Systems

가교 구조와 불화 아르기닌 개질 구조를 지닌
생체환원성 고분자 유전자 전달체

February 2020

Seoul National University
Department of Biosystems & Biomaterials
Science and Engineering

Lee, Gyeong Jin

Bioreducible Polymers with Crosslinked Structure and Fluorinated Arginine-functionalization for Gene Delivery Systems

Advised by Prof. Kim, Tae-il

Submitting a Ph.D. Dissertation of Agriculture
November 2019

Seoul National University
Department of Biosystems & Biomaterials Science and Engineering
Lee, Gyeong Jin

Confirming the Ph.D. Dissertation written by
Lee, Gyeong Jin
January 2020

Chair	Hyun, Jinho	(Seal)
Vice Chair	Kim, Tae-il	(Seal)
Examiner	Lee, Ki Hoon	(Seal)
Examiner	Kwak, Seon Yeong	(Seal)
Examiner	Jeong, Ji Hoon	(Seal)

Abstract

Bioreducible polymers have been extensively used for gene delivery systems due to their selective degradability in reducing conditions. Although bioreducible polymers have been studied for decades, studies about their cellular behavior are scarce.

In this dissertation, two kinds of bioreducible polymers for gene delivery were investigated to examine the effect of polymer structure on gene delivery mechanisms such as polyplex formation, transfection efficiency, cellular uptake pathways, and so on. One is crosslinked bioreducible polymer (polypropylenimine-cystamine bisacrylamide, PPI-CBA), the other is fluorinated arginine functionalized bioreducible polymers (heptafluorobutyrated arginine functionalized poly(cystamine bisacrylamide-diaminohexane), FR-PCH).

In the first part, a study on the extraordinary bioreducible behavior of PPI-CBA is described. In this study, it was found that the extraordinary reductive behavior of crosslinked polymer in comparison with linear bioreducible polymer. PPI-CBAs were synthesized successfully by using Michael addition reaction; they could form positively charged and nano-sized polyplexes with pDNA. Interestingly, they still retarded pDNA in reducing conditions,

which is unusual for bioreducible polymers. PPI-CBAs showed comparable efficiency to PEI25k in serum conditions, which means PPI-CBAs possessed good serum-compatibility. However, cytotoxicity of PPI-CBAs was significant and increased with concentration and crosslinking degree. Decreased intracellular glutathione (GSH) and increased reactive oxygen species (ROS) levels with an increase of the crosslinking degree suggest that GSH consumption due to re-crosslinking of degraded PPI-CBAs in cytosol might induce the increase of intracellular cytotoxic ROS. Therefore, unlike linear bioreducible polymers, crosslinked bioreducible polymer, PPI-CBAs show unique degradation and intracellular behaviors based on their crosslinked structures.

In the second part, the experiments were set to examine the effect of arginine conjugation and fluorination to linear bioreducible polymers. FR-PCHs were synthesized for gene delivery systems. They could form positively charged and nano-sized polyplexes with pDNA. Interestingly, some of FR-PCH polyplexes retarded pDNA even in reducing conditions, probably due to the hydrophobic interaction of fluoroalkyl chains. FR-PCHs showed comparable transfection efficiency to PEI25k in serum-free conditions and superior efficiency to PEI25k even in serum-containing conditions, which means FR-PCHs possessed good serum-compatibility. Good

serum tolerance was also confirmed by further experiments such as polyplex size measurement in 10% FBS (fetal bovine serum) and transfection assay in various concentrations of FBS. The polyplexes consist of FR-PCHs maintained their particle size in the presence of serum. Even at 50% of FBS, FR-PCH also showed the highest transfection efficiency. In terms of cellular uptake, fluorination enhanced membrane permeability of FR-PCHs. By using cellular uptake inhibitors, it was thought that FR-PCHs seem to use multiple pathways, but interestingly nocodazole tremendously prevented the uptake in all cell lines used. On the other hand, cytotoxicity of the polymers was significant and increased with concentration and modification degree probably due to enhanced membrane permeability of FR-PCHs. The interaction between membrane and fluoroalkyl chain would cause cell death by undermining the integrity of the cellular membranes. Nevertheless, from the results, it was confirmed that fluorination can confer not only serum-compatibility but also improved membrane permeability.

Keyword: bioreducible polymer, gene delivery, crosslinking, arginine, fluorination, cellular uptake
Student Number: 2013-21139

Table of Contents

Chapter 1. Introduction

Medicines are essential for human life. Through history, countless researchers have tried to search and develop medicines improving the life quality of mankind. Numerous diseases have been conquered; however, there are still many diseases hard to treat such as cystic fibrosis, Huntington disease, and various cancers, and so on. Many of these challenging diseases are usually genetic disorders, so it is difficult to cure by applying traditional medical treatment. As the origin of disease is gene, dysfunction of gene should be fixed for complete cure.

In 1972, a monumental paper suggesting a new concept of therapy using gene to treat such diseases was published [1]. The suggested therapy has been named gene therapy. Gene therapy means replacement of defective genes with intact genes to restore original function of a replaced gene [2,3], or suppression of defective gene overexpressing [4,5]. Delivering gene has advantages when it compares to delivering proteins or peptides. Delivering gene is more stable and affects longer than protein or peptide delivery. Although delivering gene has such advantages, naked gene is very vulnerable in human body due to various

enzymes degrading gene and has negative charge making it hard to interact with cell membrane due to the repulsive force [2-7]. These features limit the delivery of gene by itself. To treat diseases with gene therapy, development and application of potent gene delivery systems become essential to protect and deliver gene. As a consequence, many groups have researched and developed various gene delivery systems for decades [8,9].

When it comes to gene delivery systems, there are two systems with large classification. One is viral vector such as adenovirus and lentivirus. The other is non-viral vector like polymers, lipids, and so on. Viral vectors usually have high delivery efficiency because viral gene delivery systems use their original infection mechanism; however, some drawbacks such as chance of immunogenicity, carcinogenicity, and limit of cargo size. In terms of immunogenicity, it limits repetitive usage of viral vectors when immune systems were activated; the immune system would neutralize gene delivery carriers. As the alternatives to viral gene carriers, non-viral vectors have been developed. They are considered safer than viral vectors and can be modified to confer additional functions on demand because of their low immunogenicity and various composition. In addition, they do not have limit of cargo size unlike viral vectors. However, cytotoxicity and low efficiency are major

drawbacks especially in the case of polymeric gene vectors. To achieve successful gene therapy, addressing cytotoxicity and efficiency is main challenge in the field of non-viral gene delivery system development [10].

Nucleotides such as pDNA and siRNA have negative charge because they consist of phosphoester bonds [11]. When it comes to non-viral vectors, many of them have positive charge to exploit negative charge of the cargo. Cationic polymers are mainly studied due to their positive charge, ease of production and modification to adjust the properties [12]. In the case of polyethylenimine with molecular weight of 25,000 Da (PEI25k) which is considered as golden standard of non-viral gene vector, it is also cationic polymer [7,13]. Many studies developing polymeric gene delivery systems have used PEI25k as a positive control [14-19]. Positive charge on PEI makes it easy to encapsulate gene by interacting negatively charged nucleotides electrostatically; however, PEI also has drawbacks as other cationic polymers do. High molecular weight and positive charge also make it toxic limiting their usage although it is golden standard [21,21]. Usually, high molecular weight and positive charge density make more severe cytotoxicity; it is limiting their application to gene delivery [22,23].

Therefore, many works studied about the polymeric gene delivery

carriers with biodegradability to overcome the dilemma [24,25]. In the meanwhile, the biodegradable polymer also can be synthesized by crosslinking non-toxic low molecular weight compounds with biodegradable linkages. These biodegradable polymers are expected to exhibit high transfection efficiency and low cytotoxicity because of their enhanced gene condensation during systemic circulation and degradation of high molecular weight polymer to low molecular weight molecules [26-28].

Especially, bioreducible crosslinkers have been utilized to synthesize bioreducible polymeric gene carriers; bioreducible polymer is a kind of biodegradable polymer. Bioreducible polymeric gene carriers which possess internal disulfide bonds have many advantages for gene delivery systems including selective degradability and facilitated release of condensed genes from polyplexes in reducing environment [29-31] such as cytoplasm containing high concentration of glutathione (0.5-10 mM) [32]. They also have been known for possessing low cytotoxicity [33-36]. That's because the reducing condition-triggered degradation of polymer in cytoplasm prevents intracellular accumulation of polymers and excessive interaction of cationic molecules with cell membrane or cellular organelles. As a result, introducing bioreducible part in polymer have been considered as a strategy

that achieves high delivery efficiency and low cytotoxicity relative to their counterparts which is non-bioreducible.

In the meanwhile, there are other strategies dealing with the drawbacks such as PEGylation [37,38], targeting moieties [39-41]. In other words, additional modifications conferring new functions when it compares with original polymer have been applied to modulate the property and behavior of polymers. These modifications can also be combined with bioreducible polymers [42-44].

Most of the studies on bioreducible gene vectors mainly have been dealt with transfection efficiency and cytotoxicity. There are relatively few studies dealing with behavior of gene vectors, so structure-activity relationships of bioreducible gene carriers as well as basic parameters on efficient and cytotoxicity were investigated in this dissertation.

In the first part of this study, crosslinked polymers composed of PPI (polypropylenimine) and CBA (cystamine bisacrylamide) were investigated. Generation 1 PPI (PPI G1) was not used for gene delivery due to their low transfection efficiency [45]. PPIs with higher generation were usually used as PAMAM dendrimer G4 and G5 were mainly used. However, in this study, PPI G1 was used to take advantage of its low cytotoxicity derived from its low

generation [46]. Crosslinked PPI G1 dendrimers with bioreducible linkages (PPI-CBA) have not been reported for gene delivery systems so far. Therefore, high molecular weight polymers (PPI-CBAs) were synthesized by crosslinking low molecular weight PPI dendrimers with bioreducible linker, CBA, to utilize the advantages of PPI dendrimers, accomplishing high transfection efficiency and maintaining low cytotoxicity in this work. The physicochemical properties of the polymers were characterized and their potency for gene delivery systems were evaluated. In addition, interesting results about the structure-derived degradation behaviors and cytotoxicity profile of PPI-CBAs were observed, and they were further studied.

In the second part of this study, linear bioreducible polymers were synthesized by using Michael addition reaction. An amino acid, arginine, and fluoroalkyl chain (fluorination) were used to improve the efficiency of gene delivery system. As the combination of bioreducible polymer with arginine modification and fluorination was not investigated so far, the effect of combination was investigated in this study. Both arginine modification and fluorination are related with enhancing cellular uptake resulting in improved gene delivery efficiency. Although arginine modification is not a new strategy, fluorination is emerging strategy; fluorination still should be further

investigated to reveal the role in gene delivery procedure more specifically. Most of the studies reported only tested the efficiency of fluorinated polymer for gene vector. This study tries to contain not only general analysis such physicochemical property experiment and efficiency test but also analysis dealing with the effect of the combination.

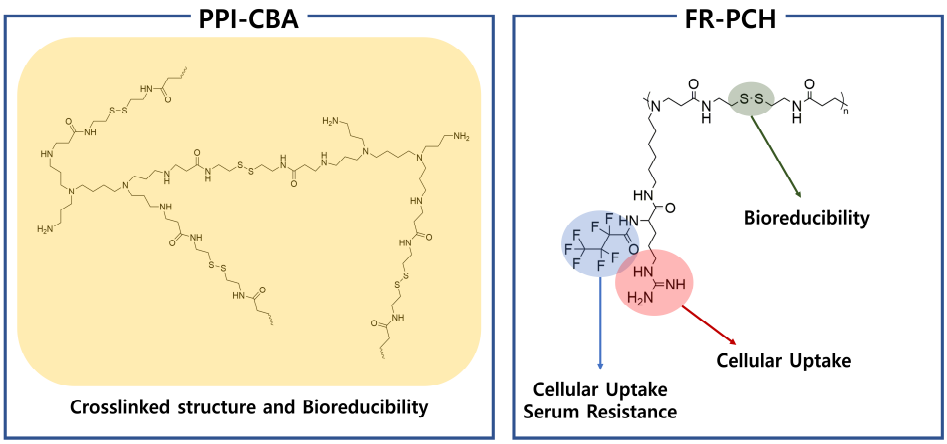

Scheme 1. Schematic explanation of the themes in the dissertation. The effect of crosslinked structure was investigated in PPI-CBA. The effect of fluorination on arginine functionalized bioreducible polymer was investigated in FR-PCH.

Chapter 2. Literature Survey

2.1. Gene Delivery Systems using Bioreducibility

2.1.1. Barriers of Gene Delivery and Reductive Environment of Cell

As mentioned above, gene delivery systems based on non-viral vector usually show lower delivery efficiency than viral vectors. Viral vectors have their own transfection mechanism. That's why they have high efficiency. On the other hand, non-viral vectors don't have their own; it makes them have relatively low efficiency. In other words, non-viral vectors cannot easily circumvent various barriers of gene delivery. With large classification, there are two kinds of barriers; extracellular barriers and intracellular barriers.

From the start of gene delivery to the site of action, all steps act as barriers [47]. When the vectors are injected into vein, components of blood such as nucleases and proteins will interact resulting the failure of delivery. The interaction of blood components also facilitates immune systems to remove the vectors. During blood circulation, vectors can be excreted through glomerular filtration. Even though vectors overcome the extracellular barriers, passing through cell membrane is a barrier. When they cross cell membrane, they must evacuate from endo-

lysosomal process before they are degraded. Then, cargo releasing, additional intracellular trafficking for gene expression, and subsequent every step is act as barriers.

Regarding these barriers, concentration gradient of reducing agent between cytosol and extracellular environment can be exploited as a gene delivery strategy. Reactive oxygen species such as peroxides, superoxides, hydroxyl radicals, and singlet oxygens are inevitable byproducts of metabolism. Although they are originated naturally and participate in various metabolism pathway, excessive concentration makes cells die by damaging genes and organelles. Therefore, to control the concentration at adequate level, several kinds of reducing agent exist inside the cell with very high level of concentration. Especially, glutathione (GSH), most abundant reducing agent, also presents at high concentration (0.5 – 10 mM). It also presents outside the cell, but the concentration is very low (micro molarity levels) when it compares to intracellular concentration [32].

2.1.2. Bioreducible Polymers for Gene Delivery Systems

Bioreducible polymers are exploiting the concentration gradient of reducing agent mentioned above to achieve higher gene delivery efficiency and lower cytotoxicity. Many studies already have

reported that higher molecular weight is favorable for successful delivery; on the other hand, it has been reported that high molecular weight usually causes more cytotoxicity [22,23]. In other words, high performance makes subsequent high risks.

Achieving high efficiency without side effects is first goal in the field of gene delivery systems. To circumvent the dilemma, biodegradable polymers have been researched for decades [24,25]. They usually composed of the linkages such as ketals [48,49], imines [50,51], ester bond [52-54], disulfide bond [55-57], and so on. They can be degraded spontaneously by the components of environment in vivo; however, most of them are degraded non-specifically because the degradation is usually progressed by hydrolysis.

On the contrary, in the case of disulfide bond, it is degraded by reducing agents. This characteristic makes it special in comparison with other biodegradable bonds. As mentioned above, extracellular environment contains much lower concentration of reducing agent, whilst intracellular environment is reducing environment. Due to it, polymers with reducible linkages such as disulfide bond can be degraded more specifically in the intracellular region. It confers bioreducible polymers spatiotemporal release ability of cargo making them more attractive than other biodegradable polymers.

They usually composed of bioreducible linkers such as dithiobis(succinimidylpropionate) (DSP), dimethyl,3,3′ −dithiobispropionimidate · 2HCl (DTBP), and N, N ’ −cystamine bisacrylamide (CBA); it fits best for the purpose of introducing bioreducibility. To make reducible polymer degrading into small pieces, disulfide bonds should be located on the backbone; disintegration of the disulfide bond causes instant decrease of molecular weight.

For decades, many researchers have been reported their studies about gene delivery systems using bioreducible polymers. Gosselin et al. used low molecular weight PEI by crosslinking with DSP or DTBP [58]. In this study, the polymers showed comparable transfection efficiency to the efficiency of PEI25k although they did not show superior performance. By analyzing the samples having different crosslinking degree, it was found that the transfection efficiency was directly related to the degree of crosslinking; more crosslinking made better performance as a vector. As predicted, all polymers synthesized in the study showed much lower cytotoxicity than PEI25k at all concentration range.

Sun et al. also studied crosslinked polymer composed of low molecular weight PEI (800 Da) [59]. In this case, CBA was used as bioreducible crosslinker. The polymer showed high transfection and

low cytotoxicity. Especially in terms of transfection efficiency, they showed superior efficiency to PEI25k although their weight ratios are higher than the weight ratio (1.3) of PEI25k; 5, 10, 15, 20, 25, and 30, respectively.

Liu et al. used DSP as crosslinker for clustering PAMAM dendrimers [60]. By crosslinking low generation (generation 2, G2) PAMAM (polyamidoamine) with bioreducible crosslinker, they synthesized the polymers showing comparable performances to PEI25k and showed superior efficiency than generation 5 (G5) PAMAM dendrimer. On the other hand, pristine G2 PAMAM just made negligible performance when it compares to the efficiency of crosslinked G2 PAMAM dendrimers. Of course, cytotoxicity of the polymers was investigated. All of them showed marginal cytotoxicity, which was almost same cytotoxicity level of G2 PAMAM.

Li et al. investigated the effect of bioreducible disulfide bond by introducing a compound which did not contain disulfide bond [61]. They used three types of crosslinkers to clustering low generation of peptide dendrimers. Two of them are synthesized in the study, which contained epoxide group for crosslinking. To investigate effect of disulfide bond on gene delivery, one of two had tertiary amine instead of disulfide bond. Third one was CBA to compare

epoxide and acrylate group. Cytotoxicity did not show significant difference among them although all of them were superior to PEI25k. In contrast, transfection efficiency of the polymers significantly different. Polymer consisted of CBA showed apparently higher efficiency than other polymers including PEI25k. It was also found that similar result was come out when they were treated under serum containing condition. In addition, they reported that hydroxyl group improved serum stability of vector despite the efficiency was not as effective as the polymer containing CBA.

Nam et al. synthesized bioreducible polymer, poly(cystaminebis(acrylamide)-diamonohexane) (poly(CBA-DAH)), which have linear structure [62]. In turn, they conjugated PEI (1,800 Da) to poly(CBA-DAH) (PCDP) through disulfide bond formation. As a result of conjugating PEI, PCDP showed higher efficiency than PEI25k and Lipofectamine 2000 even at very low weight ratio. In the meanwhile, PCDP showed negligible cytotoxicity due to their bioreducible property. Disulfide bonds and amide bonds contained in PCDP can be degraded in cells, so it was thought that the polymers disintegrated into non-toxic small molecules.

Guo et al. reported that hyperbranched poly(amido amine) (PAA) composed of 1-(2-aminoethyl)piperazine and CBA [63]. The PAAs were conjugated with RGD peptide which is tumor-specific

tissue penetration peptide via amidation reaction to enhance cellular uptake efficiency. In the study, the polymers were investigated by conducting *in vitro* and *in vivo* experiments. From the results, they displayed higher gene silencing ability and lower cytotoxicity. In addition, they successfully inhibited lung tumor growth by efficiently delivering siRNA inhibiting EGFR (epidermal growth factor receptor) *in vivo* experiment.

Wang et al. made cationic polymer containing disulfide bonds in the backbone and imidazole side groups [64]. It is a kind of linear bioreducible polymer which is consisted of bioreducible crosslinker CBA. In addition to disulfide bonds in the backbone, the polymers have adamantine groups and β-cyclodextrins. Adamantine group and β-cyclodextrin confer crosslinking ability the polymers via host-guest interaction between them. Due to the crosslinking and bioreducible linkages, they exhibited excellent polyplex stability and superior transfection efficiency to Lipofectamine 2000 which is commercially used transfection agent. Moreover, while Lipofectamine 2000 showed high cytotoxicity continuously, the polymers examined in this study did not display any cytotoxicity indicating their good biocompatibility.

Xu et al. developed a nanoparticle platform delivering siRNA comprised of poly(disulfide amide)s, cationic lipid, and lipid-PEG

[65]. Poly(disulfide amide) (PDSA) was synthesized by reacting L-cystine dimethyl ester and fatty diacid with various chain length. The platform has two sections. One is core which is composed of siRNAs, PDSAs and cationic lipids. The other is shell formed with lipid-PEG. The platform demonstrated long blood circulation and high tumor accumulation. Moreover, it showed GSH-responsive cargo release and subsequent effective gene silencing with low cytotoxicity. It indicated the platform takes advantages of lipid and bioreducible polymer well.

Ullah et al. reported a bioreducible cationic polymer called PEG-*b*-poly(disulfide-L-lysine) (PEG-SSL) [66]. It was synthesized with PEG with four acrylate arm and poly-L-lysine containing disulfide bond via Michael addition reaction. In the study, PEG-SSL displayed better biocompatibility and transfection efficiency in comparison with PEI25k used as control polymer. In the study, confocal scanning laser microscopy revealed that PEG-SSL exhibited good cellular uptake and nuclear co-localization rate implying gene delivery efficiency.

Peng et al. reported the study on hyperbranched galactose-based glycopolymers crosslinked with disulfide-containing N,N'-bis(methacryloyl)cystamine (BMAC) [67]. Reversible addition-fragmentation chain transfer (RAFT) polymerization was used in

this study to produce the polymers. In the study, it was told that disulfide bond was adopted to enhance efficiency of gene delivery and improve biocompatibility. As intended, the polymers synthesized in the study displayed low cytotoxicity and excellent gene silencing efficacy indicating the efficiency of siRNA delivery.

Rui et al. synthesized bioreducible branched polymers and tested as gene delivery carriers for CRISPR/Cas9 genome editing [68]. In the study, ester-amine quadpolymers were synthesized through three kinds of crosslinkers. The crosslinkers with different structure confer capability of modulating branching, reducibility, and hydrophobicity. This property made them complex simultaneously with DNA and RNA with more efficiency. As a result, the polymers showed high gene delivery efficiency at low weight ratio with low cytotoxicity. Moreover, due to the efficient co-delivery of DNA and RNA successfully induced CRISPR/Cas9-induced gene knockdown.

On the other hand, clustering low molecular weight moieties with crosslinkers is not the only strategy of making bioreducible polymer. Kang et al. modified low molecular weight PEI (800 Da) with 2-iminothiolane [69]. The modification with 2-iminothiolane converted the primary amines of PEI into thiol groups. Thiol groups can form disulfide bond through oxidation; in this study, DMSO was used as oxidant. The synthesized polymer showed comparable

transfection efficiency to PEI25k while they displayed low cytotoxicity.

Taranejoo et al. studied about grafting PEI (2,500 Da) on glycol chitosan (GCS-ss-PEI) via disulfide bond to use as gene vector [70]. GCS-ss-PEI was examined to evaluate the potential as gene delivery carrier. They showed much lower cytotoxicity than PEI25k. In addition, they showed higher level of GFP expression in the case of transfection assay.

Du et al. developed dendrimersome gene delivery carriers consisted of amphiphilic Janus dendrimers bearing disulfide bond [71]. Janus dendrimer consists of hydrophilic head with three amino groups and hydrophobic tail with two fatty acid; these two parts are connected with disulfide bond. As a result, the dendrimers can be self-assembled into dendrimersomes, but they can be disintegrated in reducing condition such as intracellular region releasing cargo due to the cleavage of disulfide bond. In the study, the dendrimersomes demonstrated most efficient down-regulation of target gene without any cytotoxicity during gene silencing.

Regardless of the methods constructing polymers, bioreducible polymers displayed negligible or relatively low cytotoxicity. Even the cytotoxicity was low, the polymers showed high gene delivery efficiency; many studies reported that the polymer showing

superior efficiency to commercial transfection reagents. The studies have shown the distinction of bioreducible polymers for gene delivery.

2.2. Gene Delivery Systems using Arginine

2.2.1. Role of Arginine in Gene Delivery

Utilization of arginine was originated from discovery of cell penetrating peptides (CPPs). CPPs are defined as short peptides which consist of 5-30 amino acids facilitating introduction of molecules. In other words, they are protein transduction domains which traverse biological membranes. The first discovered CPP was TAT (transactivating transcriptional activator) derived from HIV-1 (human immunodeficiency virus 1); it was found by two groups independently in 1988 [72,73]. After the first discovery, many CPPs are subsequently reported and investigated by numerous research groups. Due to extensive research on CPP, it was found that many CPPs contained arginine as main component. Based on that, artificial CPPs are made and examined cell penetrating behaviors suggesting arginine is essential component for cell penetration [74].

Further researches found that guanidine group on arginine played important role in cellular uptake of CPPs. The guanidine group on

arginine is known that it interacts with phosphate, sulfate, and carboxylate by forming bidentate complexes. When it comes to cellular uptake, it is known that the complex forming behaviors facilitates cellular uptake due to plenty of phosphates, sulfates, and carboxylates displayed on cell surface. In a paper, it was reported that congestion of guanidine-containing molecules induced by bidentate complex formation triggers macropinocytosis [75]. Besides, polyarginine motif is considered as nuclear localization sequence (NLS). NLS containing molecules are considered that they can be transported to nucleus of cell; it improves gene delivery efficiency although it is not fully investigated [76].

In the meanwhile, arginine has usually been compared with lysine because of their positive charge. Arginine and lysine are both basic amino acids with very high value of pK_a (about 12.5 and 10.5, respectively) [77,78]. The high pKa makes them enable to possess positive charge in most physiological condition. Due to the positive charge, both amino acids frequently used as a component of gene delivery carrier as shown in next section. However, in most cases, arginine usually showed superior result to lysine. Many researchers have tried to find out what makes them different.

When it comes to DNA compaction, it was concluded that arginine is superior to lysine [79]. Arginine showed stronger attraction and

weaker short-range repulsion than lysine. In addition, it was reported that arginine can form salt bridges by interacting with phosphate group of DNAs [80,81]. The bridges consist of bidentate complex or monodentate complex with additional electrostatic interaction caused by positive charge of arginine and negative charge of DNA. Although lysine can also form salt bridges, the number of them was smaller than that of arginine; guanidine group in arginine makes the differences [82-88]. In addition, the ionic interaction also stronger than lysine due to its higher pK_a [89]. Furthermore, although it was report about simulation, the interaction of arginine and lysine with lipid membrane was investigated [90]. The result revealed that arginine attracted more phosphates and water molecules in the membrane resulting in the stabilization of arginine-phosphate clusters. These phenomena make arginine effective in interfacial binding and membrane perturbation. Also, it was found that arginine maintained their positive charge even in the membrane unlike lysine.

2.2.2. Arginine Conjugated Polymers for Gene Delivery Systems

Although it was hard to expect that arginine introduced to gene vectors plays the same role, studies on arginine containing gene delivery vectors were reported. The studies have reported that

introduction of arginine to gene carriers improved efficiency of gene delivery.

Nam et al. investigated about the effect of arginine grafting. They synthesized PAMAM ester and grafted arginine and lysine respectively [91]. Also, they grafted arginine and lysine to PAMAM to examine the effect of ester bond; the ester bond can be degraded by hydrolysis making molecular weight low. As a result, arginine grafted PAMAM ester showed lower cytotoxicity while arginine grafted PAMAM showed relatively higher cytotoxicity. In terms of transfection efficiency, arginine grafted PAMAM ester was most effective among the polymers. Interestingly, arginine grafted PAMAM ester had superior transfection efficiency than PEI25k. The study showed arginine grafting can improve the efficiency of vector.

Kim et al. studied linear bioreducible polymer grafted with arginine [92]. They investigated physicochemical properties of the polymer and test it as potential gene vector. Through a series of experiments, they found that arginine grafting improved serum tolerance and transfection efficiency when it compared to PEI25k and the polymer without arginine grafting.

Ahn et al. synthesized guanidinylated dendritic polymer with PEI2k (2,000 Da), poly(amido amine) (PAMAM), and arginine

(PPR) [93]. In the study, researchers described that arginine decorating periphery of the polymers was introduced to improve the efficiency of gene vectors. Through the results from the paper, it was found that arginine conjugation increased gene delivery efficiency even in comparison with PEI25k. In addition, PPR showed lower cytotoxicity than PEI25k.

Peng et al. examined hyperbranched lysine-arginine copolymers for gene delivery carriers [94]. They used the reactivity of amine groups and carboxyl groups of L-lysine and L-arginine to polymerize them via thermal polymerization. In terms of transfection efficiency, it was found that the efficiency of polymer with only lysine was poor showing similar transfection efficiency with the efficiency of naked DNA delivery. In contrast, lysine-arginine copolymers displayed much enhanced efficiency although it was not superior to the efficiency of PEI25k; they just showed comparable efficiency. The study demonstrated that the presence of arginine enhances transfection efficiency.

Wang et al. conducted extensive research by conjugating 20 naturally occurring amino acids to PAMAM G5 dendrimers [95]. Through the modifications, they investigated the structure-activity relationship of amino acids in gene delivery. It was noteworthy that arginine conjugated dendrimers showed the highest transfection

efficiency and cellular uptake of polyplexes. The researchers concluded that arginine modifications are beneficial for DNA binding, polyplex formation, and efficient cellular uptake.

Yu et al. reported linear bioreducible polymer; however, in this study, arginine participated in polymer backbone formation through Michael addition reaction (Arg-CBA) [96]. Agmatine which is like arginine was also used (Agm-CBA); Both have guanidine group. The synthesized polymers were compared with PEI25k and Lipofectamine 2000, a commercial gene delivery reagent. When terms of cytotoxicity, Arg-CBA and Agm-CBA showed lower cytotoxicity than PEI25k and Lipofectamine 2000. Especially, Arg-CBA showed superior biocompatibility among them while biocompatibility of Agm-CBA did not show significant difference. Subsequent experiments revealed that Arg-CBA was more efficient for delivering gene displaying faster and higher cellular uptake than Agm-CBA, PEI25k, and Lipofectamine 2000. The only difference between Arg-CBA and Agm-CBA was carboxyl group, so they presumed that carboxyl group had certain role in gene delivery. However, they cannot figure out what made difference between Arg-CBA and Agm-CBA.

Li et al. modified poy(ω-aminohexyl methacrylamide)s (PAHMAA) with arginine and histidine [97]. By adjusting the ratio

of arginine to histidine, they investigated the effect of the modification such as proton buffering capacity, pDNA binding affinity, and transfection efficiency, and so on. From the results, arginine modification improved gene delivery efficiency in comparison with the efficiency of solely histidine modified polymers; histidine modified polymers showed the efficiency similar with the efficiency of naked DNA. Interestingly, certain modification ratios of arginine to histidine made the polymer much more efficient. By summarizing the results, the researchers concluded that PAHMAA-R_{18}-H_6 which have 18 arginine and 6 histidine is the most promising gene delivery vector because they exhibited low cytotoxicity, excellent transfection efficiency, and good serum compatibility derived from arginine and histidine modification.

Dhanya et al. reported interesting gene delivery system [98]. They synthesized starch-PEI containing gold nanoparticle. PEI acted as reducing agent for gold ions, and starch acted as stabilizer. Owing to gold nanoparticle formation, polymers showed alleviated cytotoxicity; however, transfection efficiency was compromised. To compensate it. the researchers modified the polymer with arginine or histidine. The results indicated that arginine-modified, gold nanoparticle containing polymers demonstrated the highest cellular uptake and transfection efficiency.

Zavradashvili et al. tried to screen novel cationic polymers as gene delivery agents [99]. They used spermine (endogenous tetraamine), N-(2-aminoethyl)-1,3-propanediamine (synthetic triamine), and arginine to make a library of cationic polymers, which was composed of 12 polymers. Through the screening, it was found that arginine-containing polymers had much more efficient than the efficiency of the polymers without arginine. The arginine-containing polymers also showed superior efficiency than commercial transfection reagents; DharmaFECT and Lipofectamine, respectively. It implied the effect of arginine on gene delivery efficiency; arginine conjugation usually improved transfection efficiency.

Lu et al. synthesized PEGylated L-arginine-modified oligo(-alkylaminosiloxanes) ($P(SiDAAr)_5PEG_3$) [100]. The backbone of polymer was consisted of oligo(-alkylaminosiloxane). Then, arginine, PEI, and PEG were conjugated to the oligo(-alkylaminosiloxane). The polymers were used as gene delivery carriers. In the study, antiluciferase siRNA inhibiting luciferase expression and anti-ABCB1 siRNA preventing efflux membrane protein from expression. The polymers showed excellent stability in the presence of excess polyanions and successfully protected the siRNA from the degradation with RNase. Without cytotoxicity, the

polymers showed almost complete knockdown of luciferase expression. In the case of anti-ABCB1 siRNA delivery, the siRNA acted as inhibitor of doxorubicin (DOX) resistance. The delivery of siRNA increased cellular uptake of DOX and enhanced cytotoxic effect of DOX in the cancer cells.

In the meanwhile, there are studies introducing guanidine group directly. Because the active part of arginine is guanidine group, researchers also have tried to make guanidinylated polymers instead of introducing arginine.

Choi et al. reported guanidinylated bock copolymers [101]. They tested efficacy of guanidinylated polymers (Guan polymer) by comparing with analogous non-guanidinylated polymer (Base polymer). As a result of guanidinylation, Guan polymers showed higher efficiency than Base polymers when they were treated to immortalized cell lines although Guan polymers displayed more cytotoxicity. However, interestingly, when they were treated to neural progenitor cells, it was found that Base polymers are more efficient. Through further experiments, the researchers concluded that the reason was the difference in susceptibility to anionic proteoglycans. Polyplex unpackaging experiment in the presence of heparin or heparan sulfate showed that Guan polymers were more susceptible than Base polymers. In the study, like arginine

conjugation, it was revealed that guanidinylation can enhance gene delivery efficiency; however, it is also revealed that guanidinylation is not always effective strategy.

Chang et al. reported the study about guanidinobenzoic acid (GBA) functionalized PAMAM G5 dendrimers [102]. Guanidinobenzoic acid has guanidine group and benzene ring in a single compound. The researchers thought that this compound could overcome steric hindrance issue in the case of conjugating various moieties on a polymer. In this study, they compared the efficiency of GBA modified polymers with benzoic acid (BA) and guanidine (GA) modified polymers respectively. In terms of gene silencing efficiency and transfection efficiency, GBA modified polymers showed superior performance in comparison with BA and GA only modified polymers suggesting the synergy of guanidine and phenyl group. In the meanwhile, when comparing the efficiency of BA only modified polymers and GA only modified polymers, GA only modified polymers more potent performance in comparison with BA only modified polymers implying the effect of guanidine modification.

Hibbitts et al. reported guanidine-containing polymers [103]. They tried to mimic the structure of oligoarginine by polymerizing PEG-based, arginine-containing polymers. It is called peptidomimetics, which is synthetic analogue mimicking the

structure and/or function of original peptide; it is not consisted of solely α-amino acids. In this study, tert-butyl N-(2-oxiranylmethyl)carbamate was used to make the backbone of the polymers. Then, primary amines of the polymer were converted into guanidine groups. This mimic was tested and evaluated with a series of experiments. As a gene delivery vector, they tested the efficiency of gene delivery. The polymers showed excellent performance by inhibiting gene expression with no cytotoxicity.

From the studies described above, it is found that arginine modification can improve the efficiency of gene delivery. Although the magnitude of enhancement was not regular, the effect of arginine has confirmed in many studies as shown.

2.3. Gene Delivery Systems using Fluorination

2.3.1. Properties of Fluoropolymers

With respect to fluoropolymers, it is easy to come up with PTFE (polytetrafluoroethylene) and its derivatives such as PCTFE (polychlorotrifluoroethylene), PVF (poly(vinyl fluoride)), PVDF (poly(vinylidene fluoride)). Like PTFE, fluoropolymers mean the polymer containing fluorine atoms. In other words, when some hydrogens attached to hydrocarbon are substituted with fluorine, they are named as fluoropolymers.

Fluoropolymers usually have extraordinary extreme physical and chemical properties favorable for various industrial applications. They have affected profoundly since their discovery in the 1930s. Most of the properties are derived from the characteristic of fluorine atoms and C−F bonds. Fluorine is the most electronegative atom (3.98). When they substitute hydrogen, C−F bond forms more dipole moment dipole (1.41 D) than C−H bond (0.40 D). In addition, fluorine has lower polarization tendency due to the high value of dipole moment derived from the electronegativity of fluorine, and C−F bond is the strongest single bond ever known. The strong bond makes fluoropolymers extremely stable. From these properties, fluoropolymers usually show excellent chemical/thermal stability, extremely low surface tension causing simultaneous hydro/lipophobicity, and high fluidity, low dielectric constant, and gas−dissolving capacity. As mentioned above, these properties make them special in various fields of industry [104,105].

2.3.2. Fluorine modification (Fluorination) in pharmaceuticals

In the field of pharmaceuticals, fluorination with fluorine and fluoroalkyl chains is also extensively adopted to develop new pharmaceuticals with high efficacy. Although it is not the form of polymer, it is found that substitution of atoms with fluorine or

fluoroalkyl chains can modulate various parameters pharmaceuticals by increasing potency, half-life, bioavailability, and so on. Strong electronegativity and other properties of fluorine can be used for modification of acidity and adjusting lipophilicity as they adjust the properties of fluoropolymers. Due to the merits of fluorinated drugs, the portion of them have been increasing; fluorination and screening of drugs have become a promising strategy of pharmaceuticals development; it is called fluorine scan [106-108].

In 1955, fludrocortisone was approved as the first fluorine containing medicine [109]. After that, fluorinated bioactive molecule have occupied important portion in pharmaceutical industry [110].

2.3.3. Fluorinated Polymers for Gene Delivery Systems

Recently, the similar attempts have been tried to examine the effect of fluorination on polymers. Researchers thought that some properties of fluorine containing drugs such as improved membrane permeability and elongated half-life *in vivo* can also be introduced if fluorination was adopted to gene delivery vectors. Although there are many differences between small molecules and polymers, they have researched various fluorinated polymers as candidates for gene delivery vectors.

Xiong et al. adopted fluoropolymer for gene delivery carrier [111].

They synthesized fluorine containing amphiphilic copolymers. Due to the simultaneous hydro/lipophobicity of fluoropolymer, they described that fluorine containing amphiphilic polymers usually displayed lower CMC (critical micelle concentration). Lower CMC means that the polymer can make more stable micelle than other polymers. Although they did not study gene delivery efficiency, they confirmed that they had synthesized the polymer suitable for gene delivery displaying low CMC, low cytotoxicity, and DNA complexing ability.

In 2014, Wang et al. published a paper on fluorinated dendrimer [112]. In the study, G5 PAMAM was grafted by heptafluorobutyric anhydride (HFBA) with various feed ratio. Although they displayed limited range of cytotoxicity, the polymers showed low cytotoxicity in that range. By using reporter genes encoding luciferase and green fluorescence protein respectively, the polymers showed superior transfection efficiency than any other controls including G5 PAMAM, PEI25k, and Lipofectamine 2000. Even though they were treated in the presence of serum (0, 10, 30, 50 % FBS), they still made superior performance.

Wang et al. published a subsequent study about fluorination [113]. In this study, they conjugated a series of fluorobenzoic acids (FBA) to G5 PAMAM dendrimers to figure out the effect of fluorination.

Furthermore, the effect of the number of fluorine atoms and the location of fluorine atoms on conjugated benzene ring were also investigated. The results revealed that the number of fluorine atoms and the location of atoms on the ring played important roles for efficient transfection. In addition, FBA-modified dendrimers showed much higher transfection efficiency than unmodified dendrimers. In the case of G5-4FBA$_{36}$ which modified with 36 FBA with 4 fluorine atoms on the ring, the transfection efficiency was superior to SuperFect and PolyFect and comparable to Lipofectamine 2000 with low cytotoxicity. It was found that cellular uptake, endosomal escape, and intracellular DNA release were efficient. From these results, it can be concluded that modification with fluoroaromatic compounds increases the efficacy of gene delivery dramatically.

Liu et al. synthesized fluorinated poly(propylenimine) (PPI) with heptafluorobutyric anhydride. G3, G4, G5 PPI dendrimers were used in the study [114]. From the results, it was found that the efficiency of gene delivery increased along with the generation of dendrimer. G5 fluorinated PPI showed the lowest value of optimal NP ratio for gene transfection although all the polymers efficiently delivered gene at very low NP ratios. Furthermore, gene delivery efficiency of the polymers was significantly improved, it was

superior to commercial transfection reagents like Lipofectamine 2000, JetPEI, SuperFect, and PolyFect.

Wang et al. published a paper dealing with self-assembled fluorodendrimers [115]. By modifying PAMAM dendrimers with heptafluorobutyric anhydride, they said fluorodendrimers had the features of lipid such as self-assembly and cell membrane affinity. From the results of experiments, it was found that self-assembled fluorodendrimers showed high transfection efficiency *in vitro* and *in vivo*, high permeability in 3D spheroids, minimal toxicity, and high stability in the presence of serum.

Lv et al. modified PEI25k with fluoroalkyl chains via oxirane or anhydride reaction [116]. The synthesized polymers showed much higher efficiency than unmodified PEI25k. Furthermore, they demonstrated comparable of superior efficiency of gene delivery to several transfection reagents such as SuperFect, PolyFect, JetPEI, and Lipofectamine 2000 even at low very low NP ratios. Especially, fluorinated PEI25k still efficiently transfected cells in 3D spheroid culture. The results suggested that fluorination enhanced the gene delivery efficiency of PEI even on spheroid cell cultures.

He et al. reported gene delivery carriers with minimal fluorination [117]. In the study, for the first time, they introduced CBT (2-chlor-4,6-bis[(perfluorohexyl)propyloxy]-1,3,5-triazine) as

fluorination reagent. The double-tailed fluorous compound, CBT, was conjugated to G1, G2, G5 PAMAM dendrimers and PEI1.8k with minimal modification degree; all the values of the modification were located between 1 and 2. Regardless of low modification degree, all the modified polymers displayed significantly improved gene delivery efficiency in comparison with their unmodified counterparts. Especially, several polymers showed comparable or superior transfection efficiency to Lipofectamine 2000. The study suggested that minimal fluorination also enhanced gene delivery efficiency although it was dependent on fluorination reagent.

Johnson et al. synthesized fluorocarbon-modified PEI (600 Da, FCPEI) and compared with hydrocarbon analogue [118]. In the study, although they did not compare the efficiency of FCPEI with other standards such as PEI25k, Lipofectamine 200, and JetPEI, gene delivery efficiency was superior to hydrocarbon analogue. Other parameters of FCPEI such as cellular uptake and serum resistance were also significantly improved in comparison with hydrocarbon-modified PEI.

Wang et al. studied about structure-activity relationships of fluorinated dendrimers [119]. G4~7 PAMAM dendrimers with various fluorination degrees were used for investigating structure-activity relationships. From the results, it was found that at least

50% of primary amines on dendrimers should be converted into fluoroalkyl chains to achieve efficient DNA and siRNA delivery. Interestingly, fluorinated G5 PAMAM showed the highest efficiency among the synthesized dendrimers although the reason was not clear.

Wang et al. applied fluorinated dendrimer to cancer treatment [120]. In the study, G4 PAMAM was modified with heptafluorobutyric anhydride. For cancer treatment, tumor necrosis factor-related apoptosis-inducing ligand (TRAIL) gene was adopted. The fluorinated PAMAM dendrimer exhibited superior gene delivery efficiency than commercial reagent such as PEI, SuperFect, and Lipofectamine 2000 resulting in much higher apoptosis of TRAIL transfected cells. Furthermore, the polymer destroyed three-dimensional cell culture efficiently *in vitro* and suppressed tumor growth *in vivo* successfully. These results indicated the potential of fluorination which increased the efficiency of gene delivery dramatically.

Wang et al. synthesized low molecular weight fluorodendrimers to deliver fluorinated drugs and TRAIL gene simultaneously [121]. Via fluorine-fluorine interaction, fluorinated drugs can be loaded in fluorodendrimers. Due to this property, fluorodendrimer can be adopted as a co-delivery carrier. In this study, G2 PAMAM

dendrimer modified with heptafluorobutyric anhydride used with self-assembled carrier. The polymer showed high gene delivery efficiency and high drug loading efficiency. When they were used as co-delivery carriers, they showed synergistic effect suggesting the potential as versatile co-delivery systems.

In the meanwhile, Xiao et al. synthesized crosslinking structured polymers incorporating fluorine into backbone of the polymers and investigated cellular uptake pathway of the polymers [122]. In other words, they synthesized fluorine containing crosslinkers and tested by constructing polymers. The crosslinkers contained various length of CF_2 chain in the middle of them and had two epoxide functional group at the both ends. In the study, low molecular weight PEI (600 Da) was used for component of the polymer. Synthesized polymers showed lower cytotoxicity in most of the cases. In terms of transfection, polymer synthesized with crosslinker containing high number of fluorine displayed lower efficiency than PEI25k; other polymers made superior performance to PEI25k in most cases. It was thought that strong interaction between the polymer and DNA may prevent the release from the polyplex ending up with low transfection efficiency. Interestingly, when it comes to cellular uptake, the uptake was increased along with the increase of serum concentration in some range, but they

did not discuss that. Through the endocytosis mechanism experiment, they found that the polymers mainly entered cells by using macropinocytosis and microtubule mediated endocytosis.

Tan et al. tested how distribution of fluorous chains affected gene delivery [123]. Via RAFT polymerization, DMAEMA (2-dimethylaminoethyl methacrylate) and HFMA (heptafluorobutyl methacrylate) were polymerized into statistical and block fluoropolymers respectively. From the results, all the polymers containing HFMA exhibited superior gene delivery efficiency. Interestingly, statistical fluoropolymers showed more efficient in gene delivery in comparison to block fluoropolymers although the reason was not revealed in this study.

Zhang et al. constructed a library of fluorinated oligoethylenimine (fOEI) [124]. Perfluorooctanyl fluoride was used for fluorination of OEI (600 Da). The researcher said that the fOEIs could readily form nanoassemblies (fOEI NAs). From the results, it was confirmed that fOEI NAs exhibited superior cellular uptake and endosomal escape even in the presence of serum. In addition, fOEI NAs demonstrated excellent colloidal stability and resistance to adsorption of serum proteins.

Chen et al. made siRNA delivery systems by using fluorinated PEI as a surfactant of perfluorodecalin (PFD) emulsion [125]. By using

emulsion, it was found that the cytotoxicity of fluorinated PEI was reduced. In the meanwhile, due to the introduction of fluorinated PEI, the emulsion demonstrated effective binding with siRNA. Moreover, the gene delivery efficiency was maintained even in the high concentration of serum conditions implying serum resistance. The efficiency was also tested in a melanoma mouse model *in vivo*. The fluorinated emulsion showed excellent silencing of Bcl2 gene inducing apoptosis and inhibiting tumor growth.

Xiao et al. also made fluorinated polymers with fluorobenzoic acid (FBA) with various number of fluorine atoms to study structure–activity relationships [126]. In the study, 600 Da of PEIs were reacted with a series of FBAs with different number of fluorine atoms. From the results, several things are found. Structure–activity relationship studies showed shielding effect of fluorine atoms. Fluorine atoms could screen the positive charge of the polymers. With good balance of shielding effect and positive charge, fluorinated polymers could condense and release DNA efficiently. In the meanwhile, it was found that more fluorine atoms could achieve more efficient cellular uptake. As a result, the polymers displayed efficient gene delivery.

Zuo et al. used carbon dots for the core of gene delivery carriers [127]. To carbon dots, PEI1.8k and tetrafluoroterephthalic acids

were conjugated via solvothermal process. PEI1.8k conferred positive charge and tetrafluoroterephthalic acid is a fluorination reagent. The fluorinated carbon dots (FCDs) displayed much higher transfection efficiency than PEI25k and Lipofectamine 2000. In comparison with non-fluorine analogue (UCD), FCD showed superior transfection efficiency to UCD implying the effect of fluorination. Moreover, in the presence of serum with high concentration, FCD still demonstrated the highest efficiency than other polymers.

Gene delivery systems adopting fluorination were extensively researched by many research groups recently. As described above, fluorinated gene delivery systems commonly were told that fluorination enhanced cellular uptake, serum stability, and consequential improvement of gene delivery efficiency. Collectively, it could be thought that fluorination was promising strategy for developing efficient gene delivery systems.

2.4. Fluorination with Other Strategies

With the progress of research on fluorinated gene delivery carriers, researchers started to combine various strategy into a polymer. As mentioned above, there are many barriers of gene delivery. To circumvent them, many researchers have been

combining many strategies into a gene delivery system. As a strategy, fluorination also have been combined with other strategies.

Wang et al. published a paper dealing with nanomicelles containing fluorocarbon core [128]. By conjugating fluorocarbon moieties to PEI (10,000 Da) by using disulfide exchange reaction, they made the elemental polymers as a component of nanomicelles. Due to the disulfide bond, it was confirmed that the polymers can release DNA in reducing environment. It means that cleavage of bond between fluorocarbon and PEI in reducing condition caused the breakdown of nanomicelles and facilitated the release of cargos. In addition, due to the fluorinated core having strong tendency of aggregation, the nanomicelles showed high gene delivery efficiency even in the presence of serum.

In the meanwhile, reactive oxygen species generated during cellular metabolism were also used trigger of polymer degradation. Liu et al. synthesized reactive oxygen species (ROS)-responsive bola-amphiphilic dendrimers [129]. The polymer was consisted of fluorinated thioacetal core with 3,5-difluorobenzalhyde and terminal PAMAM dendrons at the both ends of polymer. The polymers showed excellent siRNA delivery efficiency. ROS-sensitive property of the polymer facilitated specific and efficient release of the siRNA in the ROS-rich environment of cancer cells. In addition,

fluorine tags with ^{19}F on the polymers enabled ^{19}F−NMR analysis of the process of gene delivery.

Cai et al. synthesized bioreducible fluorinated peptide dendrimers (BFPDs) with polyhedral oligomeric silsesquioxane (POSS) core-based poly(L-lysine) G2 dendrimers, DSPs, and heptafluorobutyric acids [130]. Due to the combination, the polymer had relatively low cytotoxicity and high gene delivery efficiency superior to PEI25k. The efficiency was maintained even in vivo experiments suggesting the merit of the combination of bioreducibility and fluorination.

After a year, Cai et al. published a paper on subsequent research of BFPD [131]. In this study, BFPDs were used for siRNA delivery. As described above, the polymers also showed excellent performance and good biocompatibility in siRNA delivery. They exhibited improved physiological stability, serum resistance, enhanced intratumoral enrichment, cellular uptake, efficient endosomal escape, and facilitated intracellular siRNA release. Consequently, the polymers successfully prevented the tumor proliferation both *in vitro* and *in vivo*. In comparison with Lipofectamine 2000, BFPD was more efficient and safe gene delivery carrier.

Chen et al. published a paper on combining fluorination and bioreducibility [132]. The researchers synthesized poly(disulfide)

using N,N−dimethyldipropylene−tiramine (DMDPTA) and CBA. Then, the polymer was further modified with HFBA for fluorination. The synthesized polymer (F−RHB) exhibited superior siRNA delivery efficiency with relatively low cytotoxicity both *in vitro* and *in vivo* suggesting the merits of combining bioreducibility and fluorination.

Deng et al. developed fluorinated, ROS−cleavable PEI [133]. In this paper, low molecular weight PEI (600 Da) was crosslinked with a linker containing diselenide. Then, fluorination was done. The synthesized polymers exhibited low cytotoxicity and high gene delivery efficiency than PEI25k. The ROS triggered degradation of diselenides when the polymer entered the cells and enhanced serum resistance and facilitated interactions with cell membrane made the polymer efficient and safe. By combining degradability triggered intracellular region and fluorination, they successfully made efficient and safe gene delivery carriers.

Gong et al. reported biodegradable fluorinated poly(β−amino ester)s (FPBAEs) [134]. The synthesis was performed by using Michael addition reaction; 1H, 1H−undecafluorohexylamine was used as fluorous compound for fluorination. From the results of the study, it was found that FPBAEs had biocompatibility probably due to biodegradability derived from ester bond. In addition, it was

revealed that fluorination significantly improved the efficiency of gene delivery in comparison with unmodified analogues (PBAEs). The efficiency was also much higher than PEI25k.

Qi et al. synthesized fluorinated acid-labile branched hydroxyl-rich polycation (ARP-F) via facile ring opening polymerization [135]. By using the polymers, in this study, they performed various experiments such as *in vitro*/*in vivo* gene delivery, in vitro/in vivo gene editing, combination with treatment of anticancer drug, temozolomide and delivery of Cas9 gene. From the results, it was found that the polymers exhibited adequate pH-responsive degradability, biocompatibility, and high gene delivery efficiency both *in vitro* and *in vivo*. In the case of tumor growth inhibition, ARP-F efficiently suppressed the growth of tumor with no systemic cytotoxicity. In combination with temozolomide, the gene delivery successfully increased the sensitivity of cancer cells to anticancer drugs implying the potential of ARP-F as a gene delivery carrier.

Chen et al. used CBA, amine functionalized methoxy PEG (mPEG-NH_2), N, N-dimethyldipropylenetriamine (DMDPTA), and HFBA to synthesized fluorinated bioreducible polymer [136]. CBA, mPEG-NH_2, and DMDPTA were used for backbone of the polymer. Then, HFBA was conjugated to secondary amine of synthesized

polymer, PEG-PCD. In the study, they examined the effect of fluorination on polymer. Bioreducible behavior of the polymers was confirmed; the polymers released DNA successfully in reducing condition. Cytotoxicity of the polymers was also relatively lower than PEI25k; it might be the effect of PEG and bioreducible backbone of polymer. To confirm the efficiency as gene delivery carrier, the researchers performed several experiments. The results indicated that fluorination improved the efficiency of delivery by enhancing cellular uptake and serum stability. in vivo experiment also showed same result suggesting the potential of fluorination.

Zhang et al. published a paper dealing with ROS-responsive gene delivery carriers [137]. By using thioacetal linkers containing fluorobenzene moiety, ROS-responsive fluorinated polymer was synthesized via ring opening polymerization with tris(2-aminoethyl)amine (TAEA). By varying the number of fluorine on fluorobenzene, they investigated the effect on gene delivery. From the structure-activity relationship studies, it was found that the increasing number of fluorine atoms on the linkage induced better transfection efficiency and serum tolerance. Among the polymers, TAEA-S-4F which had 4 fluorine atoms (the highest number of fluorine in this study) showed the best performance. It was thought

that good cellular uptake and endosome escape ability derived from fluorine effect are the reason for the best performance. In the meanwhile, it was also found that to exert the effect of fluorine, enough amount of fluorine should present on the polymer. For example, TAEA-S-1F and TAEA-S-2F exhibited lower gene delivery efficiency than TAEA-S-0F which had no fluorine on benzene ring.

Although there were a few researches for combination of fluorination with other strategies, fluorination apparently attracted attention of many researchers. The combination of fluorination strategy with others would make opportunities for developing new efficient and safe gene delivery carriers.

Chapter 3. Crosslinked Bioreducible Polymer for Gene Delivery System

3.1. Materials and Methods

3.1.1. Materials

Poly(propylene imine) (DAB-Am-4 G 1.0, PPI G1), N, N'-cystamine bisacrylamide (CBA), polyethylenimine (PEI25k, 25 kDa), agarose, ethidium bromide, gel loading solution, sodium acetate, and 3-[4,5-dimethrylthiazol-2-yl]-2,5-diphenyltetrazolium bromide (MTT) were purchased from Sigma-Aldrich (USA). Tris base and methanol was purchased from Merck (Germany). HPLC grade water was purchased from Duksan (Korea). DL-dithiothreitol (DTT) was purchased from Biosesang (Korea). Hydrochloric acid was purchased from Junsei (Japan). pDNA (pCN-Luci) was amplified by using Escherichia coli DH5α and obtained by using PureLink HiPure Plasmid Filter Purification kit (Invitrogen, USA). Dulbecco's Modified Eagles' Medium (DMEM), Dulbecco's Phosphate Buffered Saline (DPBS), Fetal Bovine Serum (FBS), Penicillin-Streptomycin (P/S), Trypsin-EDTA (0.25%), and Quant-iT™ PicoGreen® kit were purchased from Invitrogen (USA). Luciferase assay system and reporter lysis

buffer were purchased from Promega (USA). BCA™ protein assay kit was purchased from PIERCE (USA). Glutathione Detection Kit was purchased from Millipore (USA). Cellular Reactive Oxygen Species Detection Assay Kit was purchased from abcam (USA). All other chemicals were purchased and used without further purification.

3.1.2. Synthesis and characterization of crosslinked PPIs

Crosslinked PPIs were synthesized by Michael addition reaction of PPI G1 and CBA according to the slightly modified method from a previous report [138]. First, PPI G1 was dissolved in methanol/water solution (9:1, v/v). Then, various molar amounts of CBA (PPI:CBA = 1:0.25, 1:0.5, 1:1, or 1:2, respectively) were prepared in reaction bottles and PPI solutions were added to the bottles with continuous stirring. After 24 h of reaction under N2 atmosphere in the dark, the solutions were diluted with ultra-pure water and acidified to pH 4 with 1 M HCl. Then, the product solutions were dialyzed against ultra-pure water for 48 h using dialysis membranes (MWCO = 3,500). The products, crosslinked PPIs, were obtained after lyophilization. The synthesis of the polymers was confirmed by ^{1}H NMR (600 MHz, AVANCE 600, Brucker, Germany). The synthesis scheme of PPI-CBAs was

shown in Scheme 2. The molecular weights of PPI-CBAs were measured by gel permeation chromatography (GPC) (YL-9100, Young Lin Instrument, Korea). The samples were dissolved at a concentration of 10 mg/mL. The assay was run on Ultrahydrogel 250 column (USA) with 1% formic acid as an eluent at 1.0 mL min-1 of flow rate. Poly(ethylene glycol)s with various molecular weights were used as standards for analysis. Carbon, nitrogen, hydrogen, and sulfur composition ratios of the polymers were also analyzed by elemental analyzer (Flash EA 1112, Thermo Electron Corporation, USA). To confirm the degradation behavior of PPI-CBAs in reducing condition, the molecular change in the presence of 5 mM DTT was measured at pre-determined time; 0.5, 1, 1.5, 2, 3, 4 h. Except for the DTT incubation, the condition for GPC measurement was same.

3.1.3. Agarose gel electrophoresis

pDNA condensing ability of PPI-CBAs was examined by agarose gel electrophoresis. PPI-CBA polyplexes were prepared in HEPES buffer (pH 7.4) at various weight ratios ranging from 0.5 to 4. Agarose gel (0.7% w/v) containing ethidium bromide solution (0.5 ㎍/mL) was prepared in TAE (Tris-Acetate-EDTA) buffer. After 30 min of incubation at room temperature, the samples were

electrophoresed at 100 V for 20 min. The polyplexes were also incubated in the presence of 5 mM DTT for 30 min at 37 ℃ and electrophoresed in order to examine the behavior of the polyplexes in reducing condition. The pDNA bands were visualized with UV illuminator (GelDoc XR+ gel documentation system, Bio-Rad, USA).

3.1.4. PicoGreen assay

PicoGreen assay was performed to examine the degradation behavior of PPI-CBAs quantitatively by detecting the dissociated pDNA from the polyplex in reducing condition. Linear bioreducible polymer, poly(cystaminebisacrylamide-diaminobutane) (poly(CBA-DAB)) and PEI25k were used as controls. Poly(CBA-DAB) was synthesized according to the slightly modified method from previous report [139]. After formation of polyplex in TE buffer at a N/P ratio of 5 (0.25 ㎍), each polyplex was incubated in 5 mM DTT solution for pre-determined time; 0, 0.5, 1, 1.5, 2, 3, 4 h, respectively. Then, PicoGreen reagent dissolved in TE buffer was added to the polyplex solution and incubated for 4 min. Fluorescence was measured with an excitation wavelength of 480 nm and emission wavelength of 520 nm using a microplate reader (Synergy H1, BioTek, USA). Results were presented as a relative fluorescence intensity (RFI, percentage values relative to value of

pDNA only). All experiments were performed in triplicate.

3.1.5. Average size and Zeta-potential value measurement of PPI-CBA polyplexes

The average sizes and Zeta-potential values of PPI-CBA polyplexes were measured by using Zeta-sizer Nano ZS (Malvern Instruments, UK) with He-Ne laser beam (633 nm) at 25 ℃. 0.5 mL of polyplex solutions (0.5 ㎍ pDNA) were prepared in ultra-pure water at various weight ratios ranging from 0.5 to 20. After 30 min of incubation, the solutions were diluted to final volume of 1 mL. The measurements were performed 3 times.

3.1.6. Cytotoxicity of polymers

The cytotoxicity of the polymers was estimated by MTT assay. HeLa, human cervical adenocarcinoma cell line, was maintained in DMEM supplemented with 10% FBS and 1% P/S in humidified atmosphere containing 5% CO_2 at 37 ℃. Then, the cells were seeded on a 96-well cell culture plate at a density of 1 x 10^4 cells/well in 100 ㎕ of DMEM containing 10% FBS and 1% P/S. As the cells achieved 70-80% confluency after 24 h of incubation, the cells were treated with PPI-CBA solutions (serum-free DMEM) with various concentrations for 4 h. PEI25k and PPI G1 were used

as controls. Then, the media were exchanged with fresh DMEM containing 10% FBS. After 24 h of incubation, 25 μL of MTT solution (2 mg/mL in DPBS) was added to each well and further incubated for 2 h. The media were carefully removed and 150 μL of DMSO was added to each well to dissolve formazan crystal formed by proliferating cells. The absorbance was measured at 570 nm by using a microplate reader. Results were presented as relative cell viability (RCV, percentage values relative to value of untreated control cells). All experiments were performed in quadruplicate.

3.1.7. Transfection experiments in vitro

HeLa cells were seeded on a 24-well cell culture plate at a density of 5 x 10^4 cells/well and grown until they achieved 70-80% confluency. Before transfection, medium of each well was exchanged with fresh DMEM for the assay in serum-free condition or with DMEM (10% FBS) for the assay in serum condition, respectively. The cells were then exposed to polyplex solutions (0.5 μg pDNA) with various weight ratios for 4 h. PEI25k polyplex (weight ratio = 1) and PPI G1 polyplexes (weight ratio = 60) were used as controls. After exchange with fresh medium containing 10% FBS, the cells were further incubated for 2 days. Then, each medium was aspirated, and the cells were rinsed with DPBS and

shaken for 30 min at room temperature with 120 μL of Reporter Lysis Buffer. Luciferase activities of cell lysates (20 μL) were measured by luciferase assay on a microplate reader and the total amounts of cellular proteins were examined by using a BCA™ Protein Assay Reagent Kit. The normalized results were presented in terms of relative light unit (RLU)/mg cellular protein. All experiments were performed in triplicate.

3.1.8. Measurement of intracellular glutathione (GSH) level

Effect of PPI-CBAs to intracellular GSH level was examined in HeLa cells. GSH assay was performed according to the slightly modified method from the manufacturer's given protocol. The cells were seeded on a 12-well cell culture plate at a density of 2×10^5 cells/well. After the cells achieved 70-80% confluency after 24 h of incubation, the cells were treated with PPI-CBAs with various concentrations (serum-free DMEM) for 4 h. Then, the cells were washed with ice-cold wash buffer and treated with lysis buffer on ice for 10 min. After collection of cell lysates by ultracentrifuge, the supernatants were mixed with prepared monochlorobimane (MCB) solutions. After 1.5 h of incubation at room temperature without light, the fluorescence of the solutions was measured by using a microplate reader with a 380/460 nm filter. Finally, intracellular

GSH levels of samples were presented in terms of relative fluorescence intensity (RFI) to a value of untreated cells. All experiments were performed in triplicate.

3.1.9. Measurement of intracellular reactive oxygen species (ROS) level

Effect of PPI-CBAs to intracellular ROS level was also examined in HeLa cells. ROS assay was performed according to the slightly modified method from the manufacturer's given protocol. The cells were seeded on a 96-well black plate at a density of 2.5 x 10^4 cells/well. After the cells achieved 70-80% confluency after 24 h of incubation, the cells were washed with supplied 1X buffer. Then, the cells were treated with 2',7'-dichlorofluorescein diacetate (DCFDA) solution for 45 min without light. After washing with 1X buffer, PPI-CBA solutions with various concentrations were treated to the cells for 4 h without light. PPI G1 and poly(CBA-DAB) were also used as controls. The fluorescence of each well was subsequently measured by using a microplate reader (excitation: 485 nm, emission: 535 nm). Finally, intracellular ROS levels of samples were presented in terms of relative fluorescence intensity (RFI) to a value of untreated cells. All experiments were performed in triplicate.

3.2. Results and discussion

3.2.1. Synthesis and characterization of PPI-CBAs

To synthesize PPI-CBAs, Michael addition reaction was used. A series of feed ratios (PPI:CBA = 1:0.25, 1:0.5, 1:1, and 1:2) were set to compare their characteristics. The synthesis scheme containing expected polymer structure for PPI-CBAs is presented in Scheme 2. Higher feed ratio (PPI:CBA=1:3) also has been tried; however, the solution turned solidified soon probably due to the extensive crosslinking. In addition, as described above, the reaction time was fixed. Further reaction also resulted in solidification of the product. Furthermore, because the reaction was step-wise, it was thought that tuning of the reaction composition rather than varying time parameter had more impact. The synthesis of the polymers was confirmed by ^{1}H NMR (Figure 1) as follows.

^{1}H NMR (D_2O): δ PPI G1 (-$NCH_2C\mathbf{H_2}C\mathbf{H_2}CH_2N$-) = 1.81, δ PPI G1 (-$NCH_2C\mathbf{H_2}CH_2N$-) = 2.14, δ CBA (-$NCH_2C\mathbf{H_2}CONHCH_2CH2SS$-) = 2.77, δ CBA (-$CH_2C\mathbf{H_2}SSC\mathbf{H_2}CH_2$-) = 2.89, δ (protons next to amines) = 3.13-3.37, δ CBA (-$NCH_2CH_2CONHC\mathbf{H_2}CH_2SS$-) = 3.58

Experimental ratios of polymer composition between PPI G1 and CBA were calculated by comparing the integrals of specific protons

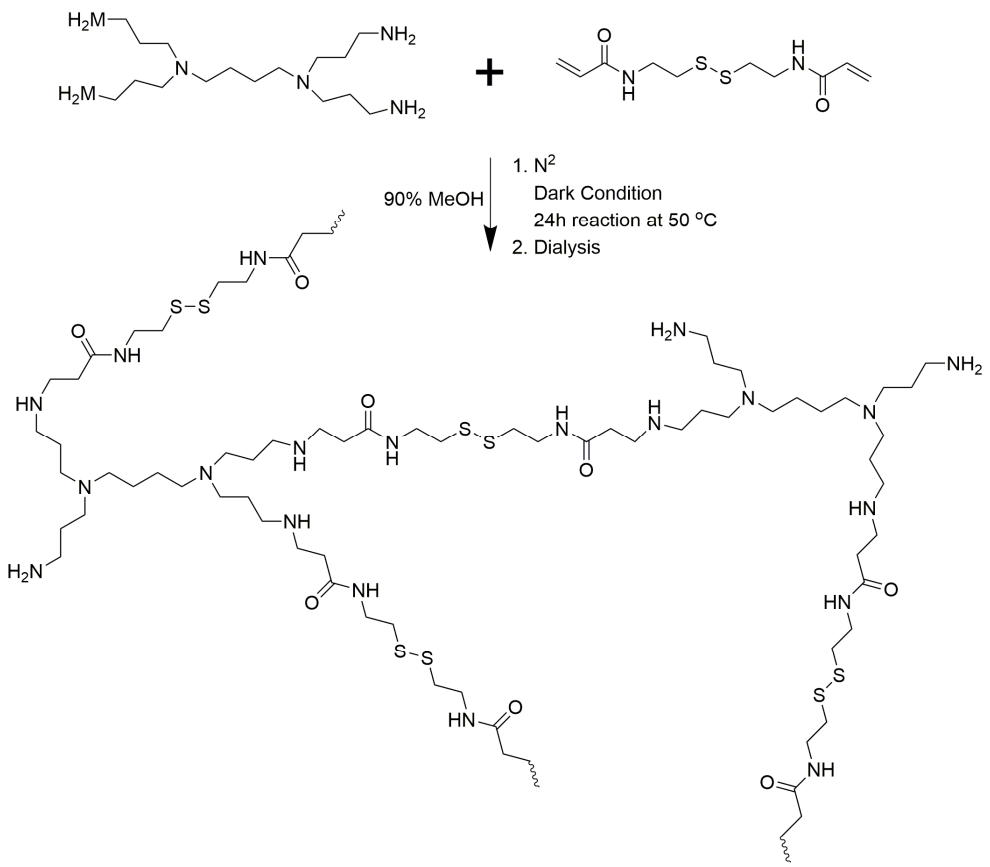

Scheme 2. Synthetic scheme of PPI-CBAs. Michael addition reaction was used to synthesize PPI-CBAs.

from PPI G1 (−$NCH_2C\mathbf{H_2}C\mathbf{H_2}CH_2N$−) and CBA (−$NCH_2CH_2CONHC\mathbf{H_2}CH_2SS$−). Table 1 shows the chemical properties of PPI−CBAs. PPI−CBAs were named after the composition ratios; P4C2, P4C3, P4C5, and P4C9, respectively. The proportion of CBA in PPI−CBAs was increased along with the increase of CBA amount added. The discordance between feed ratios and composition ratios was thought that it would be derived from the removal of unreacted PPI G1 during purification. Emerging steric hindrance during reaction progress would be a significant factor for unreacted PPI G1 which is a plausible reason of the discordance.

The element (C, H, N and S) composition of each PPI−CBA was also examined by elemental analysis. As shown in Table 2, the composition ratios of S (sulfur) were increased, and those of N were decreased along with the increase of CBA portion in PPI−CBAs. When the composition ratios of elements from elemental analysis were compared with the composition ratios of elements based on by ^{1}H NMR analysis, all the values were found in the range from 0.95 to 1.21. This result shows good correlations between these two analyses for the characterization of the structures and monomer compositions of PPI−CBAs. Molecular weights of PPI−CBAs were measured by GPC. Weight average molecular weights

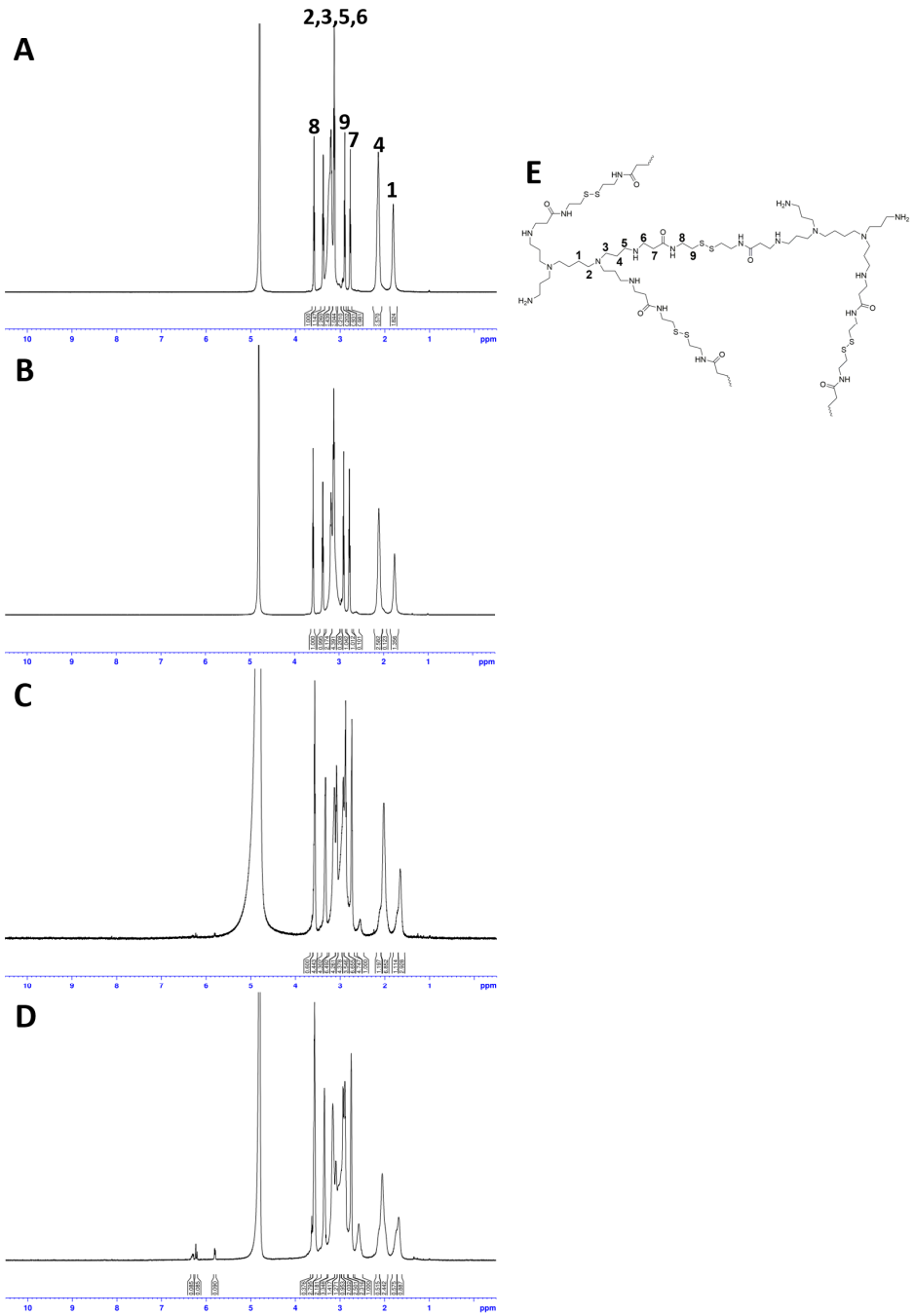

Figure 1. 1H NMR spectra of PPI-CBAs. (A) P4C2, (B) P4C3, (C) P4C5, (D) P4C9, and (E) the structure of PPI-CBAs.

Table 1. Chemical properties of synthesized PPI-CBAs.

	Initial feed ratio (PPI:CBA)	Experimental composition ratio (PPI:CBA)	M_n (kDa)	M_w (kDa)	PDI	Charge density (Da/+)
P4C2	1:0.25	1:0.5	4.62	6.81	1.47	53.1
P4C3	1:0.5	1:0.75	8.67	15.5	1.78	63.9
P4C5	1:1	1:1.24	9.79	22.8	2.33	85.6
P4C9	1:2	1:2.17	18.9	66.4	3.52	129.0

Table 2. Elemental analysis result of synthesized PPI-CBAs.

Elements	P4C2	P4C3	P4C5	P4C9
C	39.49 [a] (0.58) [b] 0.98 [c]	40.21 (0.57) 0.98	40.72 (0.56) 0.98	38.97 (0.54) 0.97
H	9.19 (0.13) 1.19	8.52 (0.12) 1.12	8.38 (0.11) 1.14	8.06 (0.11) 1.21
N	14.98 (0.22) 0.96	14.43 (0.21) 0.95	13.86 (0.19) 0.96	12.48 (0.17) 0.97
S	5.00 (0.07) 0.98	7.44 (0.11) 1.07	9.94 (0.14) 1.03	12.43 (0.17) 1.01

[a] Found value of the element (%) in each PPI-CBA

[b] Relative ratio of the element among total elements in each PPI-CBA

[c] Relative ratio between elemental analysis value and NMR analysis value of each element

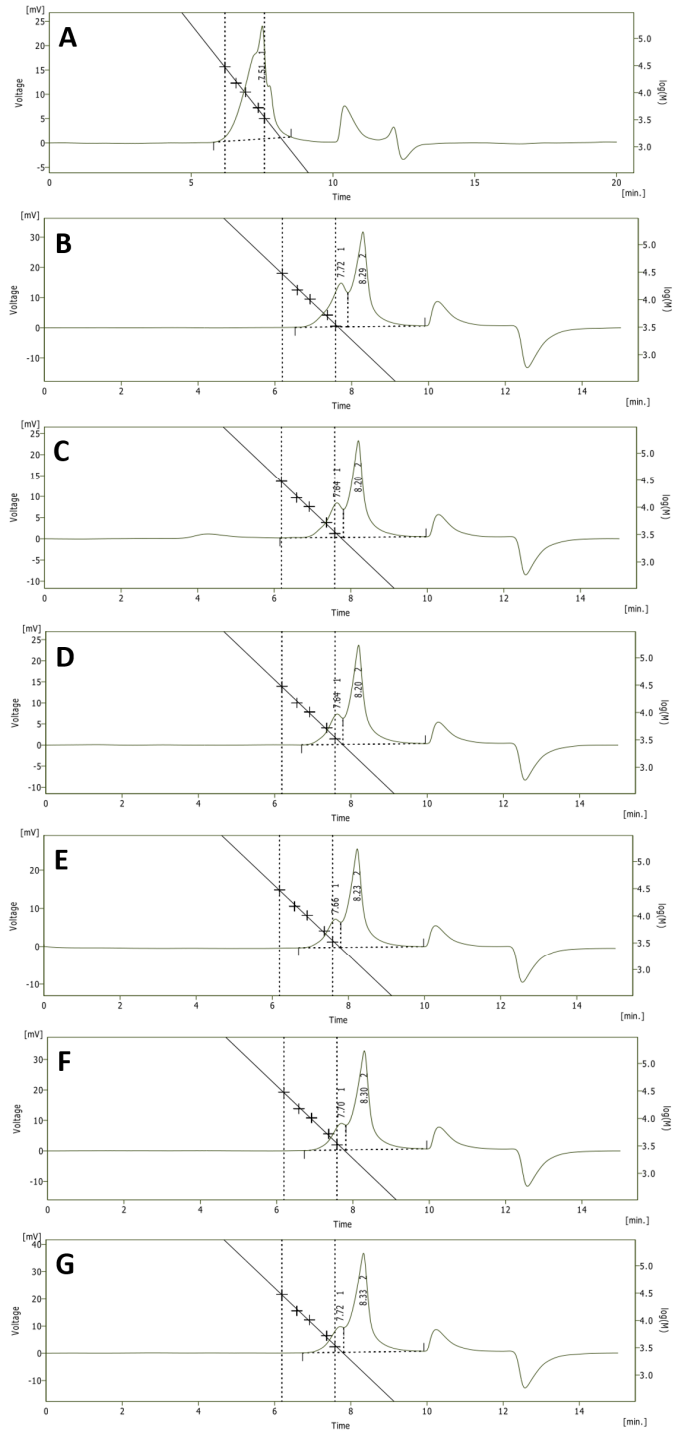

Figure 2. Chromatograms of P4C2 incubated with 5 mM DTT. (A) 0 h, (B) 0.5 h, (C) 1 h, (D) 1.5 h, (E) 2 h, (F) 3 h, (G) 4 h.

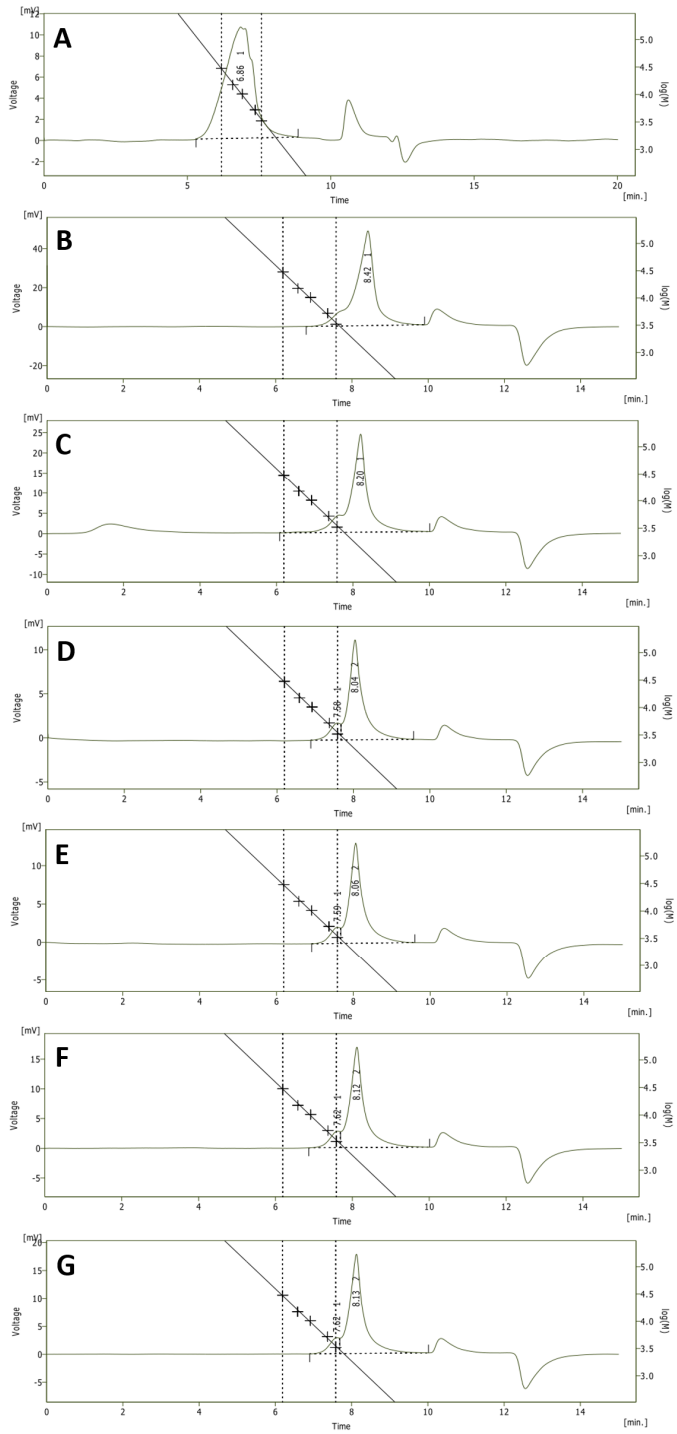

Figure 3. Chromatograms of P4C3 incubated with 5 mM DTT. (A) 0 h, (B) 0.5 h, (C) 1 h, (D) 1.5 h, (E) 2 h, (F) 3 h, (G) 4 h.

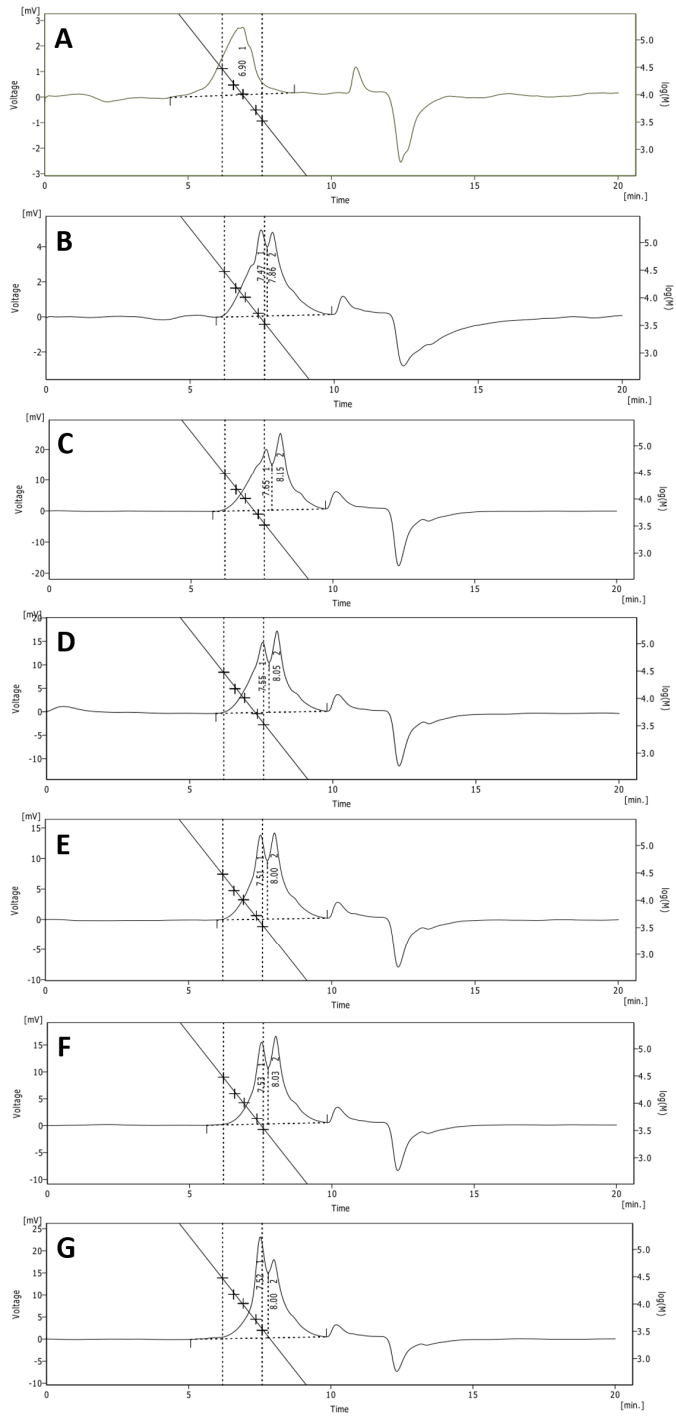

Figure 4. Chromatograms of P4C5 incubated with 5 mM DTT. (A) 0 h, (B) 0.5 h, (C) 1 h, (D) 1.5 h, (E) 2 h, (F) 3 h, (G) 4 h.

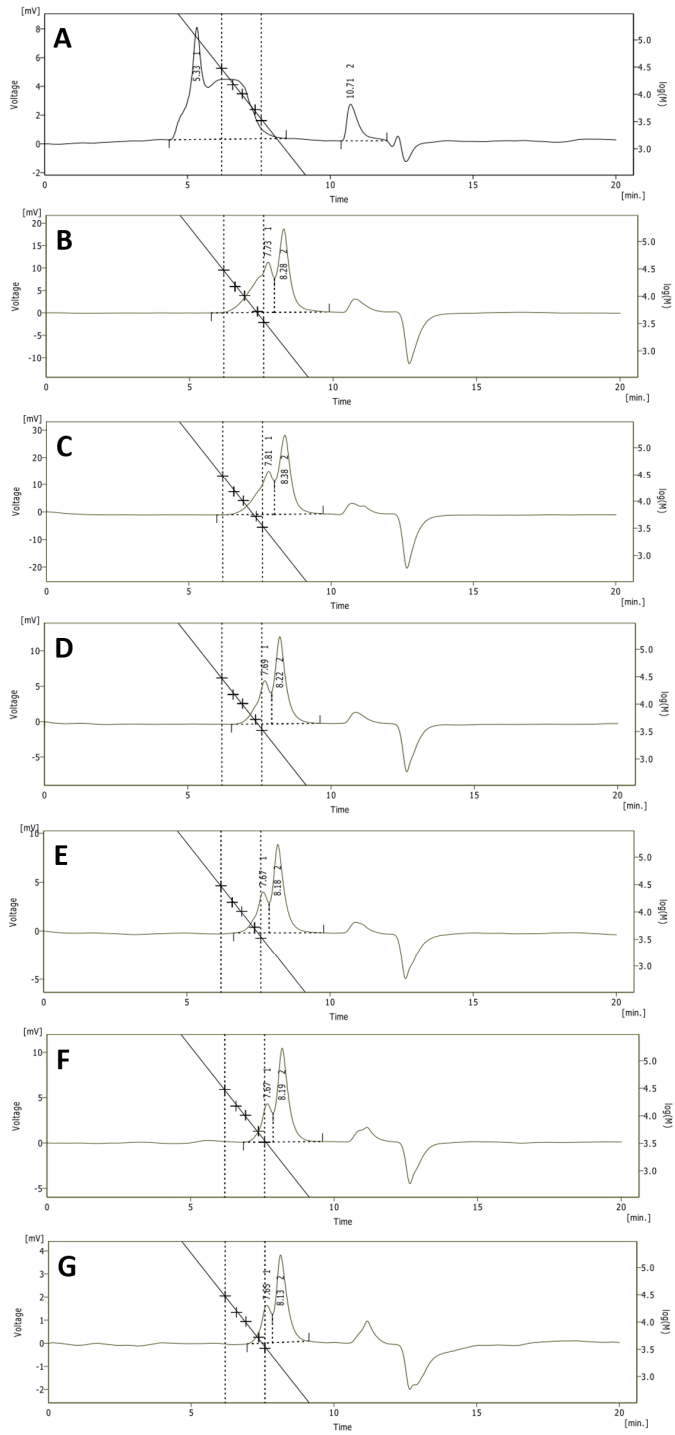

Figure 5. Chromatograms of P4C9 incubated with 5 mM DTT. (A) 0 h, (B) 0.5 h, (C) 1 h, (D) 1.5 h, (E) 2 h, (F) 3 h, (G) 4 h.

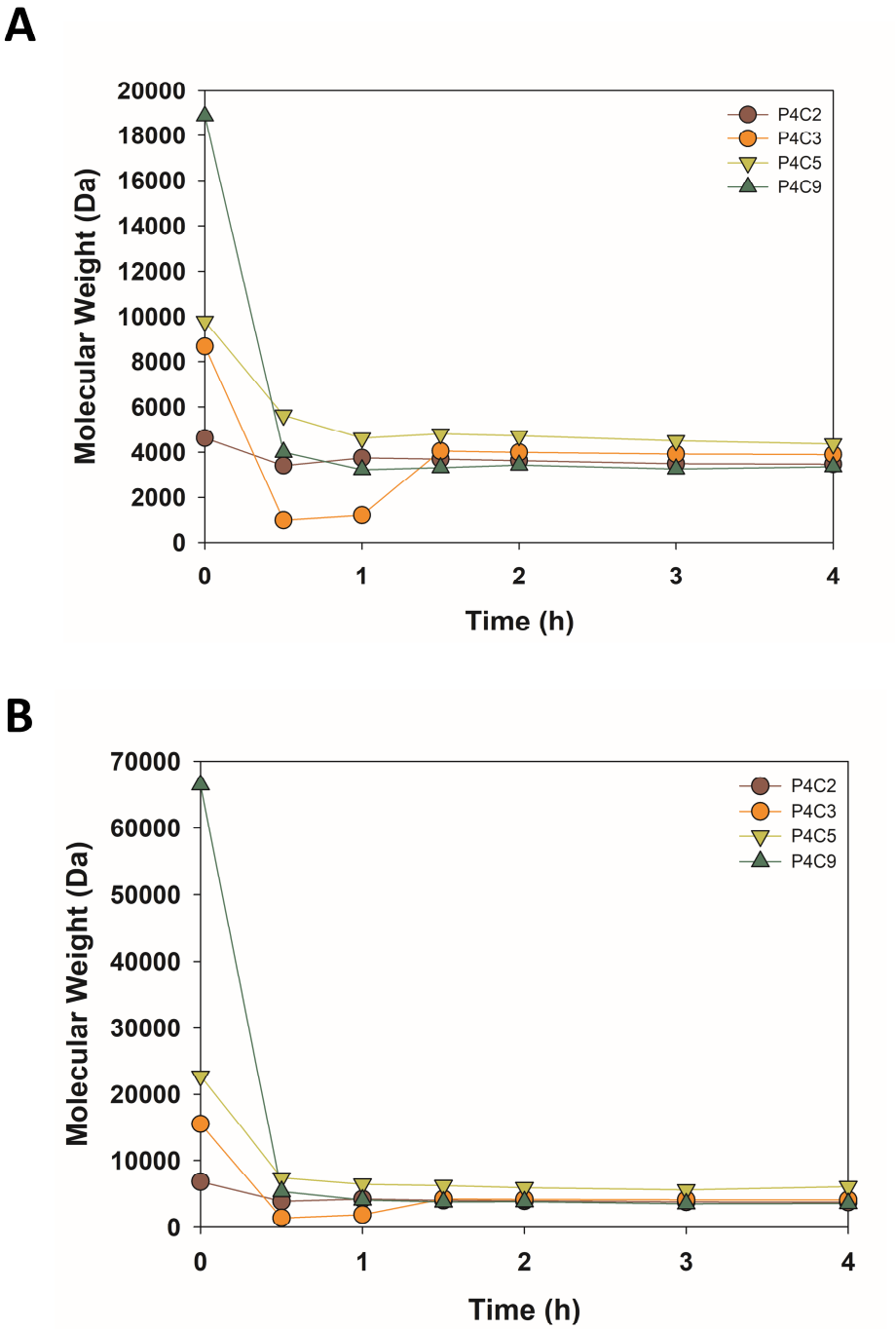

Figure 6. The molecular weight changes of PPI-CBAs in the presence of 5 mM DTT for 4 h. The plots display number-average (A) and weight-average (B) molecular weight.

(M_w) of PPI-CBAs ranged from 6.81 kDa to 66.4 kDa. Molecular weights of PPI-CBAs and polydispersity index (PDI) of the molecular weights were found to be increased with the increase of the added CBA amounts probably due to the increase of the crosslinking degree, as shown in Table 1.

As shown in Figure 2-6, degradation profiles were summarized. Interesting results were displayed. All PPI-CBAs showed resistance to degradation in reducing environment unlike linear bioreducible polymer completely degraded [140]. Although the portion of peak 1 and 2 was different, most of PPI-CBAs degraded into low molecular weight compounds (~1000 Da). However, they remained high molecular weight portion until 4 h of incubation. Moreover, in the case of P4C2, it recovered the molecular weight significantly during the DTT incubation. It can be speculated that PPI-CBAs had some extent of resistance to reducing environment and it could recover their disulfide bond after the cleavage.

3.2.2. Agarose gel electrophoresis

Agarose gel electrophoresis was performed in order to examine pDNA condensing abilities of PPI-CBAs. In the absence of DTT, a reducing agent, P4C2 and P4C3 could condense pDNA completely at

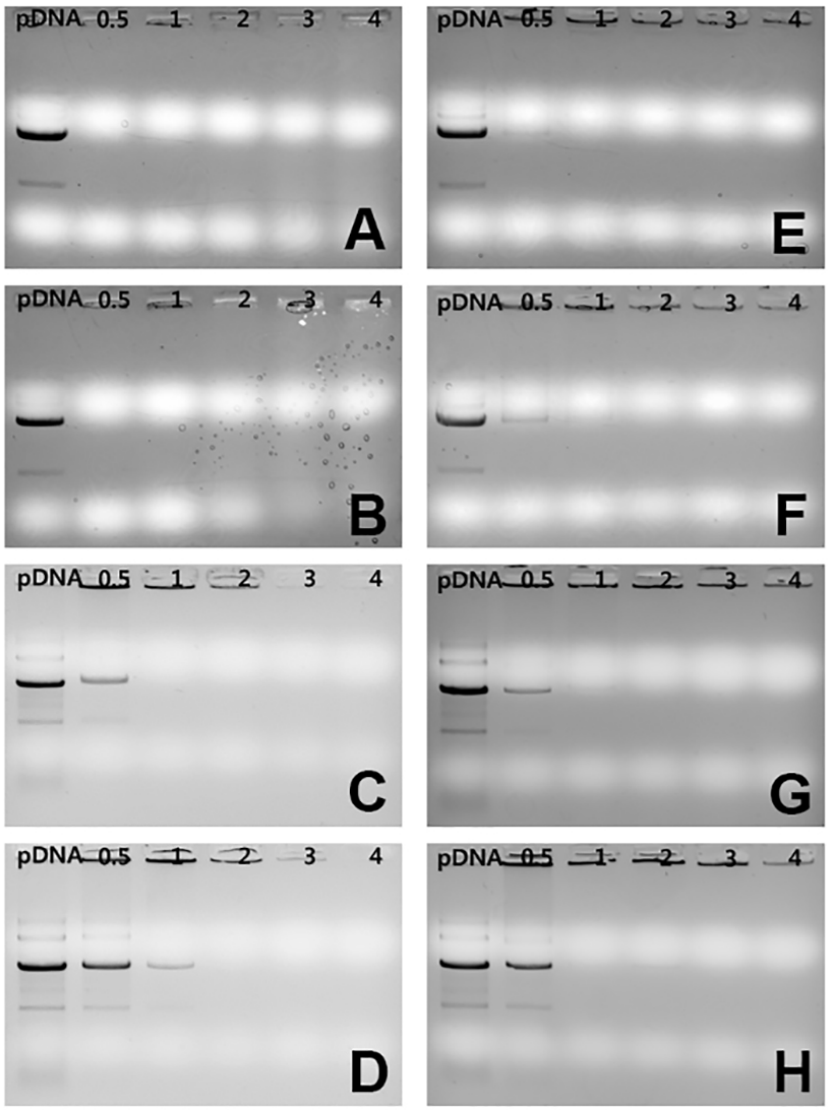

Figure 7. Agarose gel electrophoresis results of PPI-CBA polyplexes in the absence of DTT (A-D) and in the presence of DTT (5 mM) (E-H). (A) and (E): P4C2, (B) and (F): P4C3, (C) and (G): P4C5, (D) and (H): P4C9. Numbers show the weight ratio of polyplexes.

a weight ratio of 0.5 but P4C5 and P4C9 could condense pDNA at higher weight ratios (1 and 2, respectively) (Figure 7A–D), which means that PPI–CBAs could condense pDNA at low weight ratios and that pDNA condensing ability of PPI–CBAs were increased with the increase of the charge density. Table 1 shows the charge density of the polymers.

Usually, it was reported that bioreducible polymers could release pDNA from the polyplexes in reducing condition due to their degradation by cleavage of internal disulfide bonds [78,141]. However, interesting results were obtained for the electrophoresis in reducing condition (5 mM DTT). In Figure 7E–H, it was observed that PPI–CBAs still could condense pDNA even at low weight ratios in reducing condition, in contrast to other cross-linked bioreducible polymers. This result demonstrated that PPI–CBA polyplexes were not disrupted in reducing condition and that some mechanism could stabilize PPI–CBA polyplex structures even in reducing condition. In addition, pDNA bands getting strong at a weight ratio of 0.5 (Figure 7E–H) also showed that pDNA condensing ability of PPI–CBAs were increased with the increase of the charge density.

3.2.3. PicoGreen assay

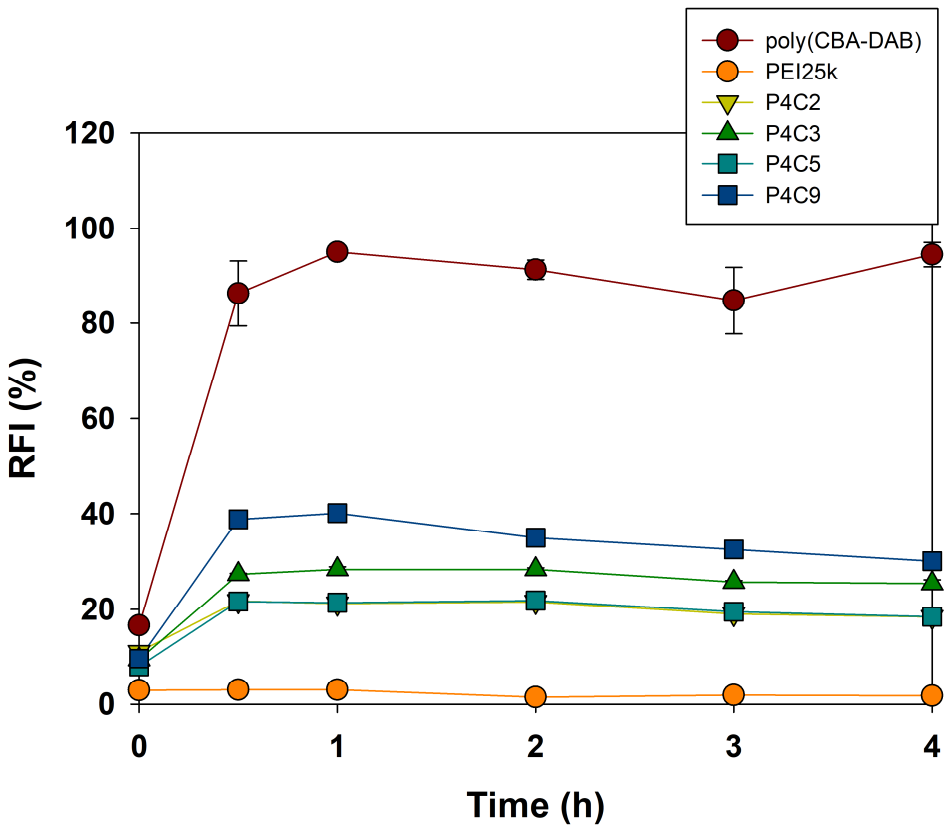

Figure 8. PicoGreen assay results. All polyplexes were prepared at a NP ratio of 5. Result was presented as a relative fluorescence intensity (RFI, percentage values relative to value of pDNA only).

In order to investigate the degradation behaviors of PPI-CBA polyplexes in reducing condition quantitatively, PicoGreen assay was performed (Figure 8). All polyplexes were prepared at a NP (nitrogen to phosphate) ratio of 5 to harmonize the electrostatic effect of polymers on polyplex formation. PEI25k and linear bioreducible polymer, poly(CBA-DAB), were used as controls. PEI25k polyplex showed very low fluorescence values irrespective of incubation time. It was thought that PEI25k polyplexes were not disrupted and stable in that condition. On the contrary, poly(CBA-DAB) polyplex showed high fluorescence values above 80% even after 30 min of incubation, meaning that poly(CBA-DAB) polyplexes could be disrupted and released most of pDNA due to degradation of the polymer structure. However, the fluorescence values of PPI-CBA polyplexes were low (< 40 %) even after 4 h of incubation in reducing condition, showing that PPI-CBA polyplexes could be degraded by cleavage of disulfide bonds, but they were just partially disrupted. When considering the number of DTT, at least 415 times of DTT to that of disulfide bonds in PPI-CBAs existed. In the case of P4C2 which possessed lowest amount of disulfide bonds, the number of DTT was about 1800 times higher. Taken together with poly(CBA-DAB) result and polymer degradation experiment results measured by GPC, it is suggested

that the disrupted PPI-CBA polyplexes may be re-stabilized by re-crosslinking of the degraded PPI-CBA fragments via auto-oxidation of their multiple terminal thiols. In the case of poly(CBA-DAB), it was thought that poly(CBA-DAB) fragments could not condense pDNA in reducing condition because even single bond degradation resulted in the whole cleavage of the linear polymers, unlike PPI-CBAs which have crosslinked structure. Therefore, it was deduced that the structures of bioreducible polymers (crosslinked structures and crosslinking degrees) would be important factors for degradation of the polyplexes in reducing condition.

3.2.4. Average size and Zeta-potential value measurement of PPI-CBA polyplexes

Average size and zeta-potential value of PPI-CBA polyplexes were measured at various weight ratios ranging from 0.5 to 20 by Zeta-sizer. As shown in Figure 9A, Z-average sizes (Z_{avg}) of all PPI-CBA polyplexes were found to be below 250 nm at higher weight ratios than 1. Interestingly, we observed the small average size (150-300 nm) of polyplexes even at low weight ratios (0.5 or 1) in which pDNA was not condensed completely by PPI-CBAs in the above agarose gel electrophoresis. It was thought to be due to

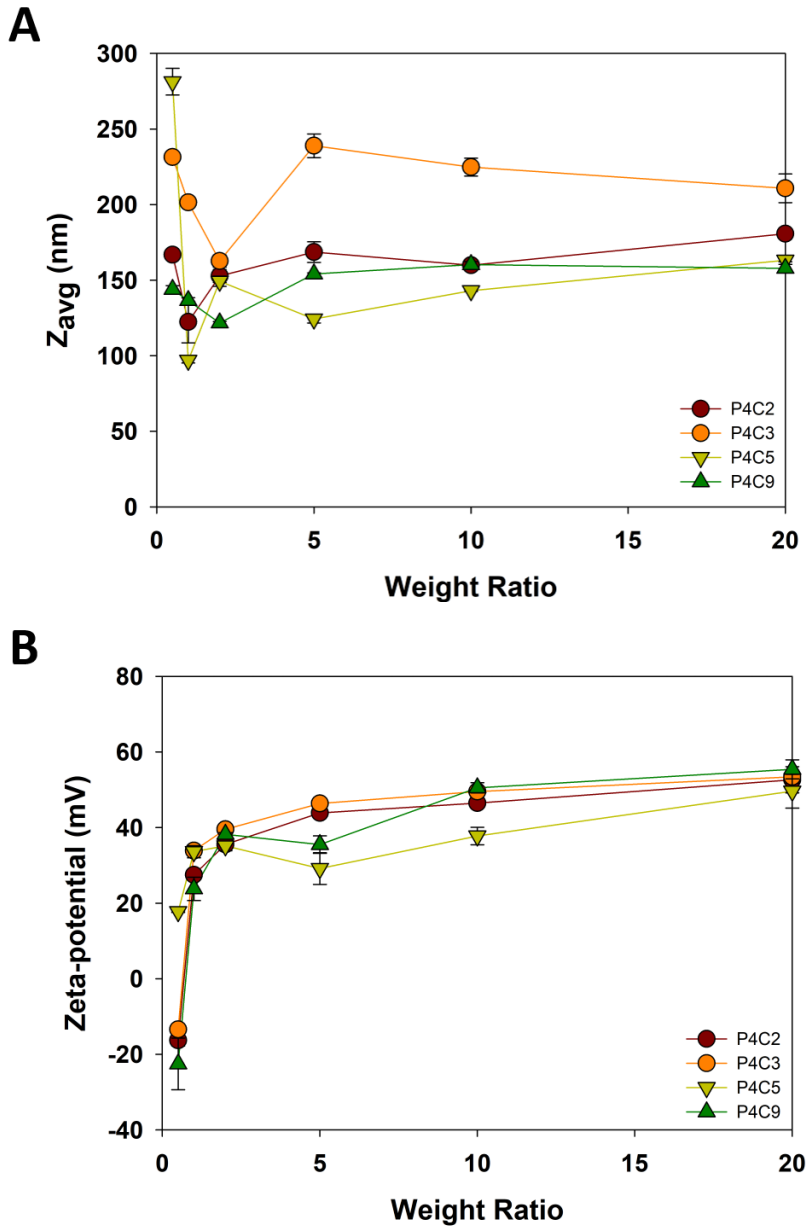

Figure 9. Average size (A) and Zeta-potential value (B) measurement of PPI-CBA polyplexes.

the partially formed polyplexes. In other words, although they could not form integral polyplexes binding pDNA tight, it would be enough to constitute the small particles.

In the case of Zeta-potential values (Figure 9B), most PPI-CBA polyplexes except P4C5 showed negative values at a weight ratio of 0.5, which meant the incomplete condensation of anionic pDNA with cationic PPI-CBAs at that ratio. Only P4C5 polyplex exhibited positive Zeta-potential value (17.8 mV) at a weight ratio of 0.5 probably due to the more expedited pDNA condensation by P4C5 than other polymers, which is well consistent with the agarose gel electrophoresis result. Zeta-potential values of PPI-CBA polyplexes were increased to positive values with the increase of weight ratios and finally reached about 50 mV at a weight ratio of 20. These results demonstrated that PPI-CBAs could form nano-sized and positively charged polyplexes with pDNA, which may lead to the efficient adsorption to negatively charged cell membrane and cellular uptake of the polyplexes [142,143].

3.2.5. Cytotoxicity of polymers

In order to examine cytotoxicity of PPI-CBAs, MTT assay was carried out with HeLa cells. In Figure 10, PEI25k showed significant cytotoxicity even at low concentrations although PPI G1 showed

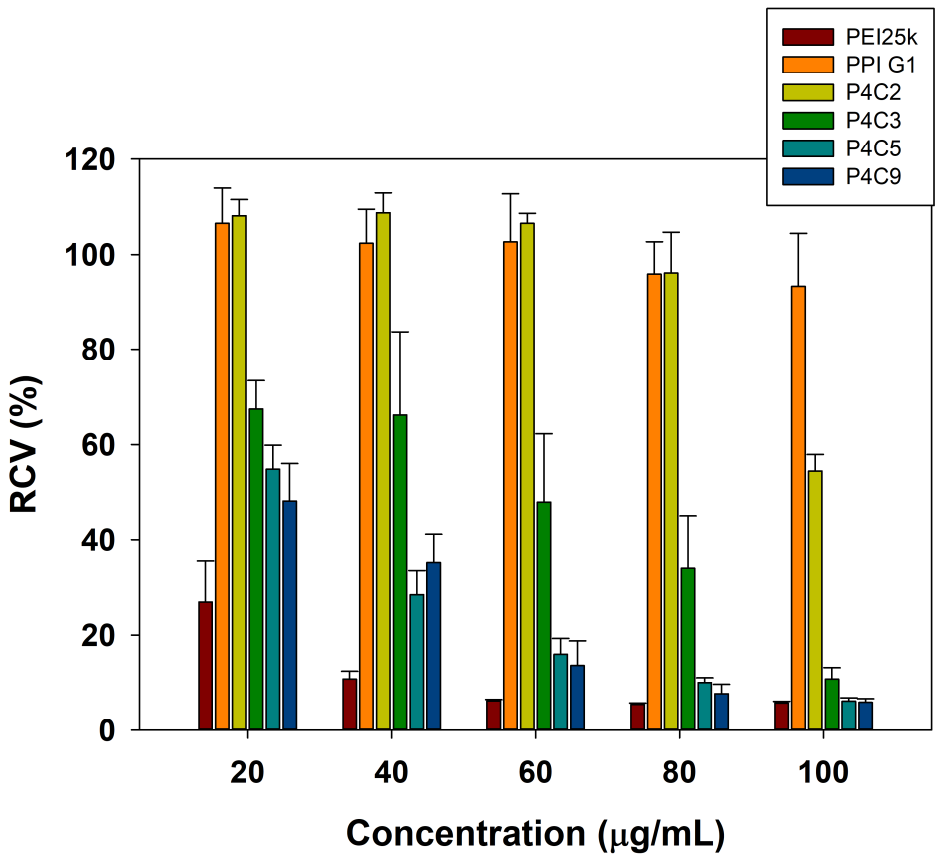

Figure 10. MTT assay result of PPI-CBAs on HeLa cells.

negligible cytotoxicity with high relative cell viability (> 90%) at all concentrations. Interestingly, PPI-CBAs-treated cells exhibited the decreased cell viability with increase of the concentration, and the cytotoxicity of PPI-CBAs was increased with increase of CBA portion in the polymers. Usually, other bioreducible polymers composed of nontoxic monomer units have been reported to show marginal cytotoxicity due to their degradation in cytosol, even if they are crosslinked [58-61,144,145]. However, bioreducible PPI-CBAs comprised of PPI G1 which is non-toxic showed considerable cytotoxicity and it was thought that it may be related with unusual degradation behaviors of PPI-CBAs in reducing condition as mentioned above. Therefore, further characterizations were performed to examine the mechanism of cytotoxicity induction in Section 3.2.7 and 3.2.8.

3.2.6. Transfection efficiency in vitro

Transfection experiments were performed by measuring transgene expression of luciferase reporter gene in HeLa cells. PEI25k (weight ratio=1) and PPI G1 (weight ratio=60) polyplexes which were prepared at their optimal conditions were used as controls. The transfection efficiency of P4C5 and P4C9 was only measured at weight ratios ranging from 5 to 20 due to their

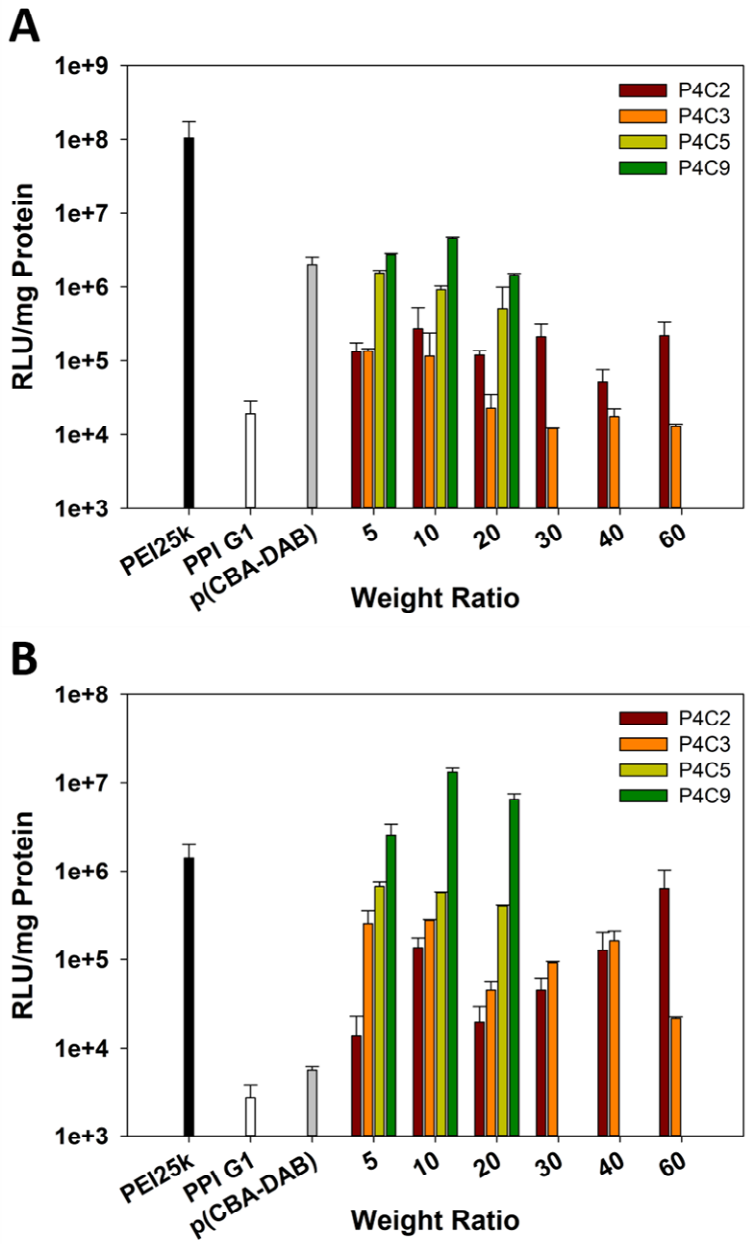

Figure 11. Transfection experiment result of PPI-CBAs on HeLa cells in serum-free condition (A) and serum condition (B).

cytotoxicity at high concentrations. In the absence of serum (Figure 11A), the transfection efficiency of PPI-CBAs was low in comparison with that of PEI25k but about 7-245 times higher at their optimized weight ratios than that of PPI G1. PPI-CBAs showed the increasing transfection efficiency with the increase of CBA portion in the polymers.

However, the transfection efficiency of PEI25k in serum condition was significantly (1/74 times) decreased in comparison with the result of serum-free condition. On the contrary, the transfection efficiency of PPI-CBAs was less decreased or even increased in comparison with the result in serum-free condition (Figure 11B). P4C9 even showed about 9 times higher transfection efficiency at a weight ratio of 10 than PEI25k in serum condition. It meant that PPI-CBAs showed a good potential for gene delivery systems in serum condition. Also, the transfection efficiency of PPI-CBAs was increased with the increase of CBA portion in the polymers, which is consistent with the result of experiment performed under the serum-free condition.

These results demonstrated that high transfection efficiency of polymeric gene carriers could be obtained by crosslinking of unit molecules with low molecular weights and that the transfection efficiency of PPI-CBAs was closely related with their

physiochemical properties such as molecular weight or crosslinking degree. In the case of P4C5 which showed the highest efficiency among PPI-CBAs, the molecular weight (22.8 kDa) was similar with PEI25k. In addition, charge density was much higher than PEI25k; 85.6 and 44, respectively. The structure also different; crosslinked versus branched structure. When considering the reports about the efficiency comparison of linear PEI and branched PEI [146] or the gene delivery study of fractured dendrimers [147] to find out what made the difference, it became complicated. In the case of branched PEI and linear PEI, branched PEI25k showed lower efficiency than linear PEI 22k although the reason was not specified. It meant that the degree of branch was not the absolute criterion of better gene delivery efficiency. In addition, it was reported that fractured dendrimer showed higher efficiency than intact dendrimer due to increased flexibility of polymer structure. It indicated that not always higher molecular weight polymer showed higher gene delivery efficiency. These reports indicated that the criteria about gene delivery efficiency were not always applied. In this study, P4C9 with higher molecular weight than PEI25k also showed lower gene delivery efficiency probably due to high cytotoxicity. When thinking about these results, it was hard to figure out the parameter making difference. Although it would need

further investigation, it can be thought that the enhanced flexibility of polymer derived from the polymerization improved efficiency of gene delivery.

3.2.7. Measurement of intracellular GSH level

Intracellular GSH levels were measured after treatment of PPI-CBAs in order to examine the effect of the polymers to the GSH levels. Several works investigating the effect of GSH depletion onto polyplex degradation and transfection efficiency reported that intracellular degradation of bioreducible polymers by intracellular GSH is an important factor for efficient transfection [145,148]. As shown in Figure 12, intracellular GSH levels were decreased with the increase of PPI-CBAs concentration. The GSH levels of PPI-CBAs treated cells were decreased to 40-60% values of untreated cells at 50 ㎍/mL of concentration. P4C2 possessing the lowest CBA portion displayed lesser decrease of GSH levels based on the concentration than other PPI-CBAs (P4C3, P4C5, and P4C9) which showed the similar decrease patterns with each other.

In the case of poly(CBA-DAB) polyplex, it was found that it consumed negligible amount of GSH unlike PPI-CBAs. In addition, in the case of 50 ㎍/mL of P4C2 treated group, the concentration of GSH (about 5 mM [149,150]) was about 433 times higher than the

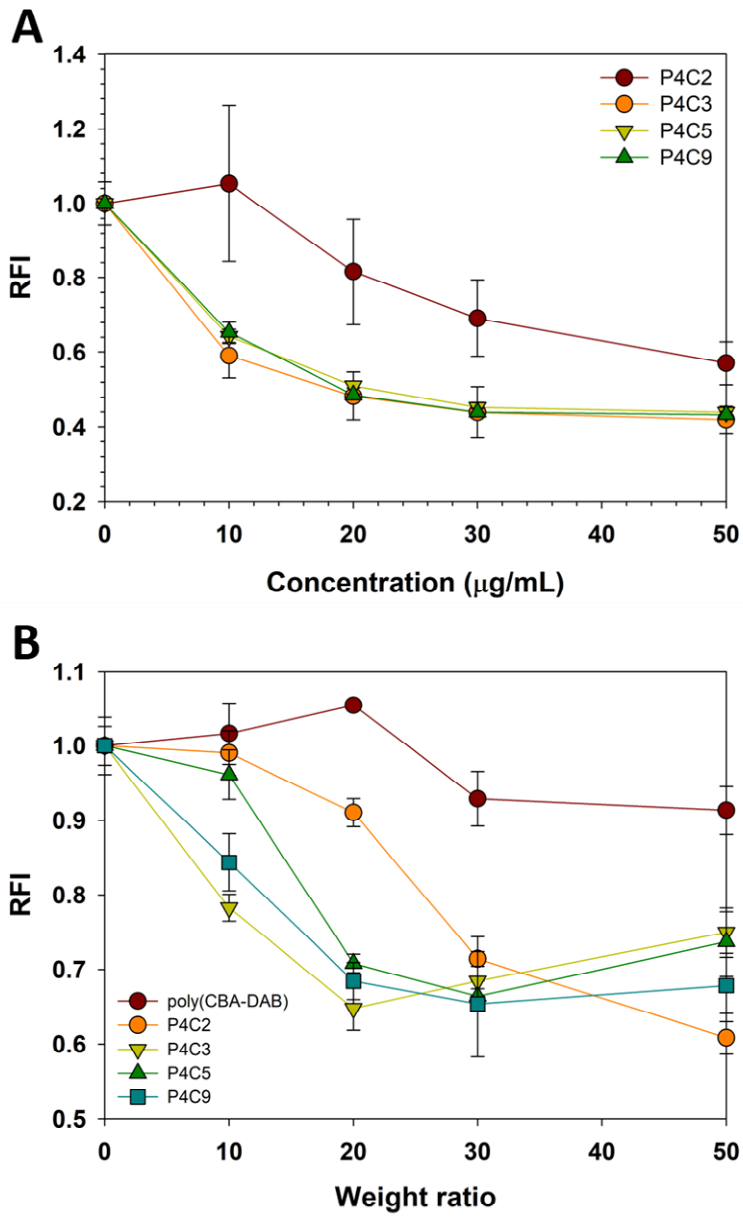

Figure 12. Measurement of intracellular GSH level after treatment of free polymers (A) and polyplexes (B). Intracellular GSH levels of samples are presented in terms of relative fluorescence intensity (RFI) to a value of untreated cells.

number of disulfide bonds existing in P4C2.

When considering PicoGreen assay, the ratio between reducing agents and disulfide bonds in GSH and ROS measurement (about 415-fold at maximum ratio) was not higher than the ratio in PicoGreen assay. Taken together with PicoGreen assay result and degradation profile measured by GPC, it can be postulated that cleavage of disulfide bonds formed by the re-crosslinks between thiols of degraded PPI-CBA fragments in cytoplasm may induce further consumption of GSH finally leading to the decrease of intracellular GSH level although regeneration of GSH and other reducing systems in cell should be considered.

3.2.8. Measurement of intracellular ROS level

Intracellular ROS levels were also measured after treatment of PPI-CBAs in order to examine the effect of the polymers to the ROS levels. Reactive oxygen species (ROS) are normal products of cellular metabolism which have important roles in cell signaling and homeostasis [151], but excessive ROS can damage cellular proteins, lipids, and DNA, leading to the decrease of cell viability making high oxidative stress condition [152,153]. The intracellular ROS levels are known to be controlled by variety of enzymes including superoxide dismutase, catalase, and small antioxidant molecules

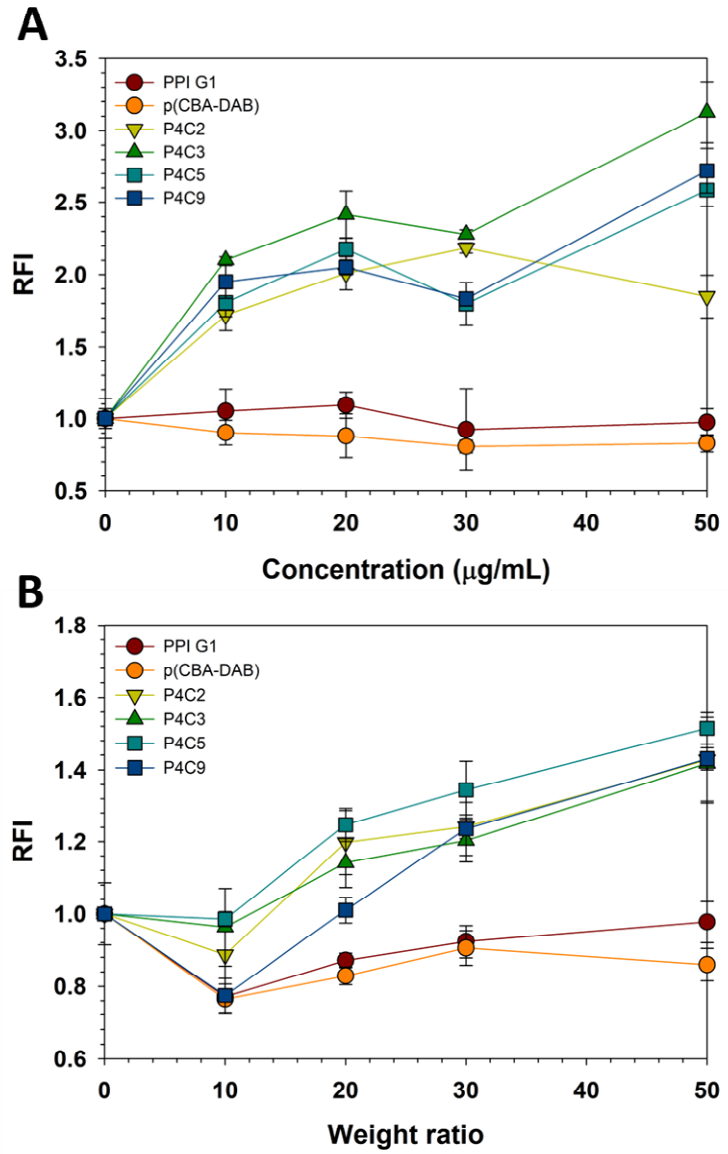

Figure 13. Measurement of intracellular ROS level after treatment of free polymers (A) and polyplexes (B). Intracellular ROS levels of samples were presented in terms of relative fluorescence intensity (RFI) to a value of untreated cells.

such as ascorbic acid or tocopherol [154]. GSH, an antioxidant, is also known to prevent the damages caused by ROS such as free radicals or peroxides [155,156]. Therefore, the effect of intracellular GSH level change induced by bioreducible PPI-CBAs to intracellular ROS level was examined to reveal the reason for unexpected cytotoxicity of PPI-CBAs. As controls, PPI G1 and linear bioreducible polymer, poly(CBA-DAB) were also used.

In Figure 13, it was observed that the increasing concentration of PPI G1 and poly(CBA-DAB) did not change the intracellular ROS level, which means that PPI, repeating unit of PPI-CBAs and linear bioreducible polymer does not affect the intracellular ROS level. No cytotoxicity of PPI G1 and poly(CBA-DAB) was identified in this work and the previous report, respectively [139]. However, the intracellular ROS levels were broadly increased with the increase of treated PPI-CBAs concentration. The ROS levels at 50 ㎍/mL of the polymer concentration (P4C3, P4C5, and P4C9) were increased to be even about three times higher than ROS level of untreated cells except P4C2 result. Relatively less increased ROS level of P4C2-treated cells may be related with less decrease of intracellular GSH level derived from P4C2 treatment. A rough correlation between the ROS levels and CBA portion in PPI-CBAs was observed in this result. This result suggested a possibility in

which the cytotoxicity of PPI-CBAs might be induced by the increase of ROS levels accompanied by decrease of GSH levels in cells and demonstrates that the cytotoxicity of bioreducible polymers may be closely related with the polymer structures. Scheme 3 shows the schematic diagram for intracellular degradation behaviors of PPI-CBAs.

The reason for difference of cytotoxicity between other crosslinked bioreducible polymers and PPI-CBAs were not revealed now but one possible explanation is that small degraded fragments of PPI-CBAs may have higher reactivity to re-crosslinking than other polymers probably due to small size of PPI G1 or short distance between reactive thiols of PPI G1 terminals.

3.3. Summary

Crosslinked bioreducible polymer, PPI-CBAs were synthesized for gene delivery systems. They could form positively charged and nano-sized polyplexes with pDNA. Interestingly, PPI-CBA polyplexes showed high stability in reducing condition, probably due to the re-crosslinking of PPI-CBA fragments. PPI-CBAs showed lower transfection efficiency than PEI25k in serum-free condition but comparable efficiency with PEI25k in serum condition, which means PPI-CBAs possessed good serum-compatibility. However,

cytotoxicity of PPI-CBAs was significant and increased with concentration and crosslinking degree. Decreased intracellular GSH and increased ROS levels with increase of the crosslinking degree suggest that GSH consumption probably due to re-crosslinking of degraded PPI-CBAs in cytosol may induce the increase of intracellular cytotoxic ROS. Therefore, unlike linear bioreducible polymers, crosslinked bioreducible polymer, PPI-CBAs show unique degradation and intracellular behaviors based on their crosslinked structures. This study would provide a deeper insight into the development of bioreducible polymeric gene carriers.

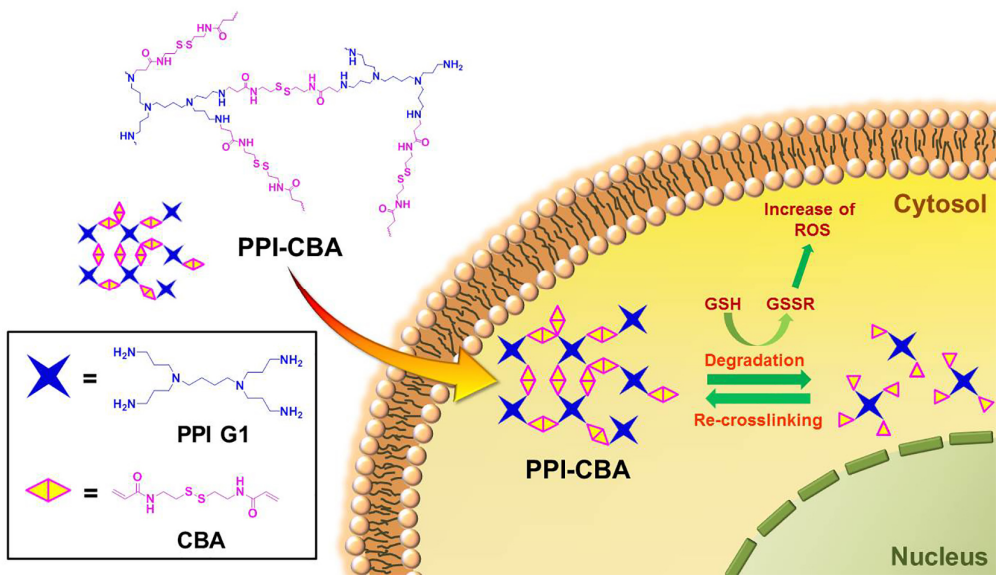

Scheme 3. Schematic diagram for the reductive degradation behaviors of PPI-CBA in cytoplasm [157].

Chapter 4. Fluoroalkylated Arginine-functionalized Bioreducible Polymer for Gene Delivery

4.1. Materials and Methods

4.1.1. Materials

N-butoxycarbonyl-1,6-hexanediamine (N-Boc-DAH), cystamine bisacrylamide (CBA), trifluoroacetic acid (TFA), triisopropylsilane (TIS), N,N-diisopropylethylamine (DIPEA), agarose, ethidium bromide, genistein (Geni), gel loading solution, sodium acetate, polyethylenimine (PEI25k, 25 kDa), 3-(4,5-dimethrylthiazol-2-yl)-2,5-diphenyltetrazolium bromide (MTT), and 4',6-diamidino-2-phenylindole dihydrochloride (DAPI) were purchased from Sigma-Aldrich (USA). Fmoc-Arg(Pbf)-OH was obtained from AnaSpec (USA). Methyl heptafluorobutyrate (MHFB) and methyl butyrate (MB) was obtained from Alfa Aesar (USA). Cytochalasin D (Cyto D) was purchased from Tocris (UK). Chlorpromazine (Chlor) was bought from TCI (Tokyo Chemical Industry Co., Ltd., Japan). Tris base, dimethylformamide (DMF), 2-(1H-benstriazole-1-yl)-1,1,3,3-tetramethyluronium

hexafluorophosphate (HBTU), heparin sodium salt (from porcine intestinal mucosa, ≥150 IU/mg), nocodazole (Noco), and methanol was purchased from Merck (Germany). HPLC grade water was purchased from Duksan (Korea). DL-dithiothreitol (DTT) was purchased from Biosesang (Korea). pDNA (pCN-Luci and gWIZ-GFP) was amplified by using Escherichia *coli* DH5α and obtained by using Nucleobond Xtra Midi kit (Macherey-Nagel, Germany). Dulbecco's Modified Eagles' Medium (DMEM), Dulbecco's phosphate buffered saline (DPBS), fetal bovine serum (FBS), penicillin-streptomycin (P/S), trypsin-EDTA (0.25%), Quant-iT™ PicoGreen® kit, and YOYO-1 iodide (1 mM solution in DMSO) were purchased from Invitrogen-Gibco (USA). Luciferase assay system and reporter lysis buffer were purchased from Promega (USA). BCA™ protein assay kit was purchased from PIERCE (USA). All other chemicals were purchased and used without further purification.

4.1.2. Synthesis of PCH

In advance of FR-PCH (heptafluorobutyrated arginine functionalized poly(cystamine bisacrylamide-diaminohexane)) synthesis, PCH (poly(cystamine bisacrylamide-diaminohexane))and R-PCH (arginine functionalized

poly(cystamine bisacrylamide-diaminohexane))were synthesized through Michael addition reaction. First, one gram of CBA and equivalent amount of N-Boc-DAH were dissolved and reacted in 4 mL of methanol/water solution (9:1, v/v). The reaction temperature was 60 ℃. After 5 days of reaction under N_2 atmosphere in the dark, 10% mole of N-Boc-DAH were added to quench residual acrylamide of CBA. After 2 days of reaction, PCH with Boc was precipitated with diethyl ether. The centrifugation condition was 4000 rpm, 10 min at 4 ℃. By using vacuum chamber, residual diethyl ether was dried overnight. To detach primary amine protection group Boc, the product was dissolved and incubated in Boc deprotection solution (TFA:TIS:dH_2O = 95:2.5:2.5, v:v:v) for 30 min on ice bath. Then, the product solutions purified by two times of diethyl ether precipitation and 48 h of dialysis against ultra-pure water using dialysis membranes (MWCO = 2,000). The product, PCH, was obtained after lyophilization.

4.1.3. Synthesis of FR-PCH and HR-PCH

R-PCH was synthesized by conjugating Fmoc-Arg(Pbf)-OH to primary amine of PCH. To conjugate, HBTU and DIPEA were additionally mixed in DMF. The reaction was performed under N_2 atmosphere at room temperature. After 2 days, Fmoc deprotection

was proceeded to prepare further modification. 20% piperidine (in DMF) was used for deprotection solution. The deprotection reaction was performed at room temperature for 30 min. Then, it was precipitated with diethyl ether twice. The centrifugation condition was 4000 rpm, 10 min at 4 ℃. To remove residual ether, vacuum chamber was used.

As a result of Fmoc deprotection, primary amine of conjugated arginine was exposed to synthesize FR-PCH and HR-PCH (butyrated arginine functionalized poly(cystamine bisacrylamide-diaminohexane)). MHFB with a series of molar ratio was used to synthesize FR-PCH, and MB was used to make HR-PCH as a control. To synthesize FR-PCH and HR-PCH, R-PCH with Pbf and MHFB (or MB) were dissolved in DMF. The reaction was proceeded at room temperature for 24 h. After the reaction, diethyl ether precipitation was carried out. Then, Pbf was removed. Vacuum dried pellets were dissolved in deprotection solution (TFA:TIS:dH_2O = 95:2.5:2.5, v:v:v). After 30 min deprotection at room temperature, ether precipitation was carried out twice for purification. The precipitates were dried in vacuum chamber overnight. To obtain purified products (FR-PCH and HR-PCH), dialysis (MWCO: 2,000) against distilled water and subsequent lyophilization were carried out.

4.1.4. Characterization of the polymers

The synthesis of the polymers was confirmed by ^{1}H NMR (600 MHz, AVANCE 600, Brucker, Germany). The molecular weight of PCH was measured by gel permeation chromatography (GPC) (YL-9100, Young Lin Instrument, Korea). The samples were dissolved at a concentration of 10 mg/mL. The assay was run on Ultrahydrogel™ Linear column (Waters, USA) with 1% formic acid as an eluent at 0.6 mL/min of flow rate. Poly(ethylene glycol)s with various molecular weights were used as standards for analysis.

4.1.5. Agarose gel electrophoresis

pDNA condensing ability of the polymers was examined by agarose gel electrophoresis. The polyplexes were prepared in HEPES buffer (pH 7.4) at various weight ratios ranging from 0.5 to 10. Agarose gel (0.7% w/v) containing ethidium bromide solution (0.5 ㎍/mL) was prepared in TAE (Tris-Acetate-EDTA) buffer. After 30 min of incubation at room temperature, the samples were electrophoresed at 100 V for 12 min. The polyplexes were also incubated in the presence of 5 mM DTT for 30 min at 37 ℃ and electrophoresed in order to examine the behavior of the polyplexes in reducing condition. The pDNA bands were visualized with UV

illuminator (GelDoc XR+ gel documentation system, Bio-Rad, USA).

4.1.6. Agarose gel electrophoresis with heparin

To examine binding affinity of polymers to pDNA, polyplexes were incubated in the presence of heparin. The detail of experiment was almost same with agarose gel electrophoresis in the presence of DTT as mentioned above (section 4.1.5). The only difference was the incubation of heparin instead of incubation of DTT. After formation of polyplexes, the polyplexes were incubated for 30min with various concentration of heparin (0 - 1000 ㎍/mL). All polyplexes used in this experiment was prepared at a weight ratio of 10 except for PEI25k; PEI25k was prepared at a weight ratio of 1.

4.1.7. Average size and Zeta-potential value measurement of the polyplexes

The average size and Zeta-potential values of the polyplexes were measured by using Zeta-sizer Nano ZS (Malvern Instruments, UK) with He-Ne laser beam (633 nm) at 25 ℃. 0.5 mL of polyplex solutions (0.5 ㎍ pDNA) were prepared in ultra-pure water at various weight ratios ranging from 0.5 to 20. After 30 min of incubation, the solutions were diluted to final volume of 1 mL. The

measurements were performed 3 times.

4.1.8. PicoGreen assay

PicoGreen assay was performed to examine the degradation behavior of polyplexes quantitatively by detecting the dissociated pDNA from the polyplex in reducing condition. After formation of polyplex in TE buffer at weight ratio of 10, each polyplex was incubated in 5 mM DTT solution for pre-determined time; 0, 0.5, 1, 1.5, 2, 3, 4 h, respectively. Then, PicoGreen reagent dissolved in TE buffer was added to the polyplex solution and incubated for 4 min. Fluorescence was measured with an excitation wavelength of 480 nm and emission wavelength of 520 nm using a microplate reader (Synergy H1, BioTek, USA). Results were presented as a relative fluorescence intensity (RFI, percentage values relative to value of pDNA only). All experiments were performed in triplicate.

4.1.9. Cytotoxicity of polymers

The cytotoxicity of the polymers was estimated by MTT assay. A549 (adenocarcinomic human alveolar basal epithelial cell line), HeLa, and C2C12 (immortalized mouse myoblast cell line) were maintained in DMEM supplemented with 10% FBS and 1% P/S in humidified atmosphere containing 5% CO_2 at 37 ℃. Then, the cells

were seeded on a 96-well cell culture plate at a density of 1 x 10^4 cells/well in 100 μL of DMEM containing 10% FBS and 1% P/S. As the cells achieved 70-80% confluency after 24 h of incubation, the cells were treated with polymer solutions (serum-free DMEM) with various concentrations for 4 h. PEI25k was used as control. Then, the media were exchanged with fresh DMEM containing 10% FBS. After 24 h of incubation, 25 μL of MTT solution (2 mg/mL in DPBS) was added to each well and further incubated for 2 h. The media were carefully removed and 150 μL of DMSO was added to each well to dissolve formazan crystal formed by proliferating cells. The absorbance was measured at 570 nm by using a microplate reader. Results were presented as relative cell viability (RCV, percentage values relative to value of untreated control cells). All experiments were performed in quadruplicate.

4.1.10. Lactate dehydrogenase (LDH) assay

A549, HeLa, and C2C12 cells were seeded on a 96-well culture plate at a density of 0.4 x 10^4 cells/well. After achieving 70-80% confluency, the cells were treated with polymer solutions with a series of concentration for 4 h. Then, the media (100 μL) was collected and LDH assay was performed by using LDH Cytotoxicity Detection Kit (Takara Biochemicals, Japan). Measured LDH level

was normalized in terms of percentage to the value of positive control (0.1% Triton-X 100). The assay was performed in triplicate.

4.1.11. Transfection experiments in vitro

A549, HeLa, and C2C12 cells were seeded on a 24-well cell culture plate at a density of 5 x 10^4 cells/well and grown until they achieved 70-80% confluency. Before transfection, medium of each well was exchanged with fresh DMEM for the assay in serum-free condition or with DMEM (10% FBS) for the assay in serum condition, respectively. The cells were then exposed to polyplex solutions (0.5 μg pDNA) with various weight ratios for 4 h. pDNA only and PEI25k polyplex (weight ratio = 1) were used as controls. After exchange with fresh medium containing 10% FBS, the cells were further incubated for 2 days. Then, each medium was aspirated, and the cells were rinsed with DPBS and shaken for 30 min at room temperature with 120 μL of Reporter Lysis Buffer. Luciferase activities of cell lysates (20 μL) were measured by luciferase assay on a microplate reader and the total amounts of cellular proteins were examined by using a BCA™ Protein Assay Reagent Kit. The normalized results were presented in terms of relative light unit (RLU)/mg cellular protein. All experiments were

performed in triplicate.

4.1.12. Observation of GFP (green fluorescence protein) expression

A549, HeLa, and C2C12 cells were seeded on a 6-well culture plate at a density of 2 x 10^5 cells/well. After achievement of 70-80% confluency, the polyplexes containing gWIZ-GFP pDNA (1 μg pDNA, optimal ratio) were treated for 4 h. The treatments were conducted under serum-free or serum condition, respectively. PEI25k polyplex (weight ratio = 1) was used as a control. The GFP expression was examined by fluorescence microscope CELENA S digital imaging system (Logos biosystems, Inc., Korea). The optimal weight ratios of polyplexes were different as follows: PCH (weight ratio 80), R-PCH (weight ratio 40), FR-PCHs (weight ratio 10), and HR-PCH30 (weight ratio 10), respectively.

4.1.13. Cellular uptake of polyplexes

Cells (A549, HeLa, and C2C12) were seeded on a 6-well cell culture plate at a density of 3 x 10^5 cells/well. After they achieved 70-80% confluency, media were exchanged for fresh serum-free DMEM. pDNA labeled with YOYO-1 iodide (1 dye molecule per 50 base pairs of nucleotides) was prepared. The cells were treated with polyplex solutions (1 μg pDNA) at optimal ratio for 4 h. Then,

the media were removed, and the wells were rinsed with ice-cold DPBS twice. After 2 min of trypsinization, the detached cells were re-suspended in DPBS. The cellular uptake of fluorescence-labeled polyplexes was examined by using BD Accuri C6 flow cytometer at a minimum of 1 x 10^4 cells gated per sample. The analysis was performed by using BD Accuri C6 software. The optimal weight ratios of polyplexes were different as follows: PCH (weight ratio 80), R-PCH (weight ratio 40), FR-PCHs (weight ratio 10), and HR-PCH30 (weight ratio 10), respectively.

4.1.14. Polyplex stability test

To investigate stability of polyplexes in different solutions (dH_2O and 10% FBS), particle size change along with time was measured. The experimental methodology was similar to DLS experiment described above (section 4.1.7). PEI25k (WR1) was used as control. The polyplexes were prepared at their optimal ratios. Then, particle size was measured with Zeta-sizer at pre-determined time; 0, 3, 6, 12, 24 h. The optimal weight ratios of polyplexes were different as follows: R-PCH (weight ratio 40), FR-PCH30 (weight ratio 10), and HR-PCH30 (weight ratio 10), respectively.

4.1.15. Serum resistance test

A549, HeLa, and C2C12 cells were seeded on a 24-well cell culture plate at a density of 5 x 10^4 cells/well and grown until they achieved 70-80% confluency. Before transfection, medium of each well was exchanged with fresh DMEM containing various FBS concentrations; 0, 10, 30, 50%, respectively. The cells were then exposed to polyplex solutions (0.5 ㎍ pDNA) at their optimal weight ratios for 4 h. The optimal weight ratios of polyplexes were different as follows: R-PCH (weight ratio 40), FR-PCH30 (weight ratio 10), and HR-PCH30 (weight ratio 10), respectively. PEI25k polyplex (weight ratio = 1) was used as control. After exchange with fresh medium containing 10% FBS, the cells were further incubated for 2 days. Then, each medium was aspirated, and the cells were rinsed with DPBS and shaken for 30 min at room temperature with 120 ㎕ of Reporter Lysis Buffer. Luciferase activities of cell lysates (20 ㎕) were measured by luciferase assay on a microplate reader and the total amounts of cellular proteins were examined by using a BCA™ Protein Assay Reagent Kit. The normalized results were presented in terms of relative light unit (RLU)/mg cellular protein. All experiments were performed in triplicate.

4.1.16. Cellular Uptake Mechanism Analysis

Cells (A549, HeLa, and C2C12) were seeded on a 6-well cell culture plate at a density of 3 x 10^5 cells/well. After they achieved 70-80% confluency, media were exchanged for fresh serum-free DMEM containing cellular uptake inhibitors were treated for 30 min; Cyto D (macropinocytosis inhibitor, 10 μg/mL), Geni (caveolae-mediated endocytosis inhibitor, 200 μM), Noco (microtubule-mediated endocytosis inhibitor, 33 μM), or Chlor (clathrin-mediated endocytosis inhibitor, 10 μM). pDNA labeled with YOYO-1 iodide (1 dye molecule per 50 base pairs of nucleotides) was prepared. The cells were treated with FR-PCH30 polyplex solutions (1 μg pDNA) at optimal ratio of 10 for 4 h. Then, the media were removed, and the wells were rinsed with ice-cold DPBS twice. After 2 min of trypsinization, the detached cells were re-suspended in DPBS. The cellular uptake of fluorescence-labeled polyplexes was examined by using BD Accuri C6 flow cytometer at a minimum of 1 x 10^4 cells gated per sample. The analysis was performed by using BD Accuri C6 software.

Cellular uptake behavior was also investigated by conducting TRF assay. Cells were seeded on a 24-well culture plate at a density of 5 x 10^4 cells/well. After achieving 70-80% of confluency, pre-treatment was performed for 30 min with the media containing the inhibitors; Cyto D, Geni, Noco, Chlor. When the pre-treatment was

completed, polyplexes were treated for 4 h in serum-free DMEM. R-PCH was used at a weight ratio of 40, and FR-PCH30 was used at a weight ratio of 10. After media exchange with serum-containing fresh DMEM, the cells were further incubated for 2 days. Further transfection assay was performed by identical method to above procedure.

4.1.17. Confocal laser scanning microscope (CLSM) observation

Intracellular behavior of treated polyplexes was observed by confocal laser scanning microscope (SP8 X, Leica, Germany). The optimal weight ratios of polyplexes were different as follows: PCH (weight ratio 80), R-PCH (weight ratio 40), FR-PCH30 (weight ratio 10), and HR-PCH30 (weight ratio 10), respectively. PEI25k (weight ratio = 1) was used as control. Cells were seeded on confocal dish at a density of 3×10^5 cells/dish. After they achieved 70-80% confluency, polyplexes prepared at their optimal weight ratio were treated for 4 h. YOYO-1 iodide labeled pDNA was used for the experiment. Then, LysoTracker RED DND-99 and DAPI was used for dyeing organelles. The images were processed through LAS X (Leica Application Suite X) software.

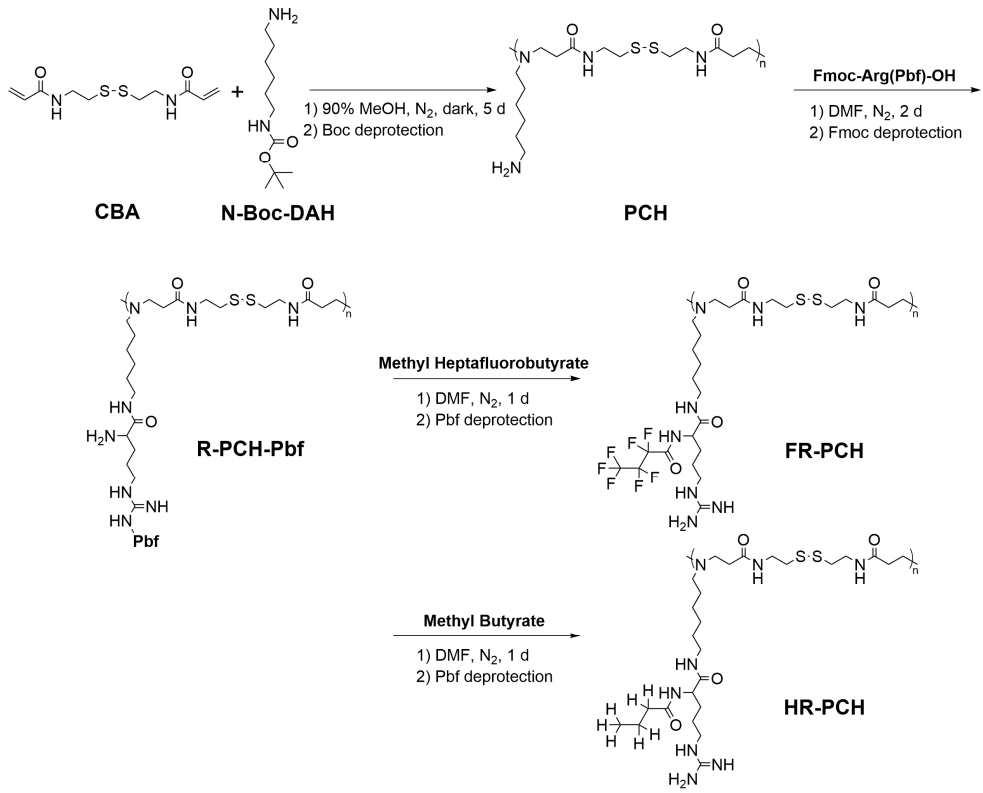

Scheme 4. Synthetic scheme of FR-PCH and HR-PCH.

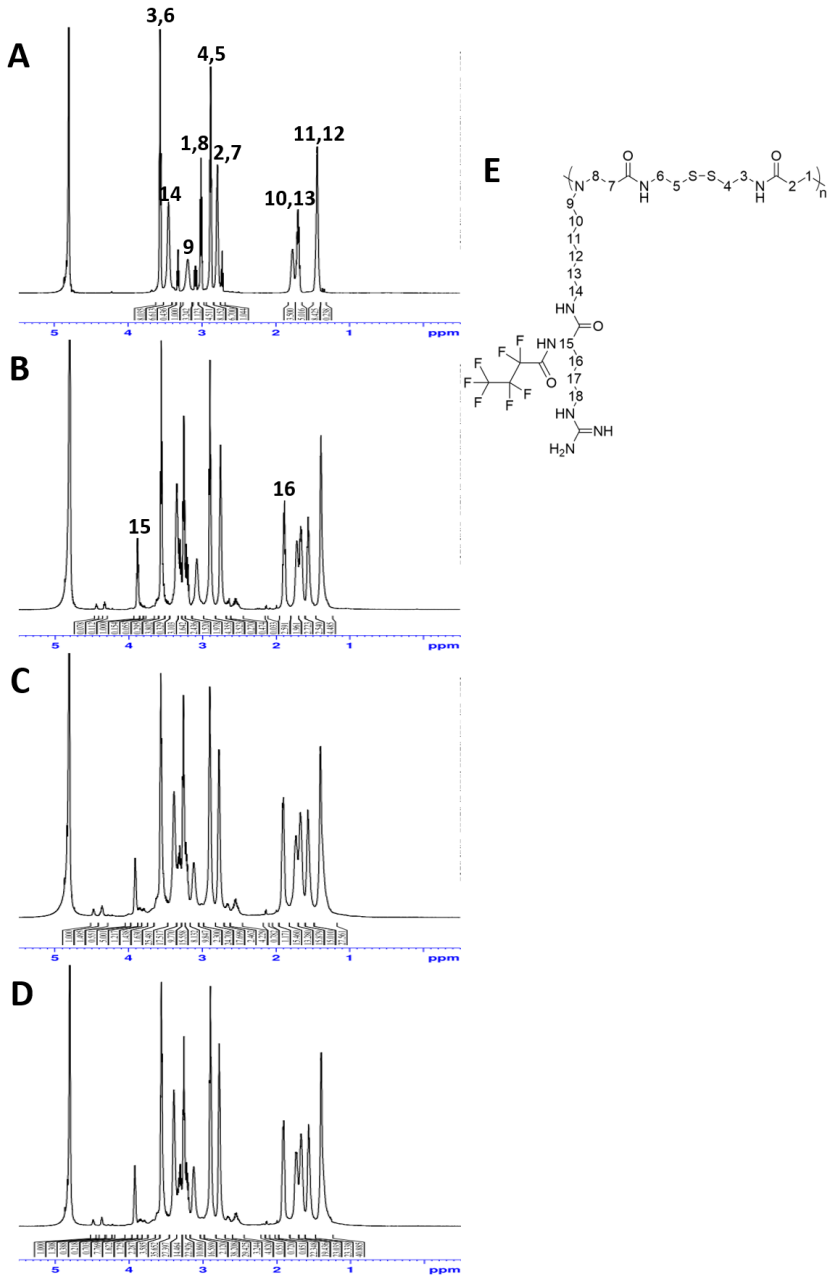

Figure 14. ^{1}H NMR spectra of the synthesized polymers. (A) PCH, (B) R-PCH, (C) FR-PCHs, (D) HR-PCH. (E) is numbered structure of FR-PCH.

4.2. Results and discussion

4.2.1. Synthesis and Characterization of polymers

To synthesize PCH, CBA and N-Boc-DAH were reacted through Michael addition reaction. After arginine grafting (R-PCH), MHFB and MB were reacted to R-PCH to prepare FR-PCH and HR-PCH, respectively. A series of feed ratios (R-PCH:MHFB = 1:0.1, 1:0.5, and 1:0.75) were set to compare their characteristics, and HR-PCH (R-PCH:MB = 1:0.75) was made as control for FR-PCH. Fluorination with the higher feed ratios also have been performed, but the experiments did not produce FR-PCHs with higher degree of modification. It was thought that instability of the reagents and emerging steric hindrance along with the progress of synthesis prevented MHFB and MB from reacting with primary amine of arginine. The synthesis scheme displaying expected polymer structure is presented in Scheme 4. The synthesis of the polymers was confirmed by ^{1}H NMR (Figure 14) as follows.

^{1}H NMR of PCH(D_2O): δ DAH ($-NH_2CH_2C\mathbf{H_2}C\mathbf{H_2}CH_2CH_2CNH_2$) = 1.40, δ DAH ($-NH_2C\mathbf{H_2}CH_2CH_2C\mathbf{H_2}CH_2CNH_2$) = 1.61-1.66, δ DAH ($-N\mathbf{H_2}CH_2CH_2CH_2CH_2CH_2CNH_2$) = 3.12, δ DAH ($-NH_2CH_2CH_2CH_2CH_2C\mathbf{H_2}CNH_2$) = 3.37, δ CBA ($-NCH_2C\mathbf{H_2}CONHCH_2CH2SS-$) = 2.77, δ CBA ($-CH_2C\mathbf{H_2}SSC\mathbf{H_2}CH_2-$) = 2.83, δ CBA (-

$NCH_2CH_2CONHC\mathbf{H_2}CH_2SS-$) = 3.52

^{1}H NMR of R-PCH, FR-PCH, HR-PCH(D_2O): δ Arginine (-$COCH(NH_2)C\mathbf{H_2}CH_2CH_2NHC(NH)CNH_2$) = 1.82, δ Arginine (-$COCH(NH_2)CH_2CH_2C\mathbf{H_2}NHC(NH)CNH_2$) = 3.22, δ Arginine (-$COC\mathbf{H}(NH_2)CH_2CH_2CH_2NHC(NH)CNH_2$) = 3.77

In the case of PCH, experimental ratios of polymer composition between CBA and DAH were calculated by comparing the integrals of specific protons from DAH (-$NH_2C\mathbf{H_2}CH_2CH_2C\mathbf{H_2}CH_2CNH_2$) and CBA (-$NCH_2CH_2CONHC\mathbf{H_2}CH_2SS-$). To confirm arginine grafting, the integrals of protons from arginine (-$COC\mathbf{H}(NH_2)CH_2CH_2CH_2NHC(NH)CNH_2$) and CBA (-$NCH_2CH_2CONHC\mathbf{H_2}CH_2SS-$) were used for calculation. The grafting of arginine was found that almost 100% of primary amines were conjugated with arginine. In the case of fluorination and alkylation, as they conjugated to R-PCH, the integral of proton derived from arginine (-$COC\mathbf{H}(NH_2)CH_2CH_2CH_2NHC(NH)CNH_2$) was diminished. Therefore, the diminished integral was calculated by comparing the integral of R-PCH, FR-PCH, and HR-PCH. The conjugation result was confirmed as 29.4, 35.3, 44.4, and 28.7, respectively. Table 3 shows the chemical properties of the polymers synthesized. FR-PCH and HR-PCH were named after the modification degree; FR-PCH30, FR-PCH35, FR-PCH45, and HR-PCH30, respectively.

Table 3. Chemical properties of synthesized polymers.

	Feed ratio (primary amine: reagent)	Degree of modification (%) [a)]	M_n (kDa)
PCH	–	–	7.9
R-PCH	–	–	11.6
FR-PCH30	1:0.1	29.4	12.9
FR-PCH35	1:0.5	35.3	13.2
FR-PCH45	1:0.75	44.4	13.6
HR-PCH30	1:0.75	28.7	12.2

[a)] Degree of modification means that the modification degrees of fluorination and alkylation, respectively.

The fluorination degree was increased along with the increase of MHFB amount added; however, it was not well correlated with feed ratio. The discordance between feed ratio and composition ratio was thought that it would be derived from the low stability of MHFB and MB during the reaction and steric hindrance. In previous report, HFBA was used as fluorination reagent to make fluorinated PEI2k [158]. In that study, fluorination degree was also not regular along with the feed ratio. It was thought that instability of anhydride form fluorination reagent affected the modification degree, so more stable form of reagent was chosen; it was more controllable than HFBA. Emerging steric hindrance along with reaction progress also would be a significant factor.

Molecular weight of PCH was measured by GPC. The result of other samples was irregular and uncertain. It was thought that grafted moieties such as arginine, MHFB, and MB interfered accurate measurement; they might interact with column used for GPC excessively. In addition, there are several differences between PEG standards used in GPC and the polymers such as charge and side chains. GPC only measures relative molecular weight of polymer by comparing calibration curve derived from standards. As a result, molecular weight of polymers was calculated based on ^{1}H NMR analysis and GPC result of PCH as shown in Table 3.

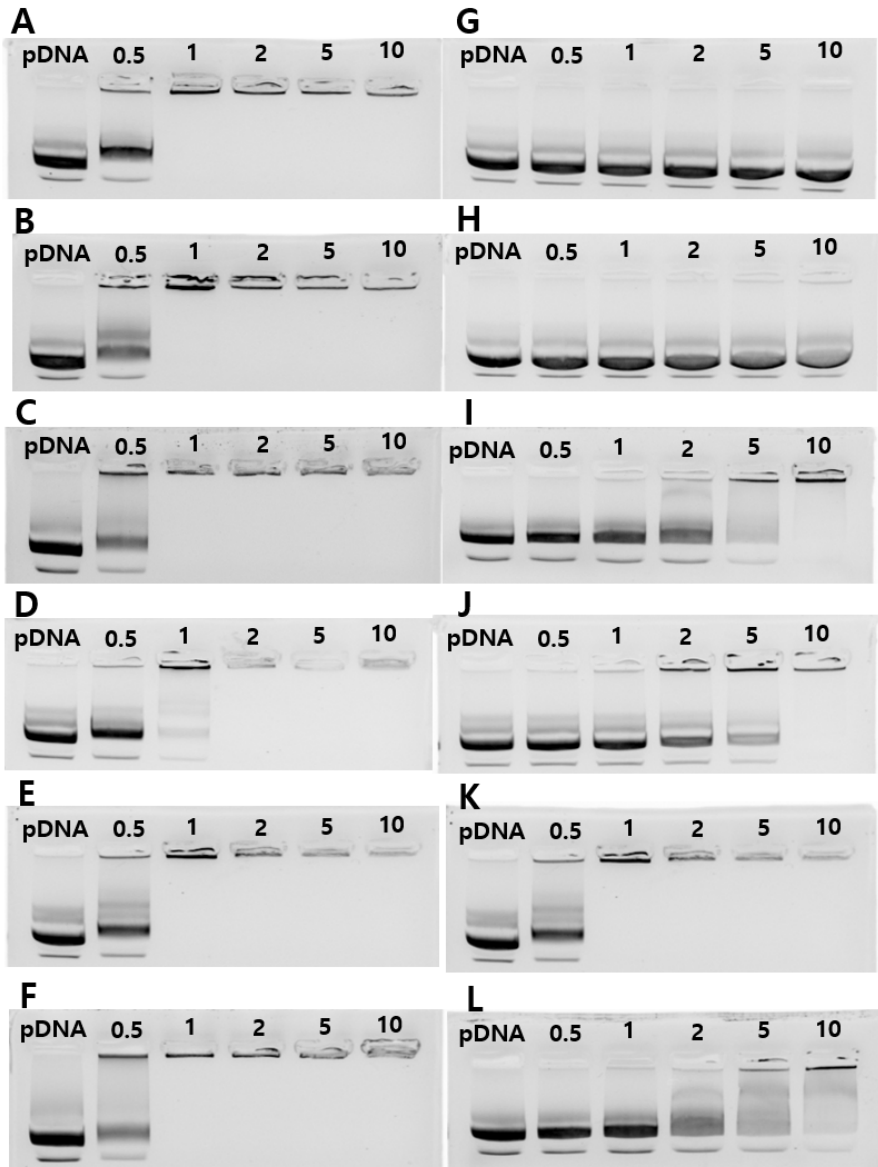

Figure 15. Agarose gel electrophoresis in the absence of DTT (A–F) and in the presence of DTT (5 mM) (G–H). (A) and (G): PCH, (B) and (H): R–PCH, (C) and (I): FR–PCH30, (D) and (J): FR–PCH35, (E) and (K): FR–PCH45, (F) and (L): HR–PCH30. Numbers show the weight ratios of polyplexes.

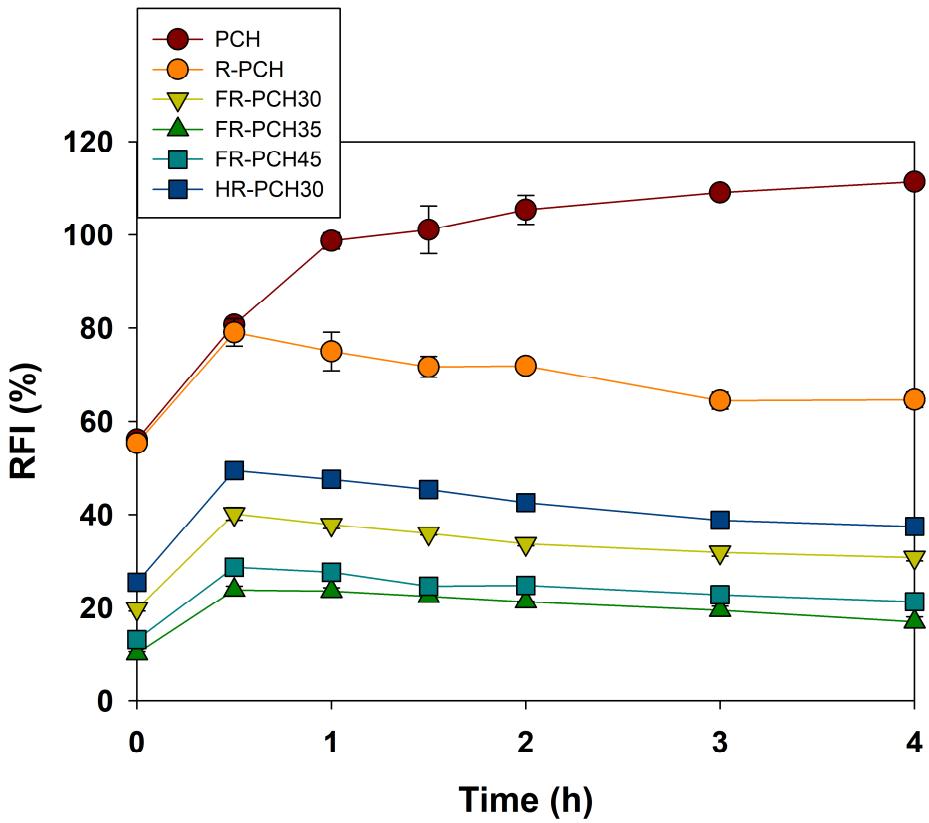

Figure 16. PicoGreen assay result. All polyplexes were prepared at a weight ratio of 10 except PEI25k which was prepared at weight ratio 1. Results were presented as a relative fluorescence intensity (RFI, percentage values relative to value of pDNA only).

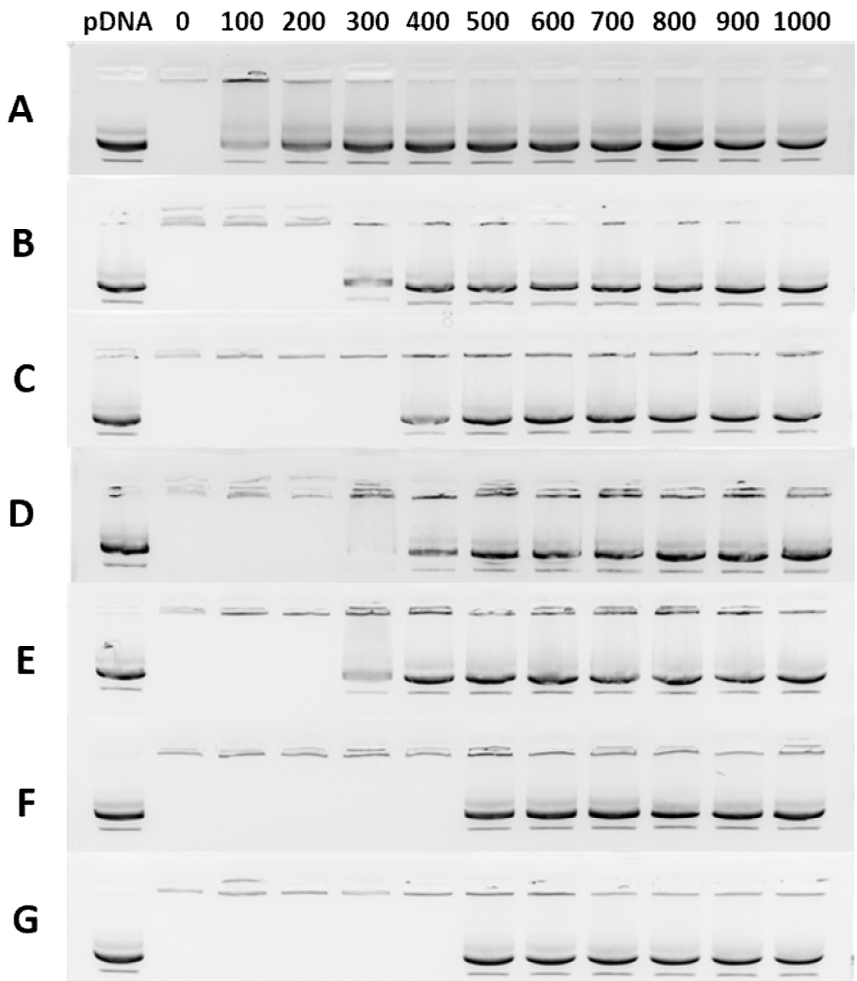

Figure 17. Agarose gel electrophoresis results in the presence of various concentration of heparin. (A): PEI25k, (B): PCH, (C): R-PCH, (D): FR-PCH30, (E): FR-PCH35, (F): FR-PCH45, (G): HR-PCH30. All polyplexes were prepared at a weight ratio of 10. Numbers display the concentration of heparin (μg/mL).

4.2.2. Characterization of polyplexes

To estimate polyplex forming ability and confirm the behaviors in reducing environment, agarose gel electrophoresis was conducted. As shown in Figure 15, all polymers except FR-PCH35 can retard pDNA at weight ratio of 1. In the case of FR-PCH35, it retarded pDNA at weight ratio of 2. It was thought that primary amine consumption due to fluorination undermined polyplex forming ability.

In the meanwhile, in the case of FR-PCH45, it recovered polyplex forming ability. It was thought that conjugated fluoroalkyl chain compensated the function of consumed primary amines. When it comes to agarose gel electrophoresis in reducing condition, all polymers except FR-PCH45 released their cargo successfully. It was thought that hydrophobic interaction of fluoroalkyl chains were still retarded pDNA even in the presence of reductant.

PicoGreen assay was used to confirm degradation behavior of polyplexes in reducing condition (Figure 16). From the result, there was apparent difference of degradation behavior. FR-PCHs and HR-PCH did not emit high level of fluorescence. It means that they still bound pDNA repelling dyes. It can be thought that they can maintain aggregated form by exploiting the hydrophobic interaction of fluoroalkyl and alkyl chains.

For further examination on DNA affinity of the polymers, agarose

gel electrophoresis in the presence of heparin was conducted; all polyplexes except PEI25k (WR 1) were prepared at a weight ratio of 10 (Figure 17). In this experiment, heparin which is negative charge-containing polysaccharide was used as competitor of pDNA. PEI25k could not retard pDNA in all concentration range. It just partially retarded at a heparin concentration of 100 ㎍/mL displaying blurred band of pDNA. While PCH started to release pDNA at a concentration of 300 ㎍/mL, R-PCH released pDNA at a concentration of 400 ㎍/mL; DNA retardation ability was improved. It was thought that arginine affected the improvement. Even though the molecular weight was increased due to arginine conjugation (from 7946 to 11621 Da), it was thought that introduction of guanidine group in addition to the presence of primary amine on arginine compensated the effect of molecular weight difference; NP (the ratio of nitrogen in polymer to phosphate in nucleic acid) ratio was increased from 35.41 (PCH) to 50.05 (R-PCH). In terms of charge density and molecular weight (NP ratio), the early release of pDNA in FR-PCH30 and FR-PCH35 can be explained. Due to the fluorination, primary amines of arginine were consumed, and the molecular weight was increased. Both factors decreased NP ratio of the polymers resulting earlier release of pDNA than R-PCH; NP ratios of two polymers were 44.93 and 44.01 at a weight ratio of 10,

respectively.

However, in the case of FR-PCH45, the decrease of NP ratio (42.67 at a weight ratio of 10) was compensated due to plenty of fluoroalkyl chain; it was thought that there was enough amount of fluoroalkyl chain for further retardation. As a result, the retardation ability FR-PCH45 was enhanced. In the case of HR-PCH30, it showed superior binding affinity to FR-PCH30. It was thought that two factors were related. One is NP ratio. The other is bulkiness of fluoroalkyl chain. NP ratio of FR-PCH30 is 44.93, and that of HR-PCH30 is 48.01. It means that HR-PCH30 has more nitrogen used for DNA binding. In the meanwhile, fluorine has slightly larger atomic diameter than hydrogen; 147 pm and 120 pm, respectively [159]. MHFB and MB have same number of carbons; the only difference is fluorine and carbon. Due to the larger size of fluorine, fluoroalkyl chain is usually bulkier and more rigid than alkyl chain [160]. Due to such properties of fluoroalkyl chain, it was thought that FR-PCH30 could not form compact polyplexes relative to HR-PCH30 allowing heparin to interact with the polymers. Summarizing these, lower NP ratio and the properties of fluoroalkyl chain made FR-PCH30 release pDNA earlier than HR-PCH30.

Through the result of DLS, particle size and Zeta-potential of polyplexes were revealed (Figure 18). In terms of particle size,

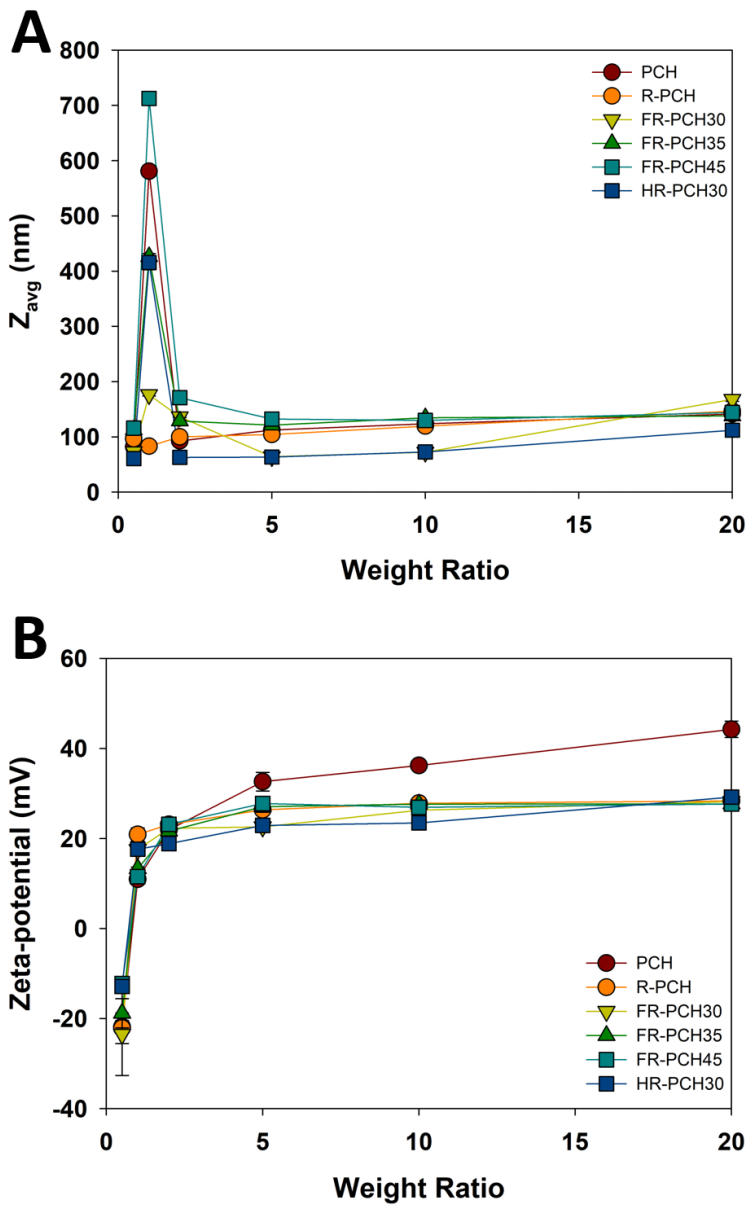

Figure 18. Average size (A) and Zeta-potential value (B) measurement of the polyplexes.

although there was minor difference, the trend was very similar. Most particle sizes were under 200 nm; it means that the polymers formed compact polyplexes. However, the particle size of them soared at weight ratio of 0.5. It was thought that combination of low Zeta-potential and hydrophobic interaction might drive them to aggregate making relatively large polyplex particles. It is also noteworthy that FR-PCH30 polyplexes made much larger nanoparticle than HR-PCH30; the size of FR-PCH30 was almost 2 time bigger than that of HR-PCH30 in some range of weight ratio. This result confirms that FR-PCH30 made less compact polyplexes than HR-PCH30 as discussed above. In the case of Zeta-potential, all polymers became positive charge at weight ratio of 1. From the result of DLS, it can be concluded that the polymers can form positively charged, compact polyplexes.

4.2.3. Cytotoxicity of polymers

Confirming cytotoxicity and safety of polymer are important part in developing gene delivery systems. When the vector was injected in body, they must not cause severe side effects. To estimate the suitability, MTT assay and LDH assay were used. Both assays were conducted with three cell lines (A549, HeLa, C2C12, respectively).

MTT assay estimates cellular toxicity of polymer by exploiting

metabolism taking place in mitochondria [161]. When MTT was treated in viable cells, succinic dehydrogenase converts tetrazolium salt form of MTT into formazan crystals which are not soluble in aqueous solutions. Therefore, amount of formazan crystal indicates the cell viability. In all cell lines, MTT assay result of the polymers showed gradually increased cytotoxicity along with the increment of fluorination degree while the cytotoxicity of PCH and R-PCH displayed similar trend and level each other (Figure 19). It was noteworthy that FR-PCH30 and HR-PCH30 showed relatively minimal cytotoxicity. In contrast, FR-PCH35 and FR-PCH45 showed similar trend of cytotoxicity regardless of cell line showing significant cytotoxicity.

As mentioned above, it was known that fluorination can modulate membrane permeability. In other words, fluorinated polymers could interact with cell membrane. Under this background, it can be presumed that the increased cytotoxicity can be derived from the interaction. Because the molecular weight of all the polymers (FR-PCHs and HR-PCH) was not so different, the factor affected cytotoxicity can be the difference in modification. Especially, the only difference between FR-PCH30 and HR-PCH was conjugated side chains.

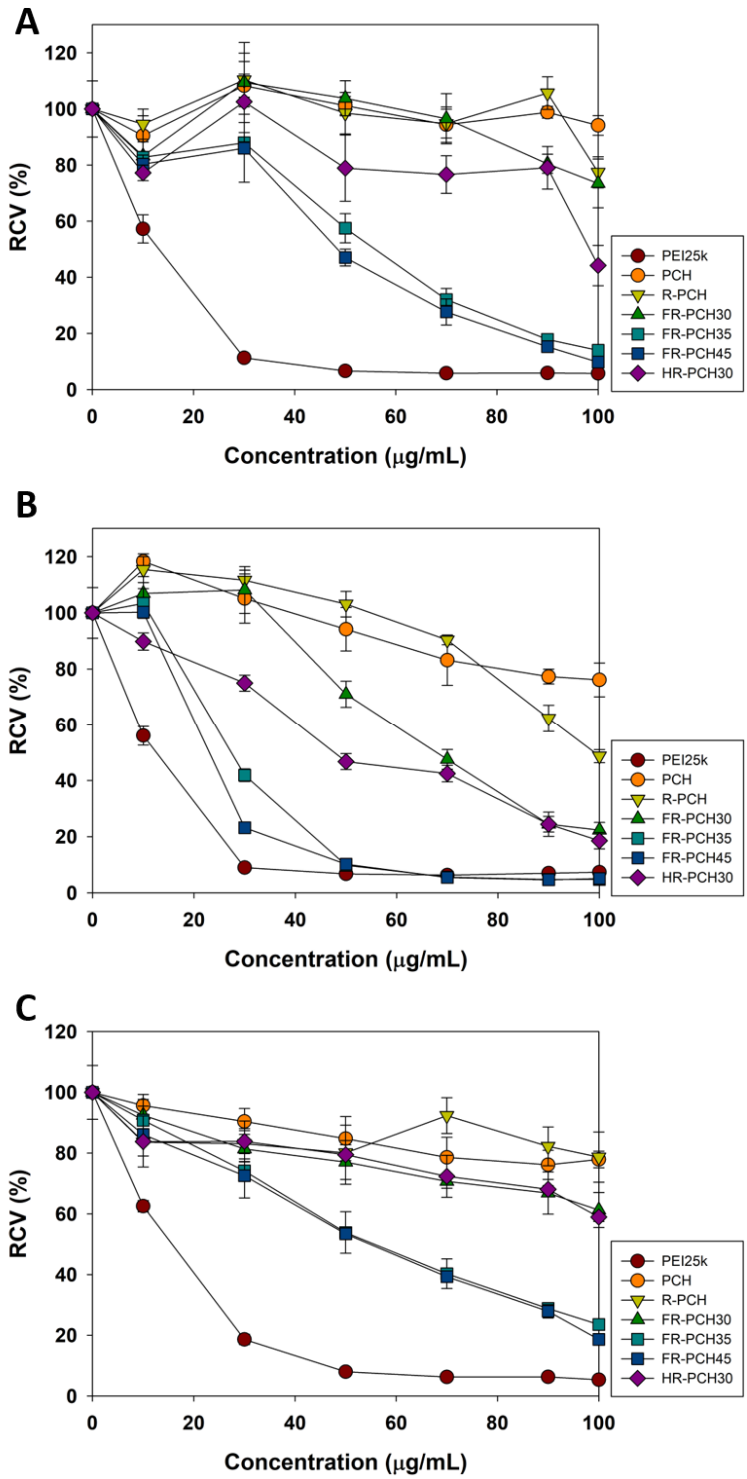

Figure 19. MTT assay result. (A): A549, (B): HeLa, (C): C2C12.

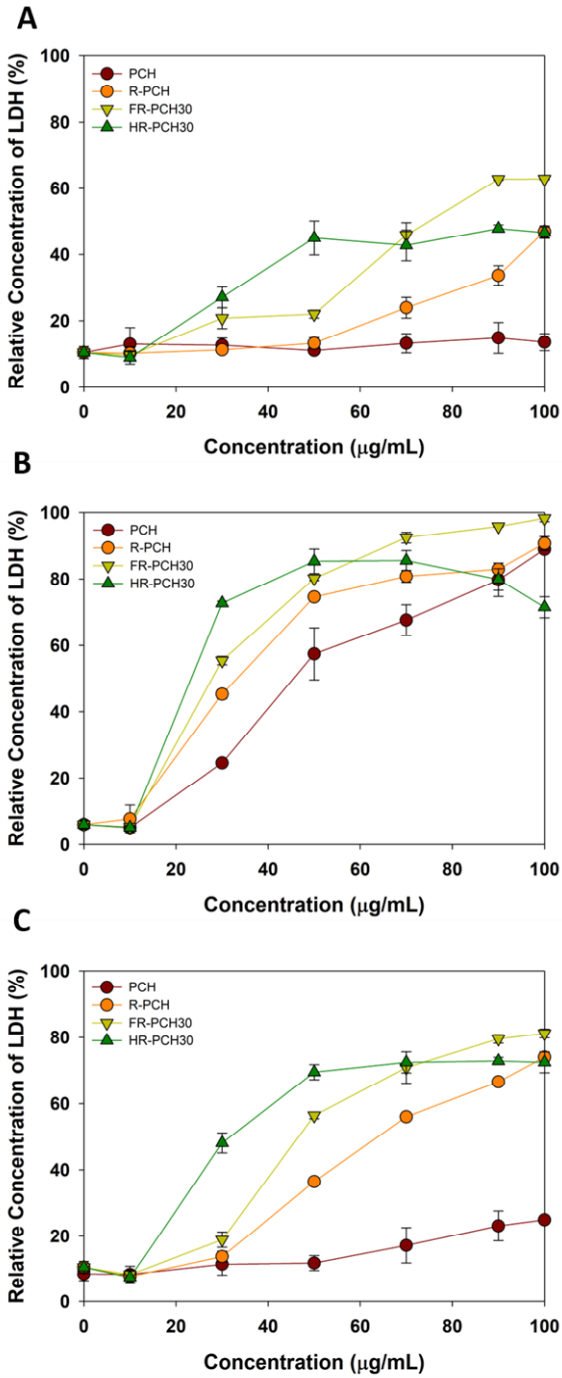

Figure 20. LDH assay result. (A): A549, (B): HeLa, (C): C2C12. The LDH values of Triton X-100 were set as 100%.

To confirm it, LDH assay was performed. As reported previously, more fluorination causes more leakage of LDH [158]. It was apparent that FR-PCH35 and 45 showed higher value than FR-PCH30. As a result, in this experiment, FR-PCH35 and 45 were not used. LDH is a cytoplasmic enzyme present in all cells. It catalyzes reversible transformation of lactate into pyruvate. When cell membrane is intact, it mainly resides in intracellular region; however, when cell membrane was damaged, it can be leaked out from cytoplasm into extracellular region [162]. As a result, it can be used as a marker of cell membrane integrity. As shown in Figure 20, although the overall shape of graphs was different, the trend of increment along with the increase of polymer concentration was apparent implying the polymers interact with the membrane. Interestingly, HeLa cell line showed extremely high values at all polymers; PCH also cause leakage of LDH. It means that cell membrane of HeLa is more vulnerable than the others. As expected, FR-PCH30 and HR-PCH30 showed higher value than the others suggesting the fluorination and alkylation enhances membrane permeability.

Summarizing the results, even though there are many factors causing cytotoxicity, it can be thought that enhanced membrane permeability as a result of the modification may induce membrane

disruption ending up with cytotoxicity.

4.2.4. Transfection efficiency *in vitro*

Transfection efficiency is the most important factor of gene delivery carriers. Not only safety but also efficacy should be tested. Even if the polymer showed good cytotoxicity, if they showed poor transfection result, they cannot be candidates of gene carrier. To demonstrate the efficiency, luciferase assay and GFP expression assay were conducted. Same as cytotoxicity experiments, the experiments were progressed in three cell lines with and without serum condition.

As shown in Figure 21, transfection results were displayed. By using three cell lines, the polyplexes were treated in the absence or presence of 10% FBS. In the case of luciferase assay with C2C12 cell line, the polyplexes were treated up to a weight ratio of 60 because of the cytotoxicity. In all experimental case, all polyplexes except PCH demonstrated the efficiency, which was comparable or superior to PEI25k, a positive control. Comparing the efficiency, FR-PCHs were better than R-PCH implicating the effect of fluorination; the effect became more apparent in the case of serum condition. The diminution of efficiency in serum condition was lesser than other polyplexes such as PEI25k, PCH, and R-PCH.

The improvement of serum tolerance after fluorination was also found in the experiment as previously reported by other researchers [124,133,136].

When it comes to GFP expression, polyplexes at their optimal weight ratio were used (Figure 22-27). In serum condition, GFP expression of PEI25k treated cells dramatically diminished comparing with the expression in non-serum condition. Interestingly, it was found that GFP expression of R-PCH was higher that of FR-PCH30 and HR-PCH30; however, when it considers the result of luciferase assay, it was feasible result. In addition, C2C12 exhibited the highest level of GFP among three cell lines. Overall, the result came out GFP expression assay was consistent with the result of luciferase assay.

From these results, it was found that fluorination had apparent effect on gene delivery efficiency even though in the presence of serum suggesting enhancement of serum tolerance.

4.2.5. Cellular uptake and serum tolerance

In previous section, it was found that fluorination can improve transfection efficiency. This section will analyze the factors affecting transfection efficiency by a series of experiments.

As mentioned above, fluorination is known for improving

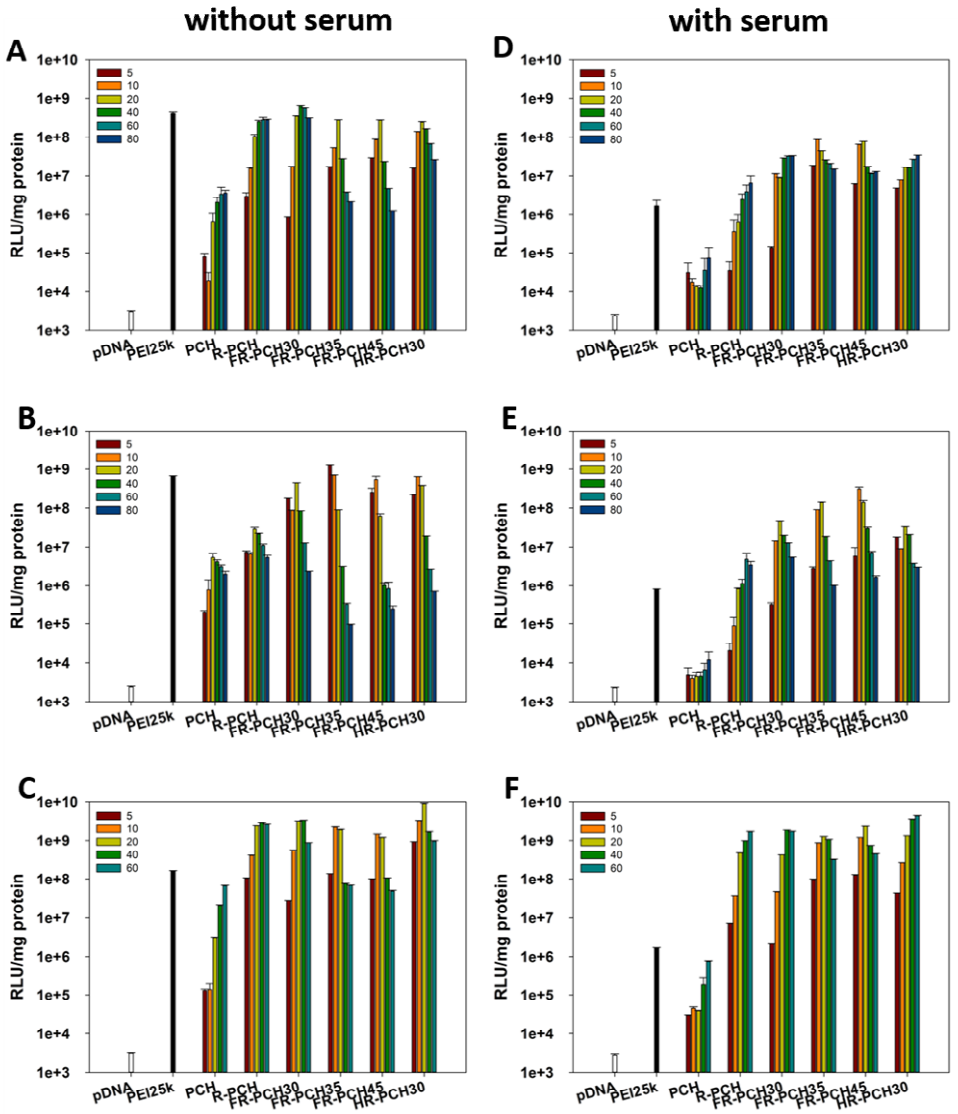

Figure 21. Transfection experiment result in the presence or absence of serum. (A) and (D): A549, (B) and (E): HeLa, (C) and (F): C2C12. The numbers mean weight ratios (WRs) of polyplexes treated.

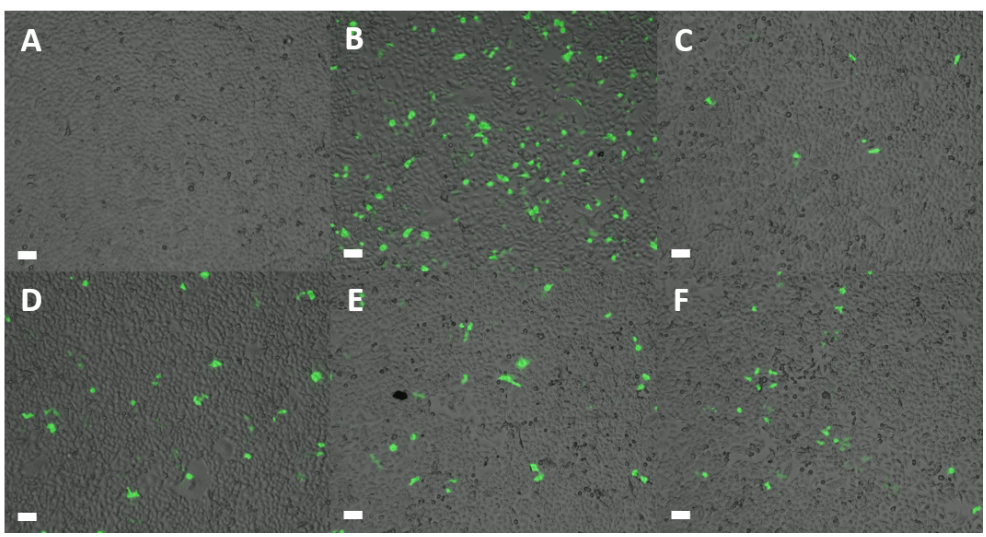

Figure 22. GFP expression result on A549 in the absence of serum. (A): Cell, (B): PEI25k WR1, (C): PCH WR80, (D): R-PCH WR40, (E): FR-PCH30 WR10, (F): HR-PCH30 WR10 (Scale bar: 100 ㎛).

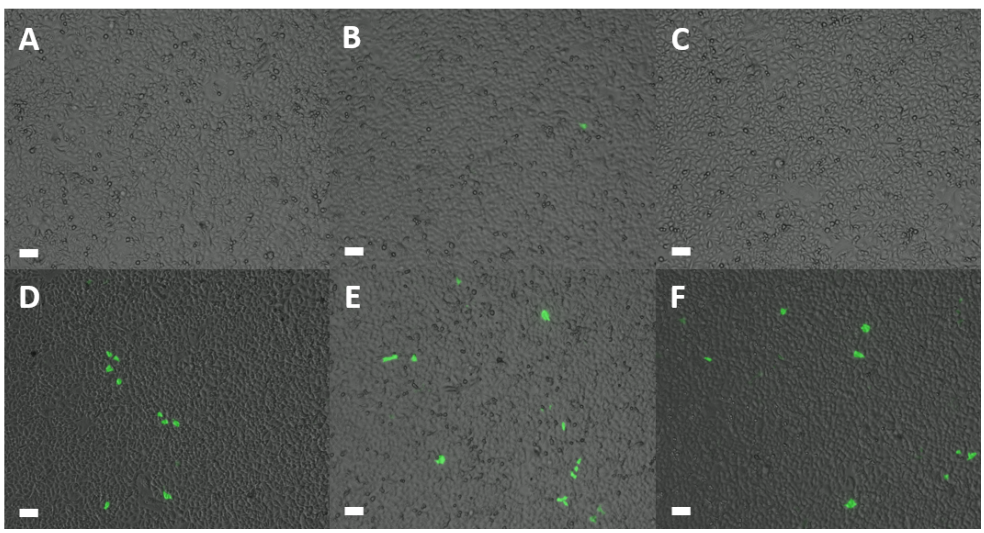

Figure 23. GFP expression result on A549 in the presence of serum. (A): Cell, (B): PEI25k WR1, (C): PCH WR80, (D): R-PCH WR40, (E): FR-PCH30 WR10, (F): HR-PCH30 WR10 (Scale bar: 100 ㎛).

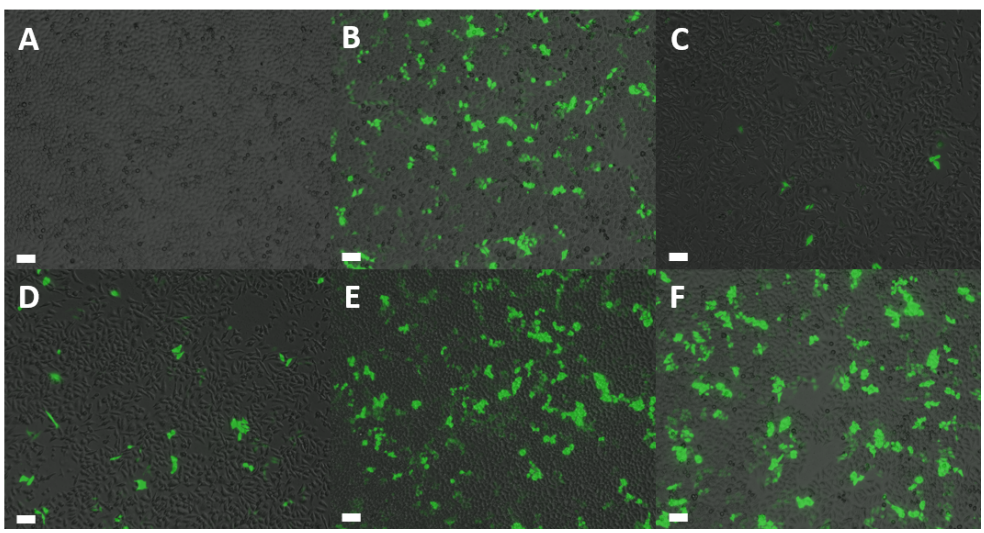

Figure 24. GFP expression result on HeLa in the absence of serum. (A): Cell, (B): PEI25k WR1, (C): PCH WR80, (D): R-PCH WR40, (E): FR-PCH30 WR10, (F): HR-PCH30 WR10 (Scale bar: 100 ㎛).

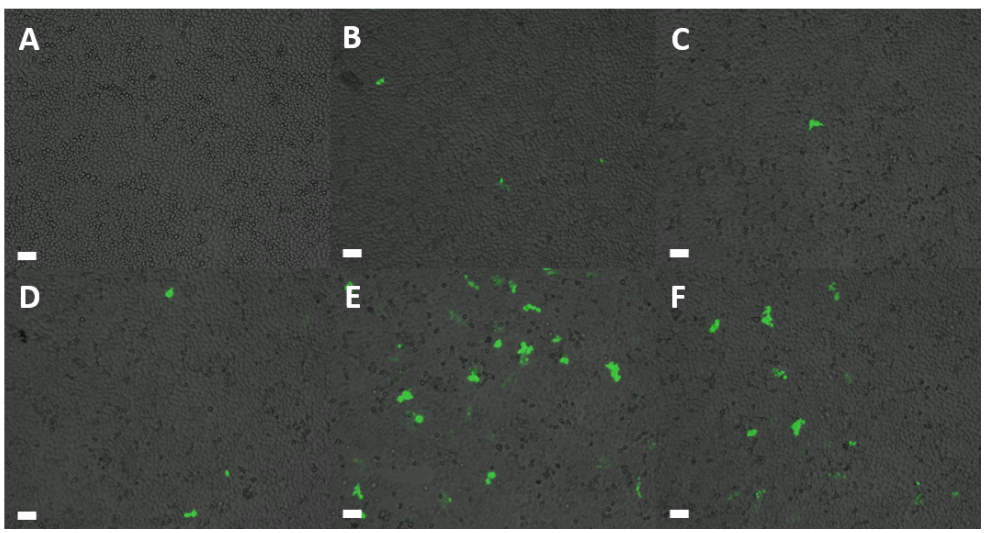

Figure 25. GFP expression result on HeLa in the presence of serum. (A): Cell, (B): PEI25k WR1, (C): PCH WR80, (D): R-PCH WR40, (E): FR-PCH30 WR10, (F): HR-PCH30 WR10 (Scale bar: 100 ㎛).

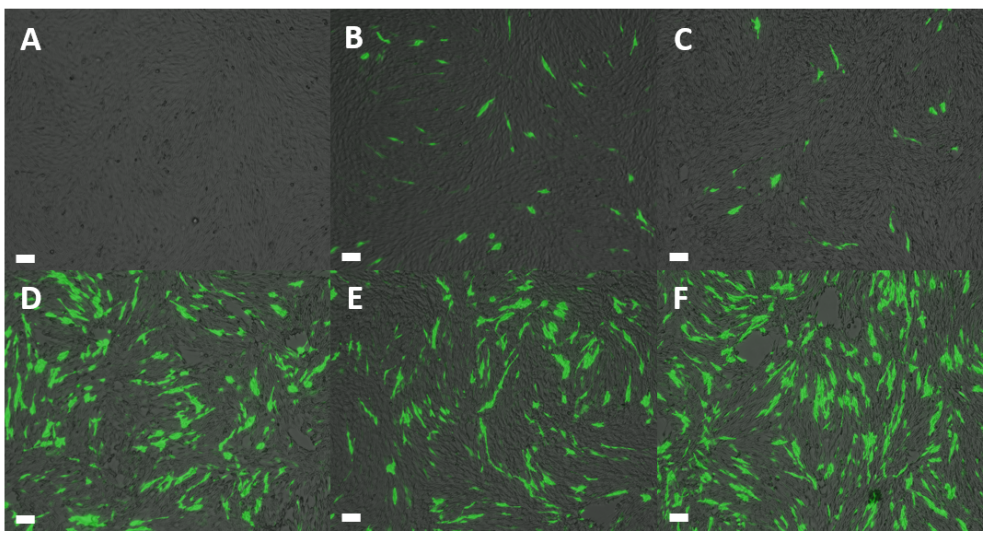

Figure 26. GFP expression result on C2C12 in the absence of serum. (A): Cell, (B): PEI25k WR1, (C): PCH WR80, (D): R-PCH WR40, (E): FR-PCH30 WR10, (F): HR-PCH30 WR10 (Scale bar: 100 ㎛).

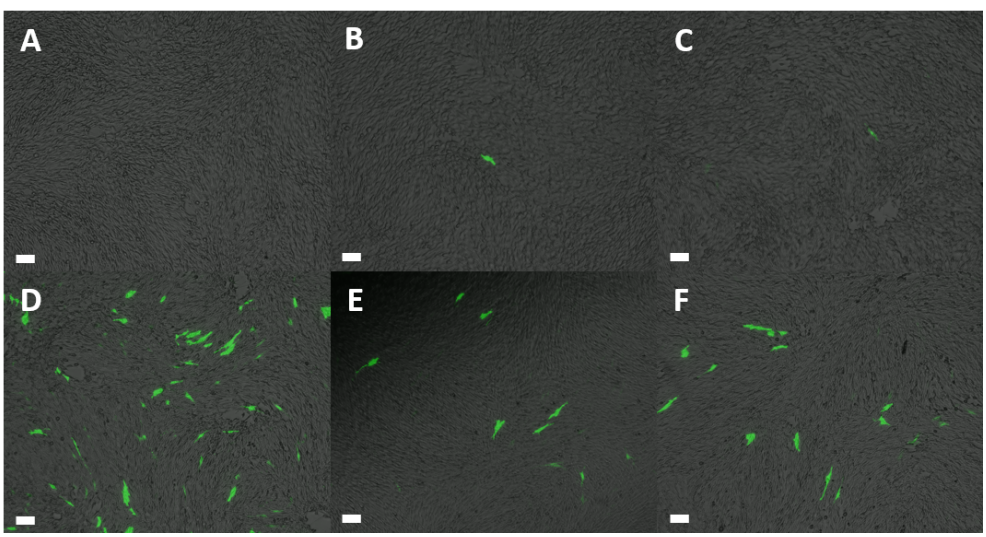

Figure 27. GFP expression result on C2C12 in the presence of serum. (A): Cell, (B): PEI25k WR1, (C): PCH WR80, (D): R-PCH WR40, (E): FR-PCH30 WR10, (F): HR-PCH30 WR10 (Scale bar: 100 ㎛).

membrane permeability. Therefore, cellular uptake efficiency was estimated by using YOYO-1 iodide labeled pDNA. As shown in Table 4, cellular uptake percentages are summarized and Figure 28-33 display histograms of each sample.

It was noteworthy that cellular uptake of FR-PCHs was usually higher than other samples. It can be thought that fluorination improved cellular uptake although the trend was not consistent among cell lines. However, by comparing with serum and without serum condition, it was reconfirmed that serum tolerance could be conferred through fluorinating polymers because the cellular uptake decrement between two condition was relatively smaller than other samples. In the meanwhile, interestingly, PEI25k in all cell lines and other polymers in several cases showed increased cellular uptake than in the presence of serum. The reason was not clear. It could be the error occurred during measurement; however, it also could be the result of interaction with the serum components such as albumin. There are studies using human serum albumin as a component of gene carrier. One of the studies dealt with ternary complex of PEI, pDNA, and human serum albumin. By incorporating human serum albumin, the transfection efficiency was improved [163]. In another study, researchers reported that human serum albumin coated

Table 4. Summarized results of flow cytometry. Numbers mean percentage of YOYO-1 iodide-containing cells in gated cells.

	PEI25k	PCH	R-PCH	FR-PCH30	FR-PCH35	FR-PCH45	FR-PCH30
A549 wo S	1.4	20.8	10.4	15.3	23.1	21.5	16.0
A549 w S	10.9	4.2	5.3	19.2	25.6	17.9	20.3
HeLa wo S	6.7	44.8	46.1	85.6	77.4	73.2	71.9
HeLa w S	10.8	27.9	50.6	60.1	59.1	65.8	66.1
C2C12 wo S	1.7	28.0	29.0	27.4	31.8	36.1	32.2
C2C12 w S	4.2	31.0	17.2	36.2	37.6	33.7	27.0

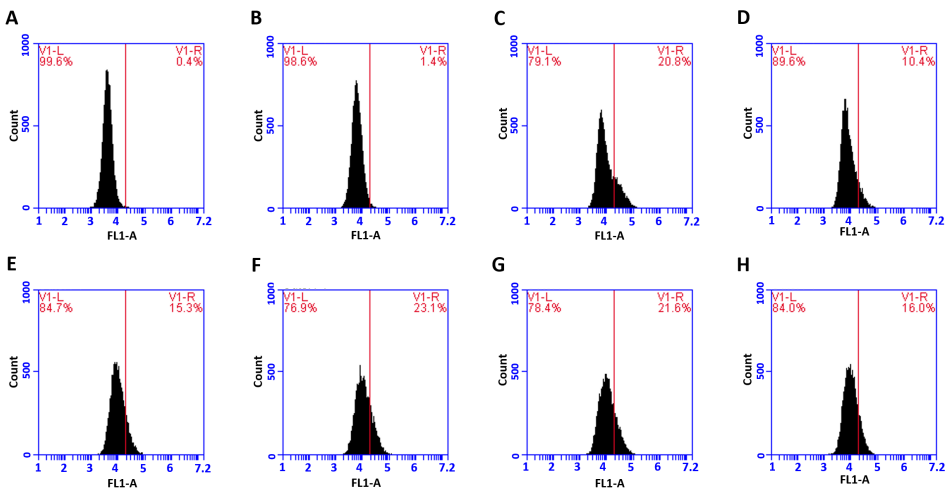

Figure 28. The cellular uptake histograms on A549 in the absence of serum. (A): Cell, (B): PEI25k WR1, (C): PCH WR80, (D): R-PCH WR40, (E): FR-PCH30 WR10, (F): FR-PCH35 WR10, (G): FR-PCH45 WR10, (H): HR-PCH30 WR10. The experiment was conducted at their optimal weight ratios (WRs).

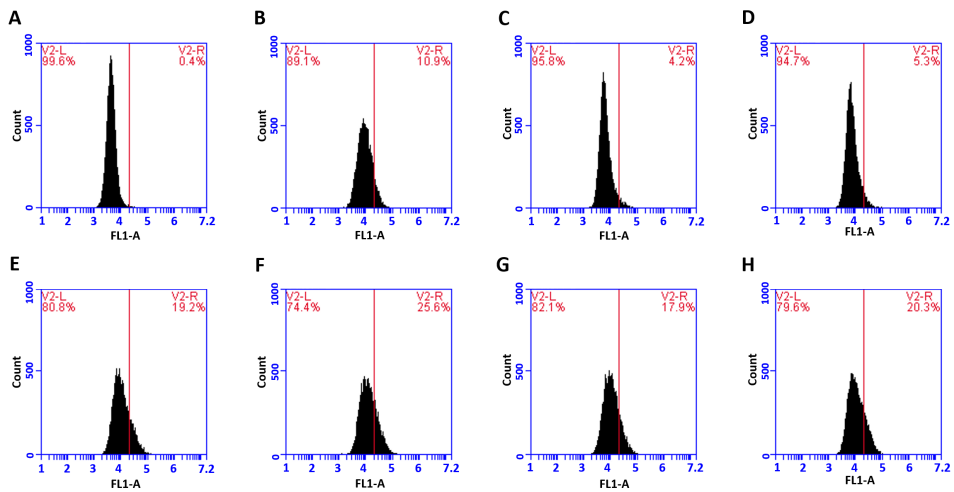

Figure 29. The cellular uptake histograms on A549 in the presence of serum. (A): Cell, (B): PEI25k WR1, (C): PCH WR80, (D): R-PCH WR40, (E): FR-PCH30 WR10, (F): FR-PCH35 WR10, (G): FR-PCH45 WR10, (H): HR-PCH30 WR10. The experiment was conducted at their optimal weight ratios (WRs).

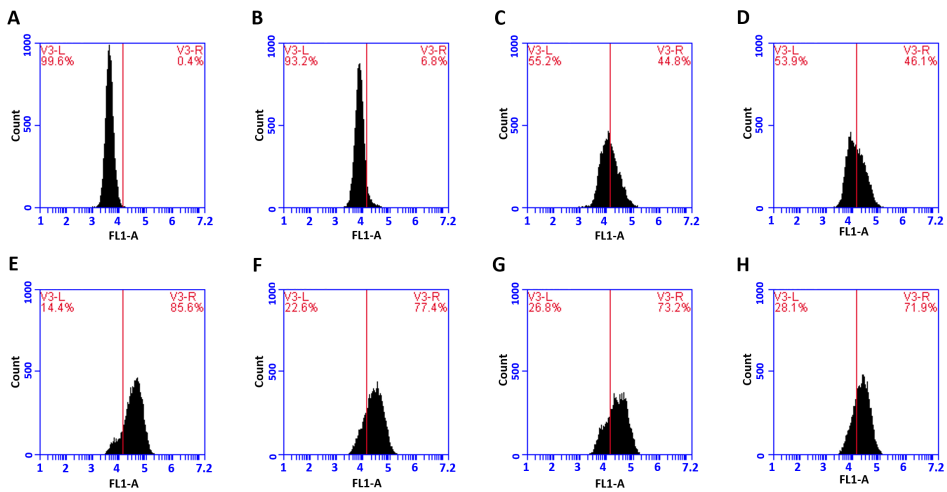

Figure 30. The cellular uptake histograms on HeLa in the absence of serum. (A): Cell, (B): PEI25k WR1, (C): PCH WR80, (D): R-PCH WR40, (E): FR-PCH30 WR10, (F): FR-PCH35 WR10, (G): FR-PCH45 WR10, (H): HR-PCH30 WR10. The experiment was conducted at their optimal weight ratios (WRs).

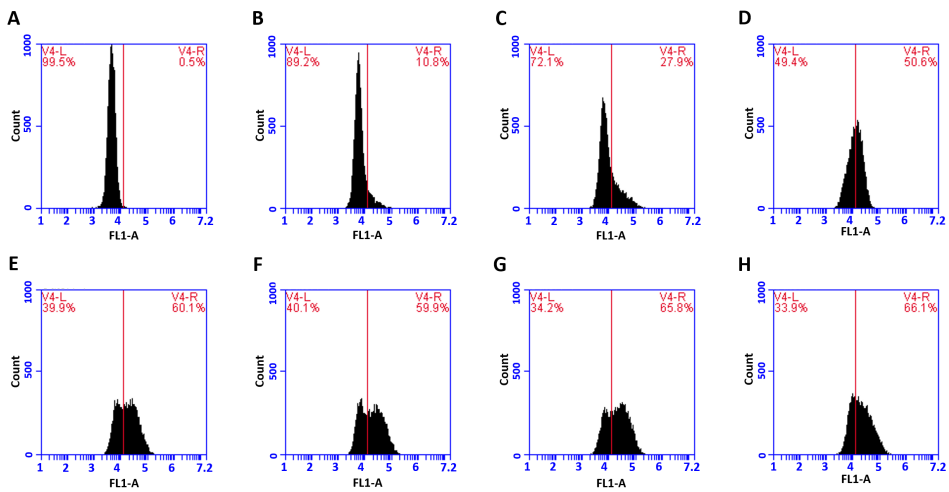

Figure 31. The cellular uptake histograms on HeLa in the presence of serum. (A): Cell, (B): PEI25k WR1, (C): PCH WR80, (D): R-PCH WR40, (E): FR-PCH30 WR10, (F): FR-PCH35 WR10, (G): FR-PCH45 WR10, (H): HR-PCH30 WR10. The experiment was conducted at their optimal weight ratios (WRs).

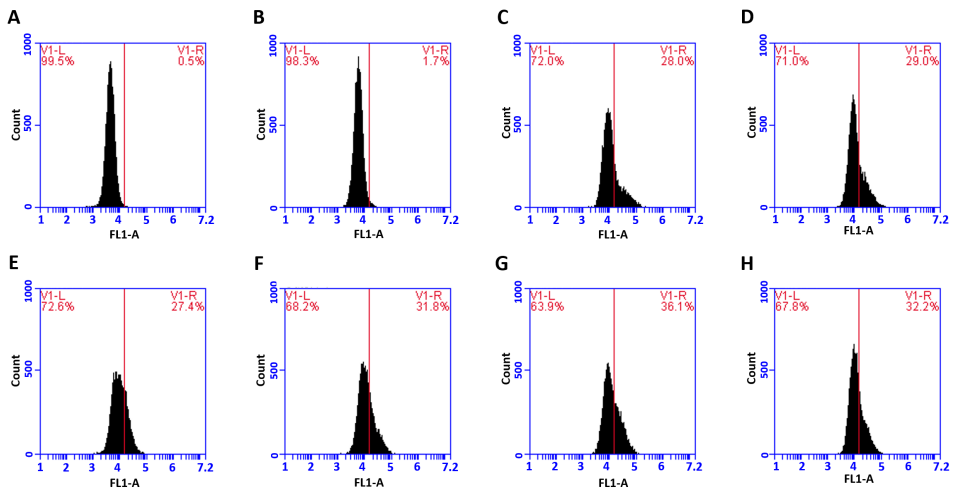

Figure 32. The cellular uptake histograms on C2C12 in the absence of serum. (A): Cell, (B): PEI25k WR1, (C): PCH WR80, (D): R-PCH WR40, (E): FR-PCH30 WR10, (F): FR-PCH35 WR10, (G): FR-PCH45 WR10, (H): HR-PCH30 WR10. The experiment was conducted at their optimal weight ratios (WRs).

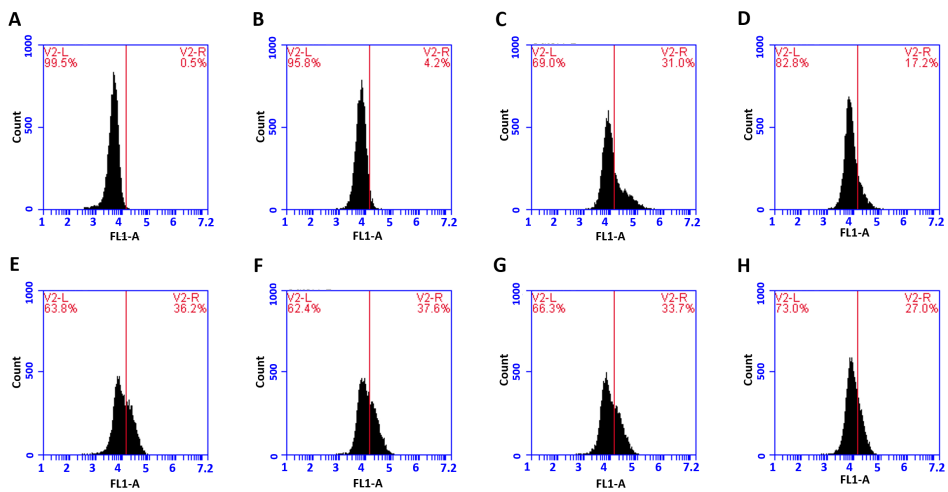

Figure 33. The cellular uptake histograms on C2C12 in the presence of serum. (A): Cell, (B): PEI25k WR1, (C): PCH WR80, (D): R-PCH WR40, (E): FR-PCH30 WR10, (F): FR-PCH35 WR10, (G): FR-PCH45 WR10, (H): HR-PCH30 WR10. The experiment was conducted at their optimal weight ratios (WRs).

lipoplexes could interact with non-specifically to receptors located on cell membrane surface, analogous to scavenger receptors, which can medicate their endocytosis [164]. It can be one of possible hypotheses for increased uptake of PEI25k in serum condition.

Consistently, the results implicated improvement of serum tolerance. In other words, serum tolerance means in some ways the stability of polyplex in serum-containing solution, so the experiment measuring particle size were conducted. As shown in Figure 34, polyplex size change is plotted.

In distilled water, the polyplexes maintained their own size almost same. Even in 10% FBS, the polyplexes except PEI25k and R-PCH also maintained their own size implicating the stability. The particle size of PEI25k and R-PCH fluctuated. The particle size of PEI25k decreased after 30 min, but it started to increase over 600 nm. In the case of R-PCH, particle size was increased at 30 min and maintained the size until 12 h, but the size was decreased at 24 h.

To confirm serum stability of polyplexes directly, transfection assay with various concentration of serum was performed. As shown in Figure 35, it was found that the efficiency of all polyplexes was decreased along with the increment of serum concentration. Despite the diminution, FR-PCH30 showed the highest level of serum resistance in comparison with other samples.

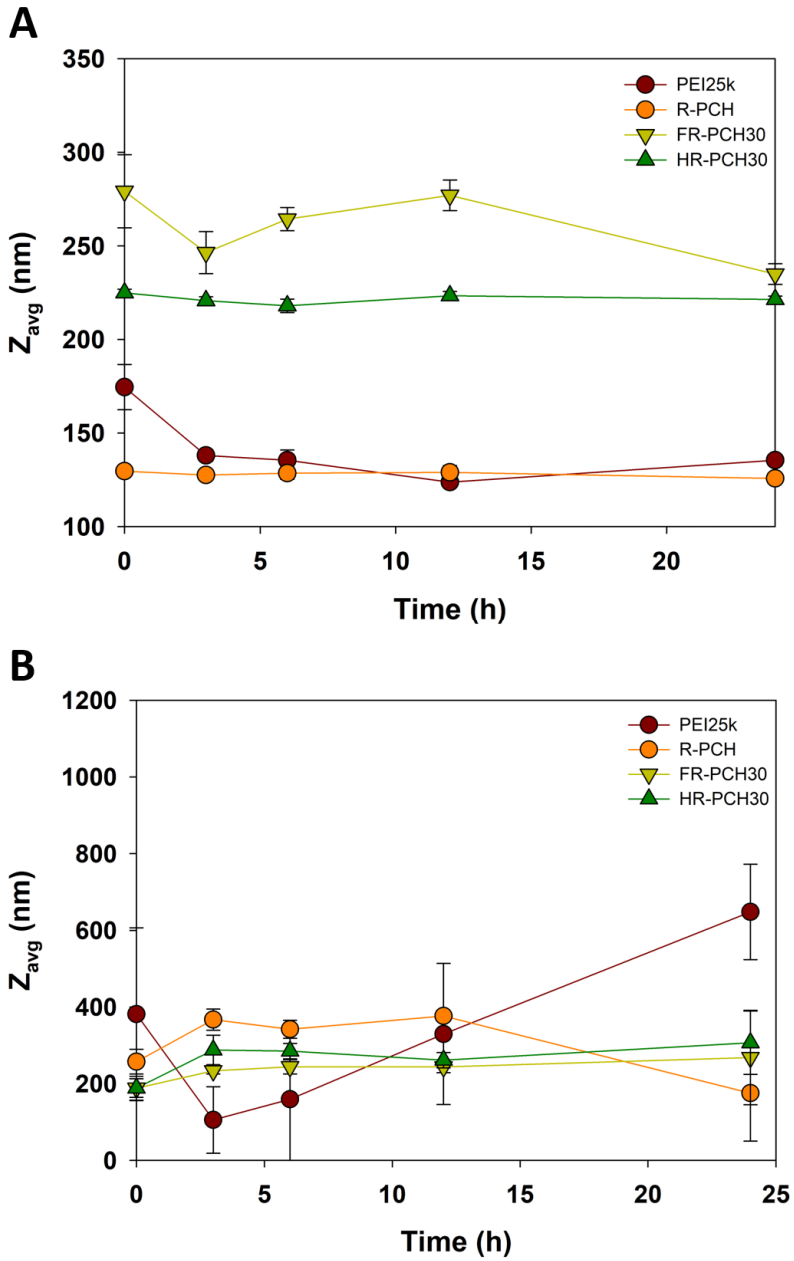

Figure 34. Polyplex stability test (A) in dH_2O and (B) in 10% FBS. All polyplexes were prepared at a weight ratio of 10. PEI25k was used as a control.

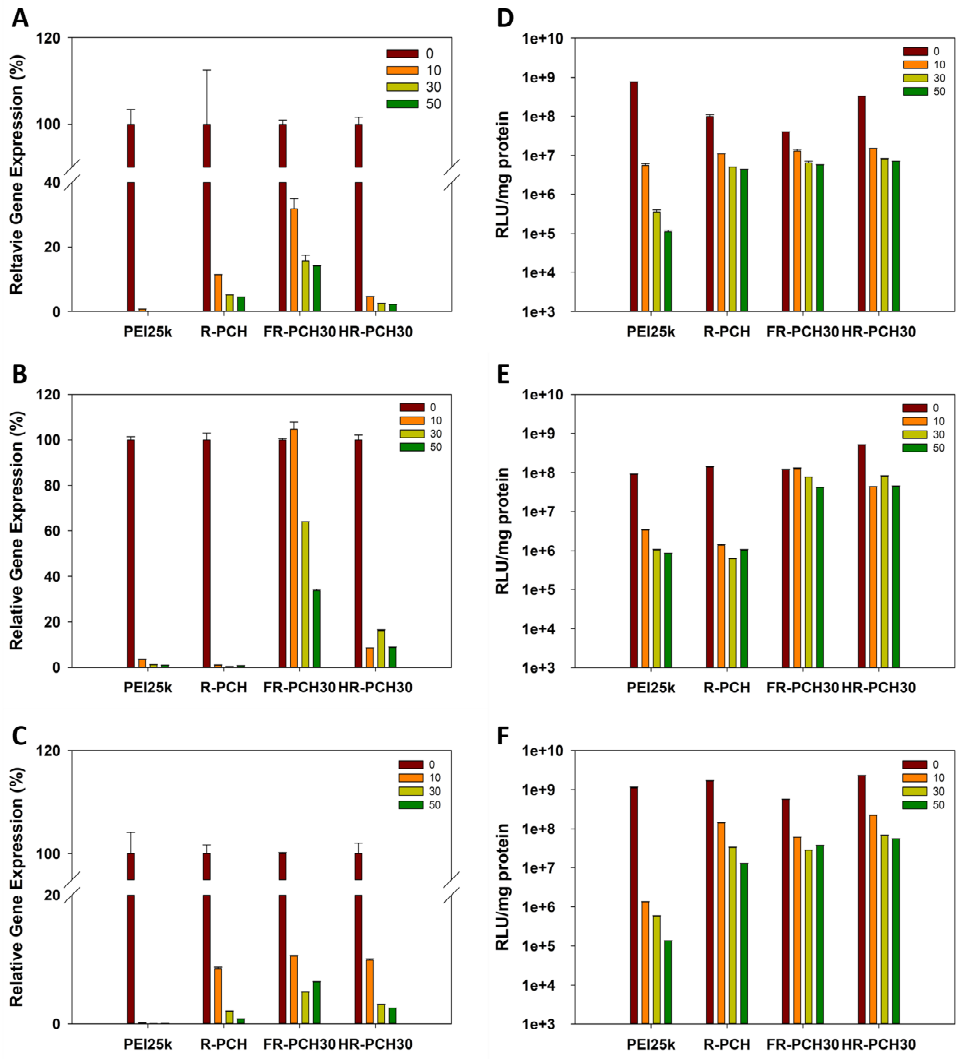

Figure 35. Transfection result in various concentration of FBS. (A) and (D): A549, (B) and (E): HeLa, (C) and (F): C2C12. The numbers mean the concentration of FBS. (A-C) was derived from (E-F) by converting the results into percentage.

Table 5. The cellular uptake results of FR-PCH30 in the presence of inhibitors. Numbers mean percentage of YOYO-1 iodide-containing cells in gated cells.

Cell	None	CytoD	Geni	Noco	Chlor
A549	13.4	20.1	25.4	7.5	17.0
HeLa	80.6	89.7	91.6	61.6	88.2
C2C12	48.3	67.1	68.5	71.7	65.0

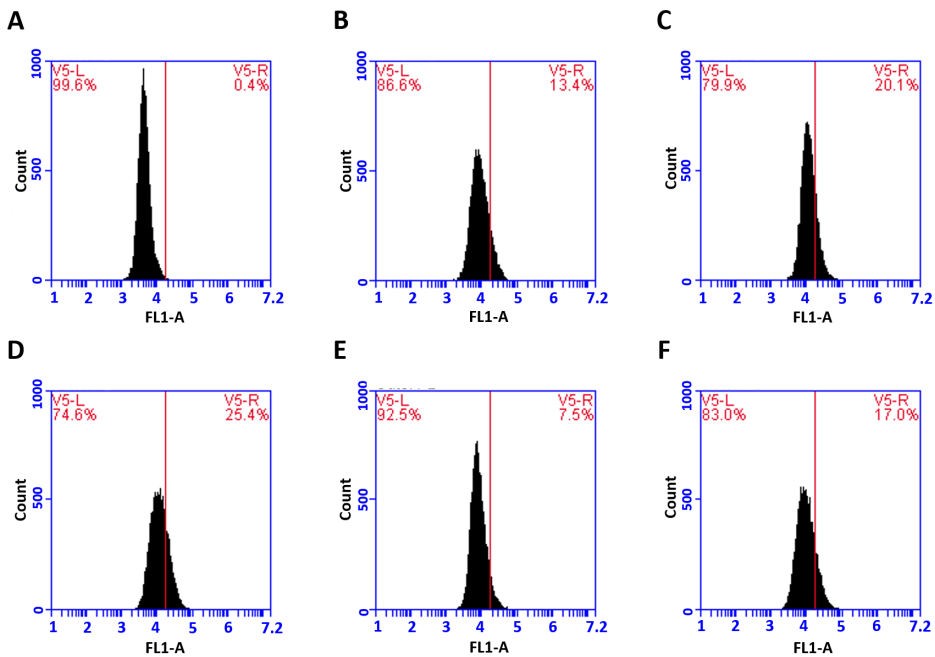

Figure 36. The cellular uptake histograms of FR-PCH30 on A549 in the presence of inhibitors. (A): Cell, (B): Non-treated, (C): Cytochalasin D-treated, (D): Genistein-treated, (E): Nocodazole-treated, (F): Chlorpromazine-treated.

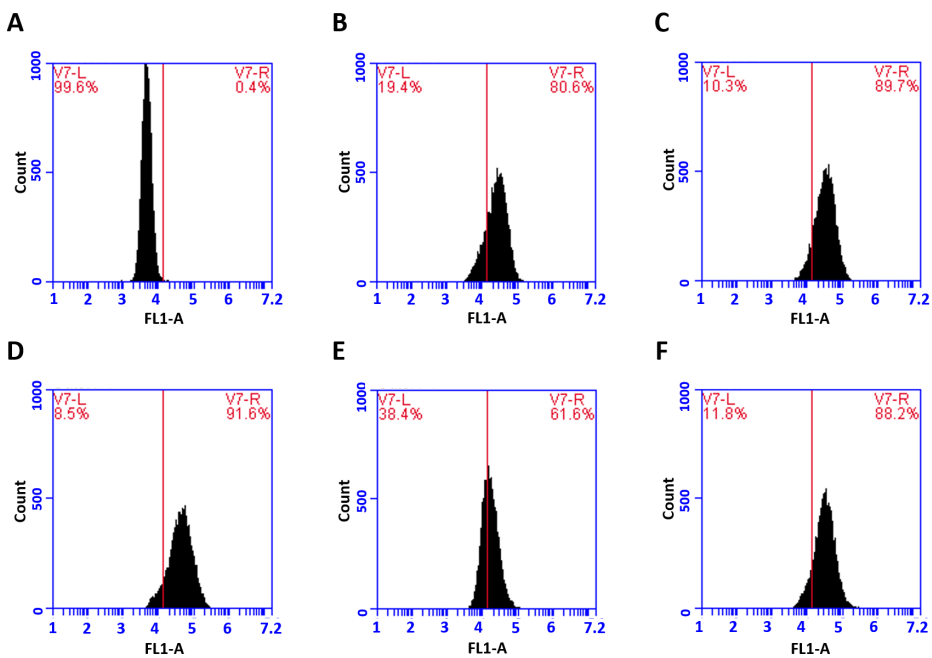

Figure 37. The cellular uptake histograms of FR-PCH30 on HeLa in the presence of inhibitors. (A): Cell, (B): Non-treated, (C): Cytochalasin D-treated, (D): Genistein-treated, (E): Nocodazole-treated, (F): Chlorpromazine-treated.

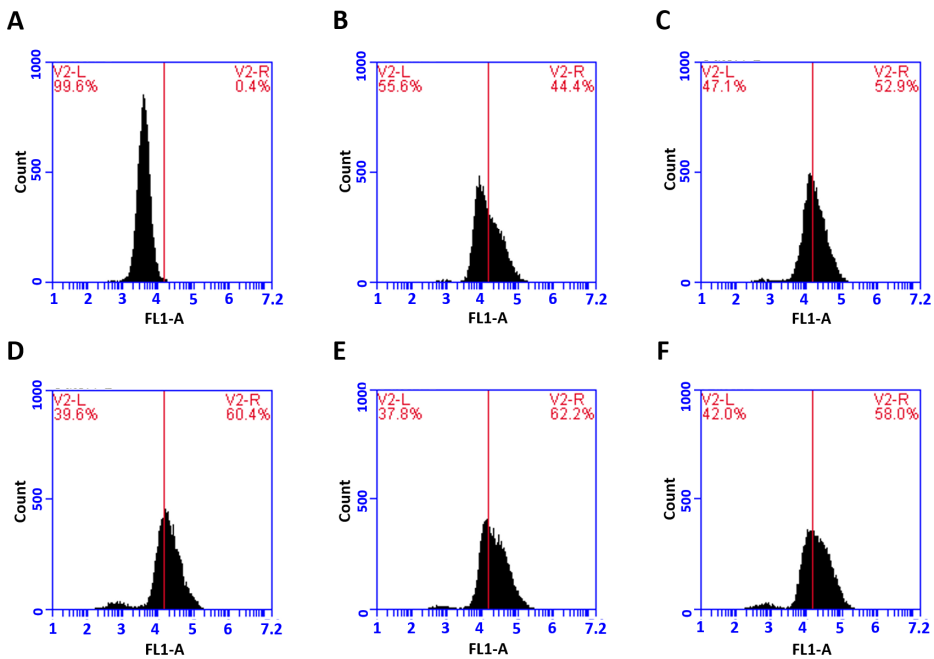

Figure 38. The cellular uptake histograms of FR-PCH30 on C2C12 in the presence of inhibitors. (A): Cell, (B): Non-treated, (C): Cytochalasin D-treated, (D): Genistein-treated, (E): Nocodazole-treated, (F): Chlorpromazine-treated.

Especially, when it comes to the transfection on HeLa, the transfection level at 50% serum was maintained with very small decrease. Also, HR-PCH30 resisted the increased concentration of serum, but it did not show the resistance comparable to FR-PCH30.

Summarizing these results, it can be thought that fluorination can confer polymer enhanced cellular uptake and serum tolerance. The enhanced cellular uptake and serum resistance from the results implied it.

4.2.6. Cellular uptake mechanism analysis of FR-PCH30

Cellular uptake is an important step during gene delivery, so many studies have been trying to find out cellular uptake pathway of their gene carrier. However, there are few articles dealt with cellular uptake pathway of fluorinated polymeric gene carrier [122]. Besides, the cellular uptake pathway of fluorinated polymer can be variable. In other words, not all fluorinated polymer would have same cellular uptake pathway. Therefore, cellular uptake pathway of FR-PCH was analyzed by using flow cytometry and luciferase assay.

When it considered flow cytometry (Table 5 and Figure 36-38), it was thought that it would be hard to specify cellular uptake pathway by using it because there was no significant difference

between cellular uptake pathways. It just can be presumed that microtubule-mediated endocytosis would relate to the uptake of FR-PCH in the case of A549 and HeLa. It was not enough to find specific route of uptake.

For further confirmation of uptake pathway, in turn, luciferase assay was used. Although total cellular uptake mechanism was not fully revealed, the expression of luciferase was final product of cellular uptake in the case of luciferase assay. By comparing the change in the transfection efficiency, analyzing of the pathway would be feasible.

From the results displayed in Figure 39, getting a basis about the uptake pathway was possible, however, it was still not possible to figure out a specific pathway. When it comes to the result from A549, transfection efficiency of R-PCH was drastically diminished at all cellular uptake pathways. On the other hand, transfection efficiency of FR-PCH30 was largely increased when Geni or Chlor were treated, respectively; transfection efficiency affected by CytoD was also increased slightly. It can be thought that FR-PCH overcome the effect of three uptake inhibitors during the cellular uptake due to fluorination. In the meanwhile, the sample affected by Noco showed extremely low efficiency; it means that microtubule-mediated endocytosis might be the main cellular uptake pathway of

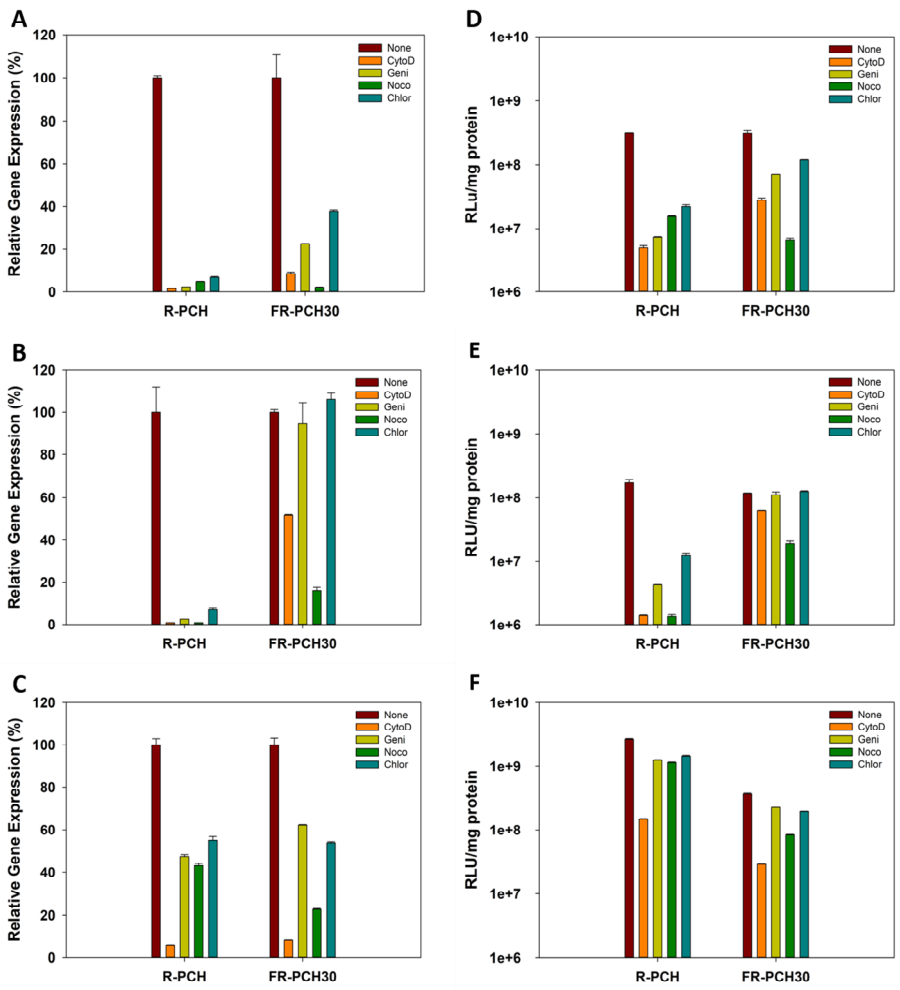

Figure 39. Transfection results in the presence of inhibitors. (A) and (D): A549, (B) and (E): HeLa, (C) and (F): C2C12. (A-C) was derived from (E-F) by converting the results into percentage.

FR-PCH when they were treated to A549. It was consistent with the result of flow cytometry (Table 5).

In the case of HeLa, apparent contrast was displayed. R-PCH showed extremely low transfection efficiency at all samples; on the other hand, FR-PCH showed negligible diminution at Geni-treated and Chlor-treated sample. It meant that FR-PCH use caveolae- In the case of HeLa, apparent contrast was displayed. R-PCH showed extremely low transfection efficiency at all samples; on the other hand, FR-PCH showed negligible diminution at Geni-treated and Chlor-treated sample. It meant that FR-PCH use caveolae-mediated endocytosis and clathrin-mediated endocytosis at negligible level. In contrast, Noco severely decreased the efficiency and CytoD diminished the efficiency by almost 50% implying that macropinocytosis and microtubule-mediated endocytosis are their gate to intracellular region. It was expected that microtubule-mediated endocytosis would be the main route from the result of flow cytometry; in that experiment, only Noco diminished the uptake. Interestingly, macropinocytosis was also specified as the route to cytosol. CytoD is known as an inhibitor of macropinocytosis because it inhibits polymerization of actin [165]; the polymerization and movement of actin is essential for macropinocytosis [166]. Combining these, it is thought that FR-PCH could overcome the

inhibition when considering the result from flow cytometry (Table 5) although the reason is not clear.

The result of C2C12 was complicated. In flow cytometry, FR-PCH was not affected by inhibitors; however, Noco affected FR-PCH more in comparison with R-PCH. Meanwhile, the effect of CytoD was weakened relatively; transfection efficiency was slightly increased in comparison with R-PCH. It implies that fluorination can make changes in the route of entry. In other words, it can be concluded that the entering tendency through microtubule-mediated endocytosis was increased, but main entry was not changed; CytoD diminished the efficiency of both R-PCH and FR-PCH30. That is, macropinocytosis was main gate of cell entry in the case of C2C12.

From these results, it can be concluded that FR-PCH uses multiple pathway for the uptake. Based on it, it is interesting that Noco inhibited well in all cell lines. Noco inhibits assemble of tubulin into microtubule [167]. As microtubules are related to intracellular transport, they also participate partially in macropinocytosis [168], clathrin-mediated endocytosis [169], and caveolae-mediated endocytosis [170]. Based on these, it can be also considered that the reason of superior inhibition by Noco is derived from the multiple role of microtubule in endocytosis. In other words,

inhibition of microtubule formation would inhibit multiple endocytosis pathway resulting in severe inhibition of gene expression. In other perspective, it can be also thought that inhibition of intracellular transport was the most critical point of gene delivery using FR-PCH when combining the results from cellular uptake analysis.

The cascade of cellular entry is so complicated and not fully revealed. Even though it was not successful analysis of cellular uptake pathway, it was clear that fluorination affected and change the tendency of cellular uptake.

4.2.7. Intracellular observation by CLSM

To observe the distribution of polyplexes, dyeing with fluorescence dyes and CLSM were conducted (Figure 40-42). In general, all three displayed similar tendency. FR-PCH30 showed most abundant green fluorescence meaning pDNA even though the result of HeLa was not so apparent as A549 and C2C12. In the meanwhile, it is noteworthy that the distribution of green fluorescence was mainly located near nucleus; it was observed in all cell lines. Recalling the function of arginine mentioned before, arginine could act as NLS for intracellular trafficking to nucleus. By considering these, it can be thought that the distribution of green

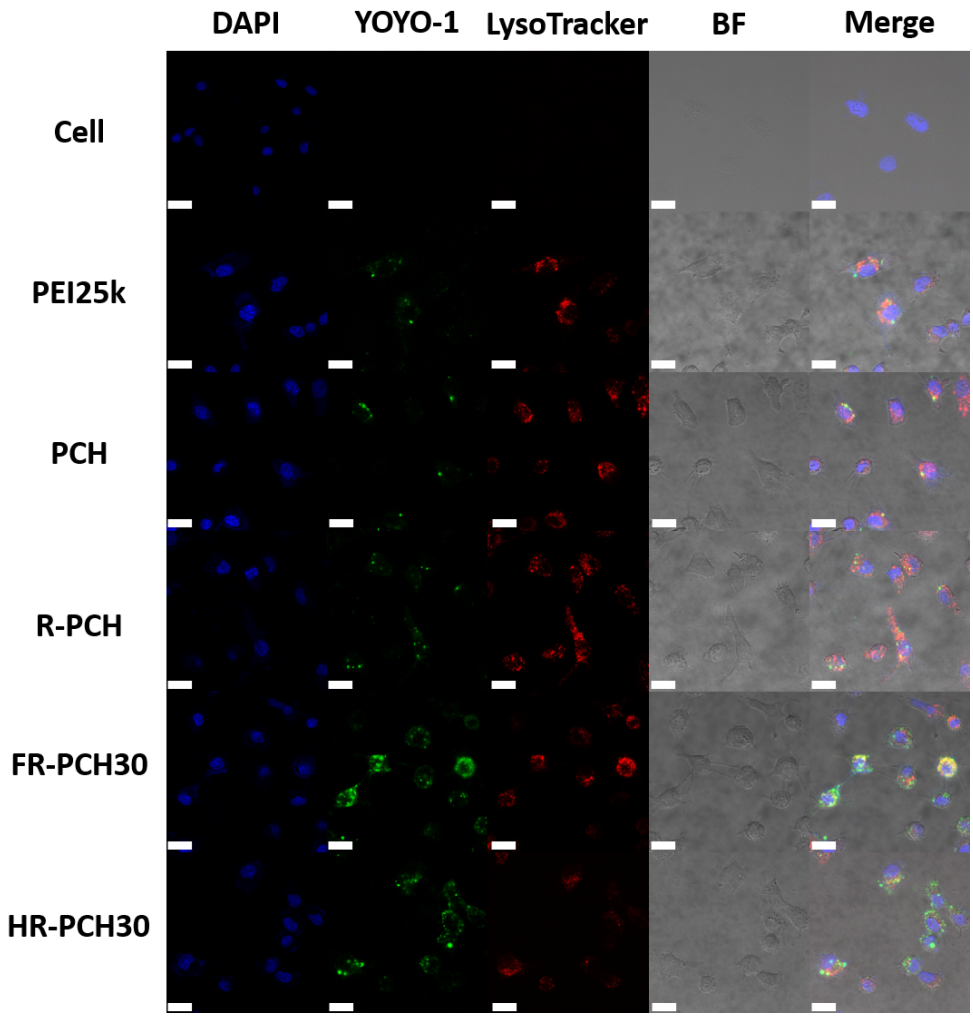

Figure 40. Intracellular observation of A549 with CLSM. DAPI: nuclei (blue), YOYO-1: pDNA (green), LysoTracker: endosome and lysosome (red). BF means bright field image (Scale bar: 20 ㎛).

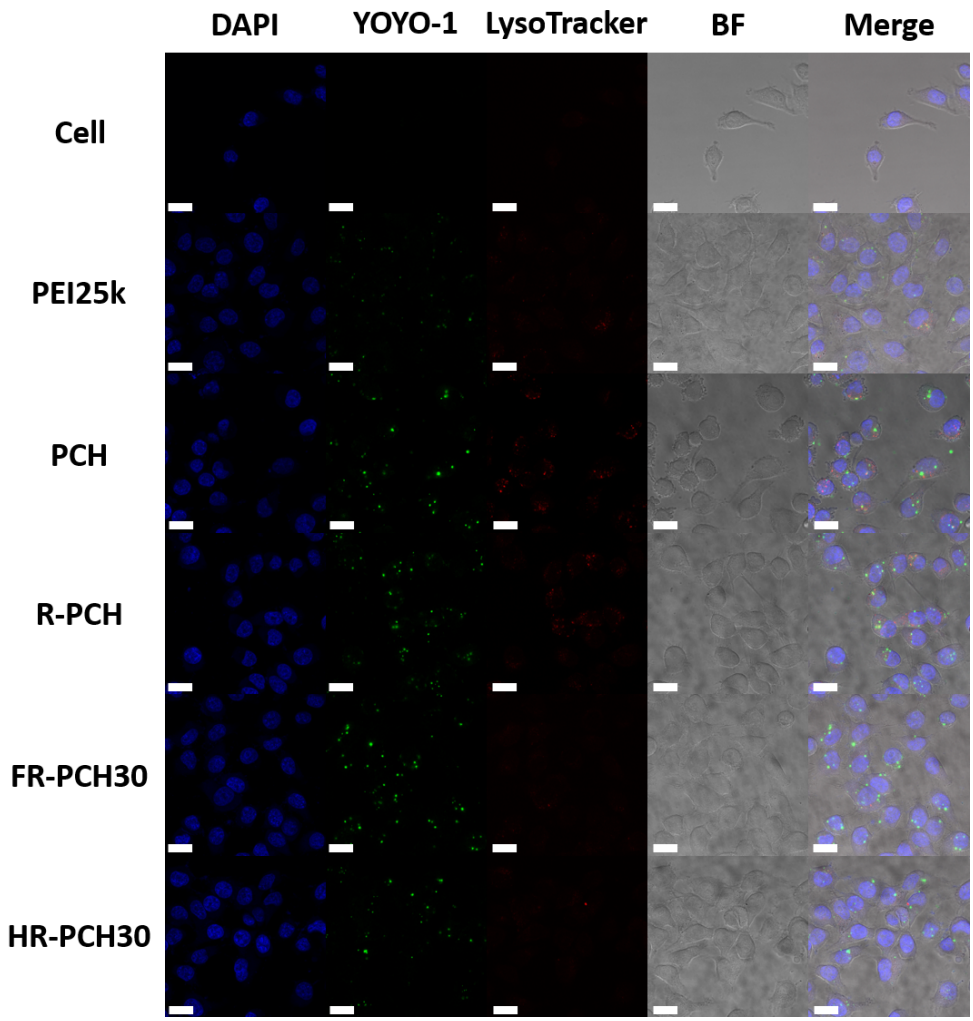

Figure 41. Intracellular observation of HeLa with CLSM. DAPI: nuclei (blue), YOYO-1: pDNA (green), LysoTracker: endosome and lysosome (red). BF means bright field image (Scale bar: 20 ㎛).

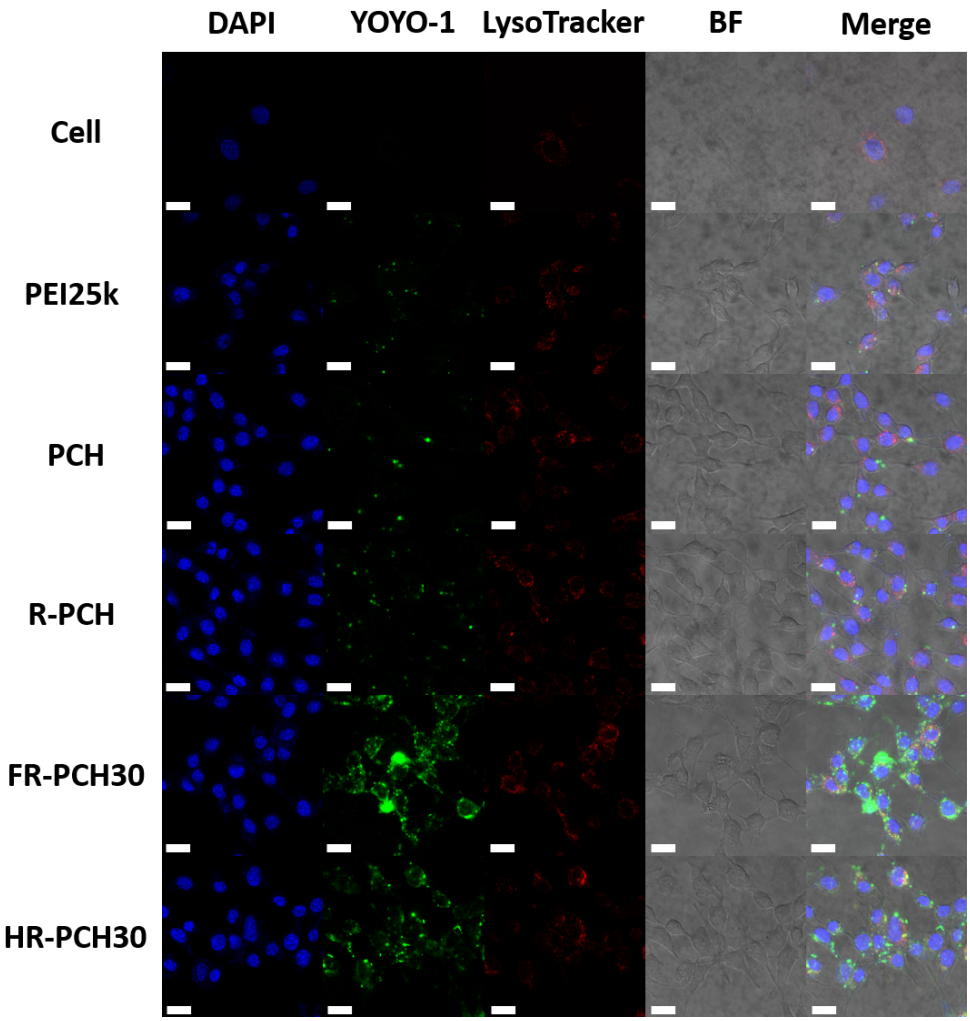

Figure 42. Intracellular observation of C2C12 with CLSM. DAPI: nuclei (blue), YOYO-1: pDNA (green), LysoTracker: endosome and lysosome (red). BF means bright field image (Scale bar: 20 ㎛).

fluorescence was a result of NLS function came from arginine.

In addition, interestingly, there were few cells containing the signal of colocalization, there are two ways plausible. One is their fast escape from endosomes. The other is endosome-independent endocytosis due to fluorination. Both hypotheses are based on the characteristic of fluorination, membrane permeability.

Summarizing these, fluorination enhances cellular uptake, and arginine confers cellular uptake enhancement and intracellular trafficking ability to nucleus. The combination of fluorination and arginine grafting can significantly enhance intracellular accumulation of YOYO-1 labeled pDNA and locates nearby nuclei.

4.3. Summary

Arginine-modified and fluorinated bioreducible polymer was synthesized for gene delivery systems. They could form positively charged and nano-sized polyplexes with pDNA. Interestingly, some of FR-PCH polyplexes retarded pDNA even in reducing condition, probably due to and hydrophobic interaction of fluoroalkyl chains. FR-PCHs showed comparable transfection efficiency to PEI25k in serum-free condition but superior efficiency to PEI25k even in serum-containing condition, which means FR-PCHs possessed good serum-compatibility. Good serum tolerance was confirmed by

further experiments such as transfection assay in various concentration of FBS. However, cytotoxicity of the polymers was significant and increased with concentration and modification degree. Nevertheless, it was confirmed that fluorination can confer not only serum-compatibility but also improved membrane permeability. Besides, fluorination resulted in changes of cellular uptake pathway. These characteristics of fluorination confer great transfection efficiency. It was also confirmed that the combination of arginine and fluorination could result in significant enhancement of gene delivery efficiency. Although this study is not enough to reveal the exact endocytosis pathway of fluorinated polymer comprehensively, this dissertation confirmed the possibility and potency of fluorination in gene delivery systems. It is expected to provide good springboard for developing fluorinated polymeric gene delivery systems.

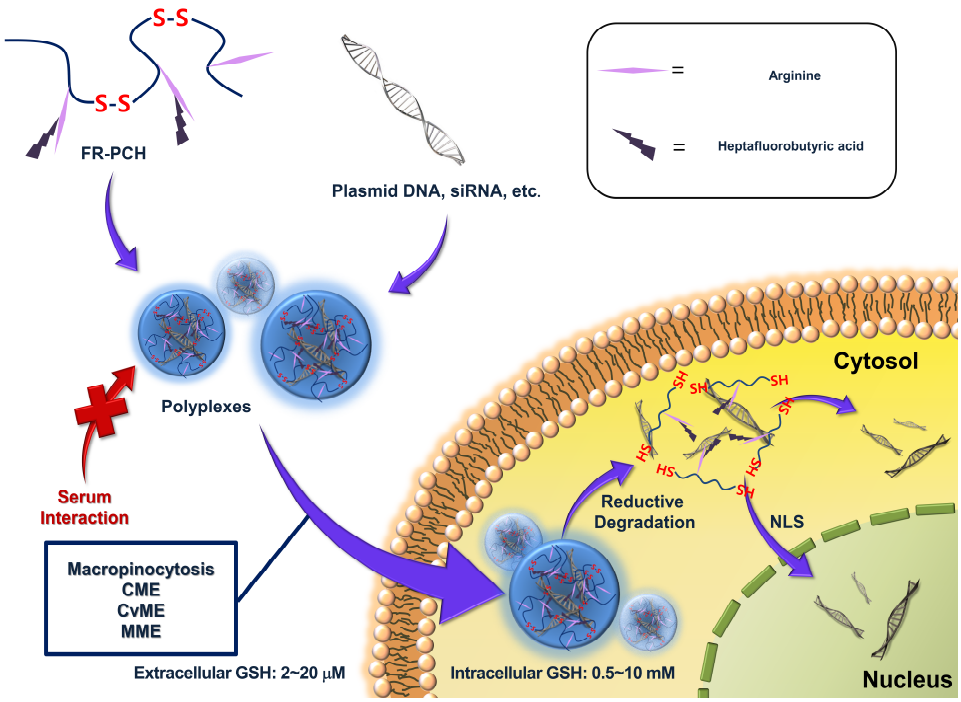

Scheme 5. Schematic diagram of gene delivery sequence with FR-PCH. Due to fluorination, FR-PCH showed serum resistance during the gene delivery. In addition, it was revealed that FR-PCH used multiple cellular uptake pathway.

Chapter 5. Conclusion

In this dissertation, two themes of bioreducible polymer were investigated in terms of structure-activity relationship; crosslinked bioreducible polymers and fluoroalkylated arginine functionalized bioreducible polymers respectively. From the results, it was found that the behavior of bioreducible polymers were critically changed along with the structure and components of the polymers such as branching, side chains.

Both polymers showed adequate basic performance for gene delivery such as polyplex formation, particle size, Zeta-potential, and transfection efficiency. All the polymers in this dissertation formed positively charged compact particles and showed comparable or superior transfection efficiency even in the presence of serum. However, PPI-CBAs and FR-PCHs showed relatively high cytotoxicity along with the polymer concentration, crosslinking and modification degree. Although the cytotoxicity trend was not new phenomenon, the resistance in reducing condition was unprecedented. From the empirical results of PPI-CBAs, it was though that thiol groups originated from cleaved disulfide bonds reacted each other forming disulfide bond again. This can be

speculated that the vicinity of free thiol groups due to crosslinked structure of PPI-CBAs made the re-crosslinking possible.

In the case of FR-PCH, from the results of electrophoresis and DLS, it was thought that fluorination conferred aggregating ability making them resistant to reducing environment. Although overall the particle size was increased, FR-PCHs still displayed small particle size partially. It was thought that the driving force was fluorine effect of fluoroalkyl side chains.

From the perspective of transfection efficiency, the study of PPI-CBAs confirmed that the crosslinking of low molecular weight compounds can achieve high transfection efficiency. The study of FR-PCHs demonstrated that the combination of arginine modification, fluorination, and bioreducibility was effective for achieving high gene delivery efficiency. It was thought that arginine improved cellular uptake and fluoroalkyl chain enhanced cellular uptake and serum resistance. In addition, it was thought that bioreducibility conferred facilitated DNA release in reducing condition and relatively lower cytotoxicity.

In the case of fluorination, it was also found that fluorination induced the change of cellular uptake pathway probably due to the permeability of fluoroalkyl chains although the mechanism was not clear.

Collectively, in this dissertation, it was found that not all bioreducible polymer behaved as reported in previous studies. The degree of branching, composition of side chains significantly changed the behavior of bioreducible polymers in extraordinary ways. This dissertation would provide further comprehension of bioreducible polymers.

References

[1] T. Friedmann, R. Roblin, Gene therapy for human genetic disease?, Science (80−.). 175 (1972) 949–955. https://doi.org/10.1126/science.175.4025.949.

[2] C. Scholz, E. Wagner, Therapeutic plasmid DNA versus siRNA delivery: Common and different tasks for synthetic carriers, J. Control. Release. 161 (2012) 554–565. https://doi.org/10.1016/j.jconrel.2011.11.014.

[3] S. Kawakami, Y. Higuchi, M. Hashida, Nonviral approaches for targeted delivery of plasmid DNA and oligonucleotide, J. Pharm. Sci. 97 (2008) 726–745. https://doi.org/10.1002/jps.21024.

[4] R.K.M. Leung, P.A. Whittaker, RNA interference: From gene silencing to gene−specific therapeutics, Pharmacol. Ther. 107 (2005) 222–239. https://doi.org/10.1016/j.pharmthera.2005.03.004.

[5] Y.K. Oh, T.G. Park, siRNA delivery systems for cancer treatment, Adv. Drug Deliv. Rev. 61 (2009) 850–862. https://doi.org/10.1016/j.addr.2009.04.018.

[6] T.G. Park, J.H. Jeong, S.W. Kim, Current status of polymeric gene delivery systems, Adv. Drug Deliv. Rev. 58 (2006) 467–486. https://doi.org/10.1016/j.addr.2006.03.007.

[7] T. Niidome, L. Huang, Gene Therapy Progress and Prospects: Nonviral vectors, Gene Ther. 9 (2002) 1647-1652. https://doi.org/10.1038/sj.gt.3301923.

[8] A. Yazdani, Z. Alirezaie, M.J. Motamedi, J. Amani, Gene Therapy: A New Approach in Modern Medicine, Int. J. Med. Rev. 5 (2018) 106-117. https://doi.org/10.29252/ijmr-050304.

[9] J. Chen, K. Wang, J. Wu, H. Tian, X. Chen, Polycations for Gene Delivery: Dilemmas and Solutions, Bioconjug. Chem. 30 (2018) 338-349. https://doi.org/10.1021/acs.bioconjchem.8b00688.

[10] E. Cevher, A. Demir, E. Sefik, Gene Delivery Systems: Recent Progress in Viral and Non-Viral Therapy, in: Recent Adv. Nov. Drug Carr. Syst., InTech, 2012. https://doi.org/10.5772/53392.

[11] D.R. Jacobson, O.A. Saleh, Counting the ions surrounding nucleic acids, Nucleic Acids Res. 45 (2017) 1596-1605. https://doi.org/10.1093/nar/gkw1305.

[12] H. Eliyahu, Y. Barenholz, A.J. Domb, Polymers for DNA delivery, Molecules. 10 (2005) 34-64. https://doi.org/10.3390/10010034.

[13] D. Pezzoli, E. Giupponi, D. Mantovani, G. Candiani, Size matters for in vitro gene delivery: investigating the relationships among complexation protocol, transfection medium, size and sedimentation, Sci. Rep. 7 (2017) 44134.

https://doi.org/10.1038/srep44134.

[14] J. Sun, F. Zeng, H. Jian, S. Wu, Grafting zwitterionic polymer chains onto PEI as a convenient strategy to enhance gene delivery performance, Polym. Chem. 4 (2013) 5810–5818. https://doi.org/10.1039/c3py00752a.

[15] Y. Yue, C. Wu, Progress and perspectives in developing polymeric vectors for in vitro gene delivery, Biomater. Sci. 1 (2013) 152–170. https://doi.org/10.1039/c2bm00030j.

[16] Y.S. Lee, S.W. Kim, Bioreducible polymers for therapeutic gene delivery, J. Control. Release. 190 (2014) 424–439. https://doi.org/10.1016/j.jconrel.2014.04.012.

[17] K. Ryu, G.J. Lee, J.Y. Choi, T. Kim, T. Il Kim, Self-Assembling Multifunctional Peptide Dimers for Gene Delivery Systems, Adv. Mater. Sci. Eng. 2015 (2015) 1–9. https://doi.org/10.1155/2015/852584.

[18] M. Wang, B. Wu, J.D. Tucker, P. Lu, Q. Lu, Poly(ester amine) constructed from polyethylenimine and pluronic for gene delivery *in vitro* and *in vivo*, Drug Deliv. 23 (2016) 3224–3233. https://doi.org/10.3109/10717544.2016.1162877.

[19] Y. Yang, H. Zhao, Y. Jia, Q. Guo, Y. Qu, J. Su, X. Lu, Y. Zhao, Z. Qian, A novel gene delivery composite system based on biodegradable folate–poly (ester amine) polymer and

thermosensitive hydrogel for sustained gene release, Sci. Rep. 6 (2016). https://doi.org/10.1038/srep21402.

[20] Y. Wang, M. Zheng, F. Meng, J. Zhang, R. Peng, Z. Zhong, Branched polyethylenimine derivatives with reductively cleavable periphery for safe and efficient in vitro gene transfer, Biomacromolecules. 12 (2011) 1032–1040. https://doi.org/10.1021/bm101364f.

[21] H. Tian, L. Lin, J. Chen, X. Chen, T.G. Park, A. Maruyama, RGD targeting hyaluronic acid coating system for PEI–PBLG polycation gene carriers, J. Control. Release. 155 (2011) 47–53. https://doi.org/10.1016/j.jconrel.2011.01.025.

[22] M. Thomas, A.M. Klibanov, Enhancing polyethylenimine's delivery of plasmid DNA into mammalian cells, Proc. Natl. Acad. Sci. U. S. A. 99 (2002) 14640–14645. https://doi.org/10.1073/pnas.192581499.

[23] M. Breunig, U. Lungwitz, R. Liebl, A. Goepferich, Breaking up the correlation between efficacy and toxicity for nonviral gene delivery, Proc. Natl. Acad. Sci. U. S. A. 104 (2007) 14454–14459. https://doi.org/10.1073/pnas.0703882104.

[24] D. Jere, H.L. Jiang, R. Arote, Y.K. Kim, Y.J. Choi, M.H. Cho, T. Akaike, C.S. Cho, Degradable polyethylenimines as DNA and small interfering RNA carriers, Expert Opin. Drug Deliv. 6 (2009)

827–834. https://doi.org/10.1517/17425240903029183.

[25] Y. Li, D. Maciel, J. Rodrigues, X. Shi, H. Tomás, Biodegradable polymer nanogels for drug/nucleic acid delivery, Chem. Rev. 115 (2015) 8564–8608. https://doi.org/10.1021/cr500131f.

[26] M. Thomas, Q. Ge, J.J. Lu, J. Chen, A.M. Klibanov, Cross–linked small polyethylenimines: While still nontoxic, deliver DNA efficiently to mammalian cells in vitro and in vivo, Pharm. Res. 22 (2005) 373–380. https://doi.org/10.1007/s11095–004–1874–y.

[27] J. Luten, C.F. van Nostrum, S.C. De Smedt, W.E. Hennink, Biodegradable polymers as non–viral carriers for plasmid DNA delivery, J. Control. Release. 126 (2008) 97–110. https://doi.org/10.1016/j.jconrel.2007.10.028.

[28] J. Liu, X. Jiang, L. Xu, X. Wang, W.E. Hennink, R. Zhuo, Novel reduction–responsive cross–linked polyethylenimine derivatives by click chemistry for nonviral gene delivery, Bioconjug. Chem. 21 (2010) 1827–1835. https://doi.org/10.1021/bc100191r.

[29] T. Il Kim, S.W. Kim, Bioreducible polymers for gene delivery, React. Funct. Polym. 71 (2011) 344–349. https://doi.org/10.1016/j.reactfunctpolym.2010.11.016.

[30] S. Son, R. Namgung, J. Kim, K. Singha, W.J. Kim, Bioreducible polymers for gene silencing and delivery, Acc. Chem.

Res. 45 (2012) 1100-1112. https://doi.org/10.1021/ar200248u.

[31] K. Ryu, T. Il Kim, Therapeutic gene delivery using bioreducible polymers, Arch. Pharm. Res. 37 (2014) 31-42. https://doi.org/10.1007/s12272-013-0275-3.

[32] G. Wu, Y.-Z. Fang, S. Yang, J.R. Lupton, N.D. Turner, Glutathione Metabolism and Its Implications for Health, J. Nutr. 134 (2004) 489-492. https://doi.org/10.1093/jn/134.3.489.

[33] Z. Guo, H. Tian, J. Xia, J. Chen, L. Lin, X. Chen, Bioreducible crosslinked low molecular weight branched PEI-PBLG as an efficient gene carrier, Sci. China Chem. 53 (2010) 2490-2496. https://doi.org/10.1007/s11426-010-4144-3.

[34] H. Park, J.W. Nichols, H.C. Kang, Y.H. Bae, Bioreducible polyspermine as less toxic and efficient gene carrier, Polym. Adv. Technol. 25 (2014) 545-551. https://doi.org/10.1002/pat.3269.

[35] K.L. Kozielski, S.Y. Tzeng, B.A. Hurtado De Mendoza, J.J. Green, Bioreducible cationic polymer-based nanoparticles for efficient and environmentally triggered cytoplasmic siRNA delivery to primary human brain cancer cells, ACS Nano. 8 (2014) 3232-3241. https://doi.org/10.1021/nn500704t.

[36] Y.K. Sung, S.W. Kim, Recent Advances in the Development of Bio-Reducible Polymers for Efficient Cancer Gene Delivery Systems., Cancer Med. J. 2 (2019) 6-13.

http://www.ncbi.nlm.nih.gov/pubmed/31032485 (accessed December 13, 2019).

[37] S. Somani, P. Laskar, N. Altwaijry, P. Kewcharoenvong, C. Irving, G. Robb, B.S. Pickard, C. Dufès, PEGylation of polypropylenimine dendrimers: effects on cytotoxicity, DNA condensation, gene delivery and expression in cancer cells, Sci. Rep. 8 (2018) 9410. https://doi.org/10.1038/s41598-018-27400-6.

[38] J.S. Suk, Q. Xu, N. Kim, J. Hanes, L.M. Ensign, PEGylation as a strategy for improving nanoparticle-based drug and gene delivery, Adv. Drug Deliv. Rev. 99 (2016) 28-51. https://doi.org/10.1016/j.addr.2015.09.012.

[39] C. Jreyssaty, Q. Shi, H. Wang, X. Qiu, F.M. Winnik, X. Zhang, K. Dai, M. Benderdour, J.C. Fernandes, Efficient Nonviral Gene Therapy Using Folate-Targeted Chitosan-DNA Nanoparticles In Vitro, ISRN Pharm. 2012 (2012) 1-9. https://doi.org/10.5402/2012/369270.

[40] S. Fumoto, S. Kawakami, M. Hashida, K. Nishi, Targeted Gene Delivery: Importance of Administration Routes, in: Nov. Gene Ther. Approaches, InTech, 2013. https://doi.org/10.5772/54741.

[41] T. Shukla, N. Upmanyu, S.P. Pandey, M.S. Sudheesh, Site-specific drug delivery, targeting, and gene therapy, in: Nanoarchitectonics Biomed., Elsevier, 2019: pp. 473-505.

https://doi.org/10.1016/b978-0-12-816200-2.00013-x.

[42] Z.Q. Yu, J.J. Yan, Y.Z. You, Q.H. Zhou, Bioreducible and acid-labile poly(amido amine)s for efficient gene delivery, Int. J. Nanomedicine. 7 (2012) 5819-5832. https://doi.org/10.2147/IJN.S37334.

[43] H.A. Kim, K. Nam, S.W. Kim, Tumor targeting RGD conjugated bio-reducible polymer for VEGF siRNA expressing plasmid delivery, Biomaterials. 35 (2014) 7543-7552. https://doi.org/10.1016/j.biomaterials.2014.05.021.

[44] R.P. Johnson, S. Uthaman, R. Augustine, Y. Zhang, H. Jin, C.I. Choi, I.K. Park, I. Kim, Glutathione and endosomal pH-responsive hybrid vesicles fabricated by zwitterionic polymer block poly(L-aspartic acid) as a smart anticancer delivery platform, React. Funct. Polym. 119 (2017) 47-56. https://doi.org/10.1016/j.reactfunctpolym.2017.07.010.

[45] B.H. Zinselmeyer, S.P. Mackay, A.G. Schatzlein, I.F. Uchegbu, The lower-generation polypropylenimine dendrimers are effective gene-transfer agents., Pharm. Res. 19 (2002) 960-7. https://doi.org/10.1023/a:1016458104359.

[46] Janaszewska, Lazniewska, Trzepiński, Marcinkowska, Klajnert-Maculewicz, Cytotoxicity of Dendrimers, Biomolecules. 9 (2019) 330. https://doi.org/10.3390/biom9080330.

[47] A.B. Hill, M. Chen, C.K. Chen, B.A. Pfeifer, C.H. Jones, Overcoming gene-delivery hurdles: Physiological considerations for nonviral vectors, Trends Biotechnol. 34 (2016) 91-105. https://doi.org/10.1016/j.tibtech.2015.11.004.

[48] M.S. Shim, Y.J. Kwon, Controlled delivery of plasmid DNA and siRNA to intracellular targets using ketalized polyethylenimine, Biomacromolecules. 9 (2008) 444-455. https://doi.org/10.1021/bm7007313.

[49] S. Maity, P. Choudhary, M. Manjunath, A. Kulkarni, N. Murthy, A biodegradable adamantane polymer with ketal linkages in its backbone for gene therapy, Chem. Commun. 51 (2015) 15956-15959. https://doi.org/10.1039/c5cc05242d.

[50] Y.H. Kim, J.H. Park, M. Lee, Y.H. Kim, T.G. Park, S.W. Kim, Polyethylenimine with acid-labile linkages as a biodegradable gene carrier, J. Control. Release. 103 (2005) 209-219. https://doi.org/10.1016/j.jconrel.2004.11.008.

[51] S. Chen, T. Jin, Poly-cross-linked PEI through aromatically conjugated imine linkages as a new class of pH-responsive nucleic acids packing cationic polymers, Front. Pharmacol. 7 (2016). https://doi.org/10.3389/fphar.2016.00015.

[52] R.B. Arote, D. Jere, H.-L. Jiang, Y.-K. Kim, Y.-J. Choi, C.-S. Cho, Biodegradable poly(ester amine)s for gene delivery

applications, Biomed. Mater. 4 (2009) 044102. https://doi.org/10.1088/1748-6041/4/4/044102.

[53] P. Mastorakos, A.L.D. Silva, J. Chisholm, E. Song, W.K. Choi, M.P. Boyle, M.M. Morales, J. Hanes, J.S. Suk, Highly compacted biodegradable DNA nanoparticles capable of overcoming the mucus barrier for inhaled lung gene therapy, Proc. Natl. Acad. Sci. U. S. A. 112 (2015) 8720-8725. https://doi.org/10.1073/pnas.1502281112.

[54] L. Song, A.X. Ding, K.X. Zhang, B. Gong, Z.L. Lu, L. He, Degradable polyesters: Via ring-opening polymerization of functional valerolactones for efficient gene delivery, Org. Biomol. Chem. 15 (2017) 6567-6574. https://doi.org/10.1039/c7ob00822h.

[55] J. Shi, J.G. Schellinger, S.H. Pun, Engineering biodegradable and multifunctional peptide-based polymers for gene delivery, J. Biol. Eng. 7 (2013). https://doi.org/10.1186/1754-1611-7-25.

[56] J. Yan, H. Zhang, F. Cheng, Y. He, T. Su, X. Zhang, M. Zhang, Y. Zhu, C. Li, J. Cao, B. He, Highly stable RGD/disulfide bridge-bearing star-shaped biodegradable nanocarriers for enhancing drug-loading efficiency, rapid cellular uptake, and on-demand cargo release, Int. J. Nanomedicine. Volume 13 (2018) 8247-8268. https://doi.org/10.2147/IJN.S179906.

[57] S. Liu, Y. Gao, D. Zhou, M. Zeng, F. Alshehri, B. Newland, J. Lyu, J. O' Keeffe-Ahern, U. Greiser, T. Guo, F. Zhang, W. Wang,

Highly branched poly(β-amino ester) delivery of minicircle DNA for transfection of neurodegenerative disease related cells, Nat. Commun. 10 (2019) 3307. https://doi.org/10.1038/s41467-019-11190-0.

[58] M.A. Gosselin, W. Guo, R.J. Lee, Efficient gene transfer using reversibly cross-linked low molecular weight polyethylenimine, Bioconjug. Chem. 12 (2001) 989-994. https://doi.org/10.1021/bc0100455.

[59] Y.X. Sun, X. Zeng, Q.F. Meng, X.Z. Zhang, S.X. Cheng, R.X. Zhuo, The influence of RGD addition on the gene transfer characteristics of disulfide-containing polyethyleneimine/DNA complexes, Biomaterials. 29 (2008) 4356-4365. https://doi.org/10.1016/j.biomaterials.2008.07.045.

[60] H. Liu, H. Wang, W. Yang, Y. Cheng, Disulfide cross-linked low generation dendrimers with high gene transfection efficacy, low cytotoxicity, and low cost, J. Am. Chem. Soc. 134 (2012) 17680-17687. https://doi.org/10.1021/ja307290j.

[61] C.Y. Li, H.J. Wang, J.M. Cao, J. Zhang, X.Q. Yu, Bioreducible cross-linked polymers based on G1 peptide dendrimer as potential gene delivery vectors, Eur. J. Med. Chem. 87 (2014) 413-420. https://doi.org/10.1016/j.ejmech.2014.09.091.

[62] J.P. Nam, S. Kim, S.W. Kim, Design of PEI-conjugated bio-

reducible polymer for efficient gene delivery, Int. J. Pharm. 545 (2018) 295-305. https://doi.org/10.1016/j.ijpharm.2018.04.051.

[63] Z. Guo, S. Li, Z. Liu, W. Xue, Tumor-Penetrating Peptide-Functionalized Redox-Responsive Hyperbranched Poly(amido amine) Delivering siRNA for Lung Cancer Therapy, (2018). https://doi.org/10.1021/acsbiomaterials.7b00971.

[64] Y. Wang, B. Ma, A.A. Abdeen, G. Chen, R. Xie, K. Saha, S. Gong, Versatile Redox-Responsive Polyplexes for the Delivery of Plasmid DNA, Messenger RNA, and CRISPR-Cas9 Genome-Editing Machinery, (2018). https://doi.org/10.1021/acsami.8b09642.

[65] X. Xu, J. Wu, S. Liu, P.E. Saw, W. Tao, Y. Li, L. Krygsman, S. Yegnasubramanian, A.M. De Marzo, J. Shi, C.J. Bieberich, O.C. Farokhzad, Redox-Responsive Nanoparticle-Mediated Systemic RNAi for Effective Cancer Therapy, Small. 14 (2018) 1802565. https://doi.org/10.1002/smll.201802565.

[66] I. Ullah, J. Zhao, S. Rukh, K. Muhammad, J. Guo, X. kui Ren, S. Xia, W. Zhang, Y. Feng, A PEG-b-poly(disulfide-l-lysine) based redox-responsive cationic polymer for efficient gene transfection, J. Mater. Chem. B. 7 (2019) 1893-1905. https://doi.org/10.1039/c8tb03226b.

[67] Y.-Y. Peng, D. Diaz-Dussan, P. Kumar, R. Narain, Tumor Microenvironment-Regulated Redox Responsive Cationic

Galactose-Based Hyperbranched Polymers for siRNA Delivery, Bioconjug. Chem. 30 (2019) 405-412. https://doi.org/10.1021/acs.bioconjchem.8b00785.

[68] Y. Rui, D.R. Wilson, K. Sanders, J.J. Green, Reducible Branched Ester-Amine Quadpolymers (rBEAQs) Codelivering Plasmid DNA and RNA Oligonucleotides Enable CRISPR/Cas9 Genome Editing, ACS Appl. Mater. Interfaces. 11 (2019) 10472-10480. https://doi.org/10.1021/acsami.8b20206.

[69] H.C. Kang, H.J. Kang, Y.H. Bae, A reducible polycationic gene vector derived from thiolated low molecular weight branched polyethyleneimine linked by 2-iminothiolane, Biomaterials. 32 (2011) 1193-1203. https://doi.org/10.1016/j.biomaterials.2010.08.079.

[70] S. Taranejoo, R. Chandrasekaran, W. Cheng, K. Hourigan, Bioreducible PEI-functionalized glycol chitosan: A novel gene vector with reduced cytotoxicity and improved transfection efficiency, Carbohydr. Polym. 153 (2016) 160-168. https://doi.org/10.1016/j.carbpol.2016.07.080.

[71] X.-J. Du, Z.-Y. Wang, Y.-C. Wang, Redox-sensitive dendrimersomes assembled from amphiphilic Janus dendrimers for siRNA delivery †, Biomater. Sci. 6 (2018) 2122. https://doi.org/10.1039/c8bm00491a.

[72] M. Green, P.M. Loewenstein, Autonomous functional domains of chemically synthesized human immunodeficiency virus tat trans-activator protein, Cell. 55 (1988) 1179-1188. https://doi.org/10.1016/0092-8674(88)90262-0.

[73] A.D. Frankel, C.O. Pabo, Cellular uptake of the tat protein from human immunodeficiency virus, Cell. 55 (1988) 1189-1193. https://doi.org/10.1016/0092-8674(88)90263-2.

[74] D.M. Copolovici, K. Langel, E. Eriste, Ü. Langel, Cell-penetrating peptides: Design, synthesis, and applications, ACS Nano. 8 (2014) 1972-1994. https://doi.org/10.1021/nn4057269.

[75] S. Futaki, I. Nakase, Cell-Surface Interactions on Arginine-Rich Cell-Penetrating Peptides Allow for Multiplex Modes of Internalization, Acc. Chem. Res. 50 (2017) 2449-2456. https://doi.org/10.1021/acs.accounts.7b00221.

[76] A. Borrelli, A.L. Tornesello, M.L. Tornesello, F.M. Buonaguro, Cell penetrating peptides as molecular carriers for anti-cancer agents, Molecules. 23 (2018) 295. https://doi.org/10.3390/molecules23020295.

[77] N.F. Hall, M.R. Sprinkle, Relations between the structure and strength of certain organic bases in aqueous solution, J. Am. Chem. Soc. 54 (1932) 3469-3485. https://doi.org/10.1021/ja01348a001.

[78] A. Borrelli, A.L. Tornesello, M.L. Tornesello, F.M.

Buonaguro, Cell penetrating peptides as molecular carriers for anti-cancer agents, Molecules. 23 (2018) 295. https://doi.org/10.3390/molecules23020295.

[79] J. Derouchey, B. Hoover, D.C. Rau, A comparison of DNA compaction by arginine and lysine peptides: A physical basis for arginine rich protamines, Biochemistry. 52 (2013) 3000-3009. https://doi.org/10.1021/bi4001408.

[80] D. Frigyes, F. Alber, S. Pongor, P. Carloni, Arginine-phosphate salt bridges in protein-DNA complexes: A Car-Parrinello study, J. Mol. Struct. THEOCHEM. 574 (2001) 39-45. https://doi.org/10.1016/S0166-1280(01)00368-2.

[81] T.I. Yusufaly, Y. Li, G. Singh, W.K. Olson, Arginine-phosphate salt bridges between histones and DNA: Intermolecular actuators that control nucleosome architecture, J. Chem. Phys. 141 (2014) 165102. https://doi.org/10.1063/1.4897978.

[82] C.L. Borders, J.A. Broadwater, P.A. Bekeny, J.E. Salmon, A.S. Lee, A.M. Eldridge, V.B. Pett, A structural role for arginine in proteins: Multiple hydrogen bonds to backbone carbonyl oxygens, Protein Sci. 3 (1994) 541-548. https://doi.org/10.1002/pro.5560030402.

[83] B. Musafia, V. Buchner, D. Arad, Complex salt bridges in proteins: Statistical analysis of structure and function, J. Mol. Biol.

254 (1995) 761-770. https://doi.org/10.1006/jmbi.1995.0653.

[84] S. Kumar, R. Nussinov, Salt bridge stability in monomeric proteins, J. Mol. Biol. 293 (1999) 1241-1255. https://doi.org/10.1006/jmbi.1999.3218.

[85] C. Strub, C. Alies, A. Lougarre, C. Ladurantie, J. Czaplicki, D. Fournier, Mutation of exposed hydrophobic amino acids to arginine to increase protein stability, BMC Biochem. 5 (2004) 1-6. https://doi.org/10.1186/1471-2091-5-9.

[86] J.E. Donald, D.W. Kulp, W.F. DeGrado, Salt bridges: Geometrically specific, designable interactions, Proteins Struct. Funct. Bioinforma. 79 (2011) 898-915. https://doi.org/10.1002/prot.22927.

[87] M. Matsutani, H. Hirakawa, M. Nishikura, W. Soemphol, I.A.I. Ali, T. Yakushi, K. Matsushita, Increased number of Arginine-based salt bridges contributes to the thermotolerance of thermotolerant acetic acid bacteria, Acetobacter tropicalis SKU1100, Biochem. Biophys. Res. Commun. 409 (2011) 120-124. https://doi.org/10.1016/j.bbrc.2011.04.126.

[88] C.-H. Chan, T.-H. Yu, K.-B. Wong, Stabilizing Salt-Bridge Enhances Protein Thermostability by Reducing the Heat Capacity Change of Unfolding, PLoS One. 6 (2011) e21624. https://doi.org/10.1371/journal.pone.0021624.

[89] O. Turunen, M. Vuorio, F. Fenel, M. Leisola, Engineering of multiple arginines into the Ser/Thr surface of Trichoderma reesei endo-1,4-β-xylanase II increases the thermotolerance and shifts the pH optimum towards alkaline pH, Protein Eng. Des. Sel. 15 (2002) 141-145. https://doi.org/10.1093/protein/15.2.141.

[90] L. Li, I. Vorobyov, T.W. Allen, The different interactions of lysine and arginine side chains with lipid membranes, J. Phys. Chem. B. 117 (2013) 11906-11920. https://doi.org/10.1021/jp405418y.

[91] H.Y. Nam, K. Nam, H.J. Hahn, B.H. Kim, H.J. Lim, H.J. Kim, J.S. Choi, J.S. Park, Biodegradable PAMAM ester for enhanced transfection efficiency with low cytotoxicity, Biomaterials. 30 (2009) 665-673. https://doi.org/10.1016/j.biomaterials.2008.10.013.

[92] T. il Kim, M. Ou, M. Lee, S.W. Kim, Arginine-grafted bioreducible poly(disulfide amine) for gene delivery systems, Biomaterials. 30 (2009) 658-664. https://doi.org/10.1016/j.biomaterials.2008.10.009.

[93] N. Young Ahn, T.-H. Kim, S. Jeong Song, J.-M. Moon, T. Hwan Ha, J. Sig Choi, Polyethylenimine-Poly(amidoamine) Dendrimer Modified with L-Arginines as an Efficient Gene Delivery Vector, Macromol. Res. 23 (2015) 726-733. https://doi.org/10.1007/s13233-015-3101-6.

[94] Q. Peng, J. Zhu, Y. Yu, L. Hoffman, X. Yang, Hyperbranched

lysine–arginine copolymer for gene delivery, J. Biomater. Sci. Polym. Ed. 26 (2015) 1163–1177. https://doi.org/10.1080/09205063.2015.1080482.

[95] F. Wang, K. Hu, Y. Cheng, Structure–activity relationship of dendrimers engineered with twenty common amino acids in gene delivery, Acta Biomater. 29 (2016) 94–102. https://doi.org/10.1016/j.actbio.2015.10.034.

[96] J. Yu, J. Zhang, H. Xing, Y. Sun, Z. Yang, T. Yang, C. Cai, X. Zhao, L. Yang, P. Ding, Novel guanidinylated bioresponsive poly(Amidoamine)s designed for short hairpin RNA delivery, Int. J. Nanomedicine. 11 (2016) 6651–6666. https://doi.org/10.2147/IJN.S115773.

[97] H. Li, T. Luo, R. Sheng, J. Sun, Z. Wang, A. Cao, Achieving high gene delivery performance with caveolae–mediated endocytosis pathway by (l)–arginine/(l)–histidine co–modified cationic gene carriers, Colloids Surfaces B Biointerfaces. 148 (2016) 73–84. https://doi.org/10.1016/j.colsurfb.2016.08.035.

[98] G.R. Dhanya, D.S. Caroline, M.R. Rekha, K. Sreenivasan, Histidine and arginine conjugated starch–PEI and its corresponding gold nanoparticles for gene delivery, Int. J. Biol. Macromol. 120 (2018) 999–1008. https://doi.org/10.1016/j.ijbiomac.2018.08.142.

[99] N. Zavradashvili, C. Sarisozen, G. Titvinidze, G. Otinashvili,

T. Kantaria, D. Tugushi, J. Puiggali, V.P. Torchilin, R. Katsarava, Library of Cationic Polymers Composed of Polyamines and Arginine as Gene Transfection Agents, ACS Omega. 4 (2019) 2090-2101. https://doi.org/10.1021/acsomega.8b02977.

[100] S. Lu, V.B. Morris, V. Labhasetwar, Effectiveness of small interfering RNA delivery via arginine-rich polyethylenimine-based polyplex in metastatic and doxorubicin-resistant breast cancer cells, J. Pharmacol. Exp. Ther. 370 (2019) 902-910. https://doi.org/10.1124/jpet.119.256909.

[101] J.L. Choi, J.K.Y. Tan, D.L. Sellers, H. Wei, P.J. Horner, S.H. Pun, Guanidinylated block copolymers for gene transfer: A comparison with amine-based materials for invitro and invivo gene transfer efficiency, Biomaterials. 54 (2015) 87-96. https://doi.org/10.1016/j.biomaterials.2015.03.008.

[102] H. Chang, J. Zhang, H. Wang, J. Lv, Y. Cheng, A Combination of Guanidyl and Phenyl Groups on a Dendrimer Enables Efficient siRNA and DNA Delivery, Biomacromolecules. 18 (2017) 2371-2378. https://doi.org/10.1021/acs.biomac.7b00567.

[103] A. Hibbitts, A.M. O'connor, J. Mccarthy, E.´ A.B. Forde, G. Hessman, C.M. O ' driscoll, S.-A. Cryan, M. Devocelle, Poly(ethylene glycol)-Based Peptidomimetic " PEGtide " of Oligo-Arginine Allows for Efficient siRNA Transfection and Gene

Inhibition, (2019). https://doi.org/10.1021/acsomega.9b00265.

[104] M. Pilarek, Liquid perfluorochemicals as flexible and efficient gas carriers applied in bioprocess engineering: An updated overview and future prospects, Chem. Process Eng. – Inz. Chem. i Proces. 35 (2014) 463–487. https://doi.org/10.2478/cpe-2014-0035.

[105] J. Gardiner, Fluoropolymers: Origin, Production, and Industrial and Commercial Applications, Aust. J. Chem. 68 (2015) 13–22. https://doi.org/10.1071/CH14165.

[106] Y. Zhou, J. Wang, Z. Gu, S. Wang, W. Zhu, J.L. Acenã, V.A. Soloshonok, K. Izawa, H. Liu, Next Generation of Fluorine-Containing Pharmaceuticals, Compounds Currently in Phase II-III Clinical Trials of Major Pharmaceutical Companies: New Structural Trends and Therapeutic Areas, Chem. Rev. 116 (2016) 422–518. https://doi.org/10.1021/acs.chemrev.5b00392.

[107] E.P. Gillis, K.J. Eastman, M.D. Hill, D.J. Donnelly, N.A. Meanwell, Applications of Fluorine in Medicinal Chemistry, J. Med. Chem. 58 (2015) 8315–8359. https://doi.org/10.1021/acs.jmedchem.5b00258.

[108] N.A. Meanwell, Fluorine and Fluorinated Motifs in the Design and Application of Bioisosteres for Drug Design, J. Med. Chem. 61 (2018) 5822–5880. https://doi.org/10.1021/acs.jmedchem.7b01788.

[109] J. Fried, E.F. Sabo, 9α-Fluoro derivatives of cortisone and hydrocortisone, J. Am. Chem. Soc. 76 (1954) 1455-1456. https://doi.org/10.1021/ja01634a101.

[110] D. O'Hagan, Fluorine in health care: Organofluorine containing blockbuster drugs, J. Fluor. Chem. 131 (2010) 1071-1081. https://doi.org/10.1016/j.jfluchem.2010.03.003.

[111] S.D. Xiong, L. Li, J. Jiang, L.P. Tong, S. Wu, Z.S. Xu, P.K. Chu, Cationic fluorine-containing amphiphilic graft copolymers as DNA carriers, Biomaterials. 31 (2010) 2673-2685. https://doi.org/10.1016/j.biomaterials.2009.12.014.

[112] M. Wang, H. Liu, L. Li, Y. Cheng, A fluorinated dendrimer achieves excellent gene transfection efficacy at extremely low nitrogen to phosphorus ratios, Nat. Commun. 5 (2014). https://doi.org/10.1038/ncomms4053.

[113] M. Wang, Y. Cheng, The effect of fluorination on the transfection efficacy of surface-engineered dendrimers, Biomaterials. 35 (2014) 6603-6613. https://doi.org/10.1016/j.biomaterials.2014.04.065.

[114] H. Liu, Y. Wang, M. Wang, J. Xiao, Y. Cheng, Fluorinated poly(propylenimine) dendrimers as gene vectors, Biomaterials. 35 (2014) 5407-5413. https://doi.org/10.1016/j.biomaterials.2014.03.040.

[115] H. Wang, Y. Wang, Y. Wang, J. Hu, T. Li, H. Liu, Q. Zhang, Y. Cheng, Self-Assembled Fluorodendrimers Combine the Features of Lipid and Polymeric Vectors in Gene Delivery, Angew. Chemie - Int. Ed. 54 (2015) 11647-11651. https://doi.org/10.1002/anie.201501461.

[116] J. Lv, H. Chang, Y. Wang, M. Wang, J. Xiao, Q. Zhang, Y. Cheng, Fluorination on polyethylenimine allows efficient 2D and 3D cell culture gene delivery, J. Mater. Chem. B. 3 (2015) 642-650. https://doi.org/10.1039/c4tb01447b.

[117] B. He, Y. Wang, N. Shao, H. Chang, Y. Cheng, Polymers modified with double-tailed fluorous compounds for efficient DNA and siRNA delivery, Acta Biomater. 22 (2015) 111-119. https://doi.org/10.1016/j.actbio.2015.04.037.

[118] M.E. Johnson, J. Shon, B.M. Guan, J.P. Patterson, N.J. Oldenhuis, A.C. Eldredge, N.C. Gianneschi, Z. Guan, Fluorocarbon Modified Low-Molecular-Weight Polyethylenimine for siRNA Delivery, Bioconjug. Chem. 27 (2016). https://doi.org/10.1021/acs.bioconjchem.6b00216.

[119] M. Wang, Y. Cheng, Structure-activity relationships of fluorinated dendrimers in DNA and siRNA delivery, Acta Biomater. 46 (2016) 204-210. https://doi.org/10.1016/j.actbio.2016.09.023.

[120] Y. Wang, M. Wang, H. Chen, H. Liu, Q. Zhang, Y. Cheng,

Fluorinated dendrimer for TRAIL gene therapy in cancer treatment, J. Mater. Chem. B. 4 (2016). https://doi.org/10.1039/c5tb02712h.

[121] H. Wang, J. Hu, X. Cai, J. Xiao, Y. Cheng, Self-assembled fluorodendrimers in the co-delivery of fluorinated drugs and therapeutic genes, Polym. Chem. 7 (2016) 2319-2322. https://doi.org/10.1039/c6py00153j.

[122] Y.P. Xiao, J. Zhang, Y.H. Liu, Z. Huang, B. Wang, Y.M. Zhang, X.Q. Yu, Cross-linked polymers with fluorinated bridges for efficient gene delivery, J. Mater. Chem. B. 5 (2017) 8542-8553. https://doi.org/10.1039/c7tb02158e.

[123] E. Tan, J. Lv, J. Hu, W. Shen, H. Wang, Y. Cheng, Statistical: Versus block fluoropolymers in gene delivery, J. Mater. Chem. B. 6 (2018) 7230-7238. https://doi.org/10.1039/c8tb01470a.

[124] T. Zhang, Y. Huang, X. Ma, N. Gong, X. Liu, L. Liu, X. Ye, B. Hu, C. Li, J.H. Tian, A. Magrini, J. Zhang, W. Guo, J.F. Xing, M. Bottini, X.J. Liang, Fluorinated Oligoethylenimine Nanoassemblies for Efficient siRNA-Mediated Gene Silencing in Serum-Containing Media by Effective Endosomal Escape, Nano Lett. 18 (2018) 6301-6311. https://doi.org/10.1021/acs.nanolett.8b02553.

[125] G. Chen, K. Wang, P. Wu, Y. Wang, Z. Zhou, L. Yin, M. Sun, D. Oupický, Development of fluorinated polyplex nanoemulsions for improved small interfering RNA delivery and cancer therapy, Nano

Res. 11 (2018) 3746-3761. https://doi.org/10.1007/s12274-017-1946-z.

[126] Y.-P. Xiao, J. Zhang, Y.-H. Liu, J.-H. Zhang, Q.-Y. Yu, Z. Huang, X.-Q. Yu, Low molecular weight PEI-based fluorinated polymers for efficient gene delivery, Eur. J. Med. Chem. 162 (2019) 602-611. https://doi.org/10.1016/j.ejmech.2018.11.041.

[127] G. Zuo, A. Xie, X. Pan, T. Su, J. Li, W. Dong, Fluorine-Doped Cationic Carbon Dots for Efficient Gene Delivery, ACS Appl. Nano Mater. 1 (2018) 2376-2385. https://doi.org/10.1021/acsanm.8b00521.

[128] L.H. Wang, D.C. Wu, H.X. Xu, Y.Z. You, High DNA-Binding Affinity and Gene-Transfection Efficacy of Bioreducible Cationic Nanomicelles with a Fluorinated Core, Angew. Chemie - Int. Ed. 55 (2016) 755-759. https://doi.org/10.1002/anie.201508695.

[129] X. Liu, Y. Wang, C. Chen, A. Tintaru, Y. Cao, J. Liu, F. Ziarelli, J. Tang, H. Guo, R. Rosas, S. Giorgio, L. Charles, P. Rocchi, L. Peng, A Fluorinated Bola-Amphiphilic Dendrimer for On-Demand Delivery of siRNA, via Specific Response to Reactive Oxygen Species, Adv. Funct. Mater. 26 (2016) 8594-8603. https://doi.org/10.1002/adfm.201604192.

[130] X. Cai, R. Jin, J. Wang, D. Yue, Q. Jiang, Y. Wu, Z. Gu, Bioreducible Fluorinated Peptide Dendrimers Capable of

Circumventing Various Physiological Barriers for Highly Efficient and Safe Gene Delivery, ACS Appl. Mater. Interfaces. 8 (2016) 5821–5832. https://doi.org/10.1021/acsami.5b11545.

[131] X. Cai, H. Zhu, Y. Zhang, Z. Gu, Highly Efficient and Safe Delivery of VEGF siRNA by Bioreducible Fluorinated Peptide Dendrimers for Cancer Therapy, ACS Appl. Mater. Interfaces. 9 (2017) 9402–9415. https://doi.org/10.1021/acsami.6b16689.

[132] G. Chen, K. Wang, Q. Hu, L. Ding, F. Yu, Z. Zhou, Y. Zhou, J. Li, M. Sun, D. Oupický, Combining Fluorination and Bioreducibility for Improved siRNA Polyplex Delivery, ACS Appl. Mater. Interfaces. 9 (2017) 4457–4466. https://doi.org/10.1021/acsami.6b14184.

[133] Q. Deng, X. Li, L. Zhu, H. He, D. Chen, Y. Chen, L. Yin, Serum-resistant, reactive oxygen species (ROS)-potentiated gene delivery in cancer cells mediated by fluorinated, diselenide-crosslinked polyplexes, Biomater. Sci. (2017). https://doi.org/10.1039/c7bm00334j.

[134] J.H. Gong, Y. Wang, L. Xing, P.F. Cui, J. Bin Qiao, Y.J. He, H.L. Jiang, Biocompatible fluorinated poly(β-amino ester)s for safe and efficient gene therapy, Int. J. Pharm. 535 (2018) 180–193. https://doi.org/10.1016/j.ijpharm.2017.11.015.

[135] Y. Qi, H. Song, H. Xiao, G. Cheng, B. Yu, F.J. Xu, Fluorinated Acid-Labile Branched Hydroxyl-Rich Nanosystems for Flexible

and Robust Delivery of Plasmids, Small. 14 (2018). https://doi.org/10.1002/smll.201803061.

[136] G. Chen, K. Wang, Y. Wang, P. Wu, M. Sun, D. Oupický, Fluorination Enhances Serum Stability of Bioreducible Poly(amido amine) Polyplexes and Enables Efficient Intravenous siRNA Delivery, Adv. Healthc. Mater. 7 (2018) 1–14. https://doi.org/10.1002/adhm.201700978.

[137] J.-H. Zhang, W.-J. Wang, J. Zhang, Y.-P. Xiao, Y.-H. Liu, X.-Q. Yu, ROS-responsive fluorinated polycations as non-viral gene vectors, Eur. J. Med. Chem. 182 (2019) 111666. https://doi.org/10.1016/j.ejmech.2019.111666.

[138] L. V Christensen, C.W. Chang, J.K. Won, W.K. Sung, Z. Zhong, C. Lin, J.F.J. Engbersen, J. Feijen, Reducible poly(amido ethylenimine)s designed for triggered intracellular gene delivery, Bioconjug. Chem. 17 (2006) 1233–1240. https://doi.org/10.1021/bc0602026.

[139] M. Ou, X.-L. Wang, R. Xu, C.-W. Chang, D. a Bull, S.W. Kim, Novel biodegradable poly(disulfide amine)s for gene delivery with high efficiency and low cytotoxicity., Bioconjug. Chem. 19 (2008) 626–33. https://doi.org/10.1021/bc700397x.

[140] Y.Z. You, D.S. Manickam, Q.H. Zhou, D. Oupický, Reducible poly(2-dimethylaminoethyl methacrylate): Synthesis, cytotoxicity,

and gene delivery activity, J. Control. Release. 122 (2007) 217–225. https://doi.org/10.1016/j.jconrel.2007.04.020.

[141] T. il Kim, M. Lee, S.W. Kim, A guanidinylated bioreducible polymer with high nuclear localization ability for gene delivery systems, Biomaterials. 31 (2010) 1798–1804. https://doi.org/10.1016/j.biomaterials.2009.10.034.

[142] Wagner, Ogris, Zauner, Polylysine–based transfection systems utilizing receptor–mediated delivery., Adv. Drug Deliv. Rev. 30 (1998) 97–113. https://doi.org/10.1016/s0169–409x(97)00110–5.

[143] I. Kopatz, J.–S. Remy, J.–P. Behr, A model for non–viral gene delivery: through syndecan adhesion molecules and powered by actin, J. Gene Med. 6 (2004) 769–776. https://doi.org/10.1002/jgm.558.

[144] Q. Peng, Z. Zhong, R. Zhuo, Disulfide cross–linked polyethylenimines (PEI) prepared via thiolation of low molecular weight PEI as highly efficient gene vectors, Bioconjug. Chem. 19 (2008) 499–506. https://doi.org/10.1021/bc7003236.

[145] S. Son, K. Singha, W.J. Kim, Bioreducible BPEI–SS–PEG–cNGR polymer as a tumor targeted nonviral gene carrier, Biomaterials. 31 (2010) 6344–6354. https://doi.org/10.1016/j.biomaterials.2010.04.047.

[146] J.W. Wiseman, C.A. Goddard, D. McLelland, W.H. Colledge, A comparison of linear and branched polyethylenimine (PEI) with DCChol/DOPE liposomes for gene delivery to epithelial cells in vitro and in vivo, Gene Ther. 10 (2003) 1654-1662. https://doi.org/10.1038/sj.gt.3302050.

[147] M.X. Tang, C.T. Redemann, F.C. Szoka, In vitro gene delivery by degraded polyamidoamine dendrimers, Bioconjug. Chem. 7 (1996) 703-714. https://doi.org/10.1021/bc9600630.

[148] Y.B. Lim, S.M. Kim, H. Suh, J.S. Park, Biodegradable, endosome disruptive, and cationic network-type polymer as a highly efficient and nontoxic gene delivery carrier, Bioconjug. Chem. 13 (2002) 952-957. https://doi.org/10.1021/bc025541n.

[149] X. Jiang, Y. Yu, J. Chen, M. Zhao, H. Chen, X. Song, A.J. Matzuk, S.L. Carroll, X. Tan, A. Sizovs, N. Cheng, M.C. Wang, J. Wang, Quantitative imaging of glutathione in live cells using a reversible reaction-based ratiometric fluorescent probe, ACS Chem. Biol. 10 (2015) 864-874. https://doi.org/10.1021/cb500986w.

[150] L. Zhao, C.D. Kroenke, J. Song, D. Piwnica-Worms, J.J.H. Ackerman, J.J. Neil, Intracellular water-specific MR of microbead-adherent cells: The HeLa cell intracellular water exchange lifetime, NMR Biomed. 21 (2008) 159-164. https://doi.org/10.1002/nbm.1173.

[151] K. Kim, K. Ryu, T. Il Kim, Cationic methylcellulose derivative with serum-compatibility and endosome buffering ability for gene delivery systems, Carbohydr. Polym. 110 (2014) 268-277. https://doi.org/10.1016/j.carbpol.2014.03.073.

[152] S.M. Moghimi, P. Symonds, J.C. Murray, A.C. Hunter, G. Debska, A. Szewczyk, A two-stage poly(ethylenimine)-mediated cytotoxicity: Implications for gene transfer/therapy, Mol. Ther. 11 (2005) 990-995. https://doi.org/10.1016/j.ymthe.2005.02.010.

[153] W.T. Godbey, K.K. Wu, G.J. Hirasaki, A.G. Mikos, Improved packing of poly(ethylenimine)/DNA complexes increases transfection efficiency, Gene Ther. 6 (1999) 1380-1388. https://doi.org/10.1038/sj.gt.3300976.

[154] W.T. Godbey, K.K. Wu, A.G. Mikos, Poly(ethylenimine)-mediated gene delivery affects endothelial cell function and viability., Biomaterials. 22 (2001) 471-80. https://doi.org/10.1016/s0142-9612(00)00203-9.

[155] H.K. Sun, H.J. Ji, T. Il Kim, W.K. Sung, D.A. Bull, VEGF siRNA delivery system using arginine-grafted bioreducible poly(disulfide amine), Mol. Pharm. 6 (2009) 718-726. https://doi.org/10.1021/mp800161e.

[156] R.M. Touyz, E.L. Schiffrin, Reactive oxygen species in vascular biology: Implications in hypertension, Histochem. Cell Biol.

122 (2004) 339-352. https://doi.org/10.1007/s00418-004-0696-7.

[157] G.J. Lee, K. Ryu, K. Kim, J. Choi, T. Kim, Crosslinked Polypropylenimine Dendrimers with Bioreducible Linkages for Gene Delivery Systems and Their Reductive Degradation Behaviors, Macromol. Biosci. 15 (2015) 1595-1604. https://doi.org/10.1002/mabi.201500141.

[158] G.J. Lee, T. Kim, Fluorination effect to intermediate molecular weight polyethylenimine for gene delivery systems, J. Biomed. Mater. Res. Part A. 107 (2019) 2468-2478. https://doi.org/10.1002/jbm.a.36753.

[159] P. Shah, A.D. Westwell, The role of fluorine in medicinal chemistry, J. Enzyme Inhib. Med. Chem. 22 (2007) 527-540. https://doi.org/10.1080/14756360701425014.

[160] N.M. Kovalchuk, A. Trybala, V. Starov, O. Matar, N. Ivanova, Fluoro- Vs hydrocarbon surfactants: Why do they differ in wetting performance?, Adv. Colloid Interface Sci. 210 (2014) 65-71. https://doi.org/10.1016/j.cis.2014.04.003.

[161] R. Hamid, Y. Rotshteyn, L. Rabadi, R. Parikh, P. Bullock, Comparison of alamar blue and MTT assays for high through-put screening, Toxicol. Vitr. 18 (2004) 703-710. https://doi.org/10.1016/j.tiv.2004.03.012.

[162] J. Weyermann, D. Lochmann, A. Zimmer, A practical note on the use of cytotoxicity assays, Int. J. Pharm. 288 (2005) 369–376. https://doi.org/10.1016/j.ijpharm.2004.09.018.

[163] S. Carrabino, S. Di Gioia, E. Copreni, M. Conese, Serum albumin enhances polyethylenimine–mediated gene delivery to human respiratory epithelial cells, J. Gene Med. 7 (2005) 1555–1564. https://doi.org/10.1002/jgm.799.

[164] S. Simões, V. Slepushkin, P. Pires, R. Gaspar, M.C. Pedroso De Lima, N. Düzgüneş, Human serum albumin enhances DNA transfection by lipoplexes and confers resistance to inhibition by serum, Biochim. Biophys. Acta – Biomembr. 1463 (2000) 459–469. https://doi.org/10.1016/S0005–2736(99)00238–2.

[165] J.F. Casella, M.D. Flanagan, S. Lin, Cytochalasin D inhibits actin polymerization and induces depolymerization of actin filaments formed during platelet shape change, Nature. 293 (1981) 302–305. https://doi.org/10.1038/293302a0.

[166] G. Bloomfield, R.R. Kay, Uses and abuses of macropinocytosis, J. Cell Sci. 129 (2016) 2697–2705. https://doi.org/10.1242/jcs.176149.

[167] K. Xu, P.M. Schwarz, R.F. Ludueña, Interaction of nocodazole with tubulin isotypes, Drug Dev. Res. 55 (2002) 91–96. https://doi.org/10.1002/ddr.10023.

[168] H.S. Kruth, N.L. Jones, W. Huang, B. Zhao, I. Ishii, J. Chang, C.A. Combs, D. Malide, W.Y. Zhang, Macropinocytosis is the endocytic pathway that mediates macrophage foam cell formation with native low density lipoprotein, J. Biol. Chem. 280 (2005) 2352–2360. https://doi.org/10.1074/jbc.M407167200.

[169] A. Kakigi, T. Okada, T. Takeda, D. Taguchi, R. Nishioka, M. Nishimura, Actin filaments and microtubules regulate endocytosis in marginal cells of the stria vascularis, Acta Otolaryngol. 128 (2008) 856–860. https://doi.org/10.1080/00016480701777373.

[170] A.W. Wong, S.J. Scales, D.E. Reilly, DNA internalized via caveolae requires microtubule–dependent, Rab7–independent transport to the late endocytic pathway for delivery to the nucleus, J. Biol. Chem. 282 (2007) 22953–22963. https://doi.org/10.1074/jbc.M611015200.

초록

생체환원성 고분자는 환원성 환경에서 선택적으로 분해될 수 있는 특징을 갖고 있어서 유전자 전달체로 널리 이용되고 있다. 하지만 수십 년 동안의 연구에도 불구하고 생체환원성 고분자의 세포 거동을 연구한 논문은 많지 않다.

본 연구에서는 크게 두 종류의 생체환원성 고분자를 다루고 있다. 첫째는 PPI-CBA로 명명한 가교 구조를 지닌 것이며, 둘째로는 FR-PCH로 명명한, 불화탄소와 아르기닌으로 개질한 생체환원성 고분자다. 첫 번째 부분에서는 PPI-CBA의 특이한 분해 거동이 주된 내용이라 볼 수 있다. PPI-CBA는 마이클 첨가 반응 (Michael addition reaction)을 이용해 합성이 진행되었는데, 합성된 고분자는 양이온을 띠고 있는 폴리플렉스 (polyplex) 나노 입자를 이룰 수 있었다. 전기영동에서 흥미로운 결과를 얻을 수 있었는데, 환원성 환경임에도 불구하고 PPI-CBA가 여전히 pDNA를 붙잡고 있었다. 한편, PPI-CBA는 세럼이 있는 상태에서 진행된 실험에서 유전자 전달 효율이 PEI25k보다 뛰어난 모습을 보여줬는데, 이는 PPI-CBA가 세럼과의 상성이 좋음을 의미한다. 그러나 독성이 문제가 되었는데, 세포 내 글루타치온 (glutathione) 과 활성 산소 농도를 측정한 결과를 통해 PPI-CBA의 분해된 부분이 끊임없이 재결합을 하면서 글루타치온을 소모하기 때문에 세포 독성이 발생하는 것으로 추측할 수 있었다. 다시 말해, PPI-CBA는 선형 구조의 생체환원성 고분자와는 다르게 독특한 분해 거동

및 세포 내 거동을 보이는 것으로 볼 수 있었다.

두번째 부분에서는 아르기닌과 불화탄소로 개질한 생체환원성 고분자인 FR-PCH에 대해 다뤘다. 마찬가지로 양이온성을 띠는 폴리플렉스 나노 입자를 형성할 수 있었는데 불화 탄소 치환이 많이 된 일부 FR-PCH는 환원성 환경에서도 pDNA를 붙잡고 있는 것을 볼 수 있었다. 이런 현상은 소수성 상호작용을 할 수 있는 불화탄소가 원인이지 않나 추측할 수 있었다. FR-PCH는 세럼이 없는 조건에서도, 있는 조건에서도 PEI25k를 능가하는 유전자 전달 효율을 보였는데, 이는 FR-PCH가 다른 고분자보다 세럼에 영향을 덜 받는다는 걸 의미한다. 세럼에 대한 상성은 다양한 농도의 세럼을 포함한 배지에서 유전자 전달 효율을 확인하는 등의 일련의 실험으로 추가적으로 확인해 볼 수 있었다. 그러나 좋은 유전자 전달 효율에도 불구하고 상대적으로 높은 세포독성을 지니는 것을 알 수 있었다. LDH가 세포 밖으로 방출되는 양을 봤을 때, 세포 독성은 불화탄소 사슬이 세포막과 강하게 상호작용하는 과정에서 유도되는 것이 아닌가 추측할 수 있었다. 그럼에도 불구하고 다양한 추가 실험을 통해, 불화탄소를 고분자에 도입하는 것이 세럼 안정성 향상이나 막 친화성 같은 것을 획득할 수 있는 좋은 방법이란 것을 다시 한 번 확인할 수 있었다. 또한, 본 연구에서는 불화탄소 사슬과 아르기닌을 갖고 있는 유전자 전달체가 어떻게 세포 내로 들어가는지 알아보기 위한 실험들도 진행되었는데, 합성한 고분자는 특정한 하나의 세포 진입 기작을 이용하는 것 같지는 않았으며 노코다졸에 크게 영향을 받는 것을 확인할 수 있었다.